The Impact of Bacterial Signaling Molecules on the Alveolar Immunity of the Lung

Dissertation der Fakultät für Biologie

der Ludwig-Maximilians-Universität München

Raphaël Prungnaud

München 2019

Aus dem

Comprehensive Pneumology Center (CPC)

Institut für Lung Biology and Diseases (iLBD)

Impact of Bacterial Signaling Molecules on the Alveolar Immunity of the Lung

Diese Dissertation wurde angefertigt unter der Leitung von meines Doktorvaters Prof. Dr. rer. nat. Anton Hartmann am Helmholtz Zentrum München und der Ludwig-Maximilians-Universität München.

Erstgutachter: Prof. Dr. rer. nat. Anton Hartmann

Zweitgutachter: Prof. Dr. Elisabeth Weiß

Tag der Abgabe: 14.10.2019

Tag der mündlichen Prüfung: 23.06.2020

ERKLÄRUNG

Ich versichere hiermit an Eides statt, dass meine Dissertation selbständig und ohne unerlaubte Hilfsmittel angefertigt worden ist. Die vorliegende Dissertation wurde weder ganz, noch teilweise bei einer anderen Prüfungskommission vorgelegt. Ich habe noch zu keinem früheren Zeitpunkt versucht, eine Dissertation einzureichen oder an einer Doktorprüfung teilzunehmen.

München, den 14.10.2019

Raphaël Prungnaud

"It's a marathon, not a sprint."

–Everyone ever

TABLE OF CONTENTS

FIGURES

TABLES

SUPPLEMENTARY FIGURES

ABSTRACT

Mammalian lungs have evolved with the environment as organs with the largest interface to the outside world. Our lungs exist in a state of homeostasis despite their consistent exposition to thousands of exogenous chemicals, particles and microorganisms carried by the air. As previously described for the gut and the skin, a high diversity of microbes lives and prospers in interaction with their host on the pulmonary surface as well, thereby connecting us to the environment. However, imbalances between beneficial and pathogenic microbes in this complex biological system can cause acute or chronic diseases. From these empirical observations, the human microbiome, in its diversity, interacts actively with the host immunity.

This project aims to investigate the effect of two classes of bacterial signaling molecules on the inflammation dynamics of the lung, focusing on differentiation of T helper (T_h) cells, activation (polarization) of alveolar macrophages (AM), and wound healing and repair during an inflammatory response. On one hand, the quorum sensing (QS) molecule 3-oxo-C_{12}-HSL (AHL), produced by the pathogenic bacterium *Pseudomonas aeruginosa* (PAO1 strain) and on the other hand the D-tryptophan (D-Trp), amino acid secreted by probiotic lactic acid bacteria, like *Lactobacillus casei*, were studied as examples of two classes of molecules involved in having a potential therapeutic interaction with the host.

First the effects of the 3-oxo-C_{12}-HSL on murine T_h cells, especially T_h17 and T_h2-cell differentiation, were investigated. 3-oxo-C_{12}-HSL increased interleukin 17 (IL-17) production of T_h17 cells. However, it did not influence interleukin 4 (IL-4) production in T_h2 differentiated cells. IL-17, mainly produced from T_h17 cells, is a pro-inflammatory cytokine responsible for the chemoattraction of leukocytes to the site of inflammation; whereas IL-4, produced from T_h2 cells and a key regulator of adaptive immunity, is also involved in M2-polarization of macrophages, thereby promoting the resolution of inflammation and wound repair. Altogether these results showed that 3-

oxo-C_{12}-HSL stimulation of differentiated T_h17 cells supported IL-17 production and might thereby promote the inflammatory response.

During a bacterial lung infection, the primary immune response is conducted by tissue resident, alveolar macrophages (AM). To study the effect of AHLs on alveolar macrophage polarization, M0-naïve AM (MH-S cell line) were polarized with lipopolysaccharide (LPS) towards M1-polarization and simultaneously treated with AHLs (60 μM). Interestingly, both the expression and secretion of the pro-inflammatory cytokines Tumor Necrosis Factor α (TNFα) and Interleukin 1 beta (IL-1β) rose by the cotreatment with AHLs, mostly 3-oxo-C12-HSL, suggesting that the development of M1 AM and thus an inflammatory response was supported. D-Trp treatment (10-100 μM), simultaneous applied to M1-polarization, led also to an increase of TNFα secretion, suggesting that D-Trp contributed to a pro-inflammatory modulation of the AM as well. Then again, both 3-oxo-C_{12}-HSL and D-Trp treatments supported alternative, IL-4 triggered AM polarization (M2-polarization), characterized by increased expression of the markers Arginase 1 (Arg1) and Mannose Receptor C-Type 1 (Mrc1). The latter results suggest that M2-polarization could be enhanced by 3-oxo-C_{12}-HSL and D-Trp, thereby eventually promoting M2 dependent repair pathways during the resolution phase of inflammation. In aim to test the influence on repair pathways, a lung epithelium coculture model, consisting of AM (MH-S) and alveolar epithelial cells type 2 (AECII; LA-4 and MLE-12 cell lines) was investigated. The coculture wound healing assays however revealed that 3-oxo-C_{12}-HSL, and D-Trp to a lesser extent, inhibited in vitro epithelial barrier function and healing independently even from a by LPS induced inflammatory response. Similarly, *Pseudomonas aeruginosa's* culture supernatant, containing secreted AHL, greatly impaired epithelial wound healing. Also *in vivo*, in an acute lung injury (ALI) model, created by intratracheal LPS delivery into the lung of BALB/c mice, therapeutically treatment with 3-oxo-C_{12}-HSL, at a dose of 1200 μM (corresponding to a local strong PAO1 infection) failed to reduce polymorphonuclear neutrophil (PMN) recruitment in the airspace of the lung after acute lung injury. This altogether rejects the hypothesis of therapeutic effects of AHL during inflammatory conditions of the lung.

In contrast, D-Trp treatment reduced PMN recruitment in the ALI model, accompanied by a trend in declined bronchoalveolar lavage (BAL) levels of the chemokine (C-X-C motif) ligand 1 (CXCL1), while L-Trp had no comparable effect. mRNA analysis of the whole lung homogenate confirmed that the expression of CD11b (a marker for PMNs and inflammatory macrophages) was mildly reduced after D-Trp instillation. These results collectively confirmed the anti-inflammatory effects of D-Trp in an injured lung. Since D-Trp can have transcriptional signaling activity via the aryl hydrocarbon receptor (AhR), whose immunological importance is gaining more and more attention, the involvement of this pathway was investigated in bone marrow derived macrophages (BMDM) from $AhR^{-/-}$ (AhR^{tm1Bra}) mice. D-Trp treatment of BMDM caused an AhR dependent expression of the prototypic AhR target gene cytochrome P450-1A1 (Cyp1a1) and also indoleamine 2,3-dioxygenase 1 (Ido1), while L-Trp had no effect. Since Ido1 metabolizes tryptophan to kynurenine, which in turn is sensed by AhR, this suggests a positive feedback loop. Finally, D-Trp but not L-Trp treatment of BMDM also reduced the expression of the LPS stimulated M1 markers interleukin-6 (Il-6) and Nos2, and enhanced the by IL-4 stimulated M2 markers Arg1 and Mrc1, all in an AhR dependent manner.

In summary, the results suggest not the investigated AHL 3-oxo-C_{12}-HSL, but rather D-tryptophan as a potential target of respiratory medicine, due to its receptor specific immunomodulatory, anti-inflammatory role on macrophages and alveolar macrophages, which might be used to alleviate pulmonary inflammation or support its resolution.

ZUSAMMENFASSUNG

Die Lungen von Säugetieren haben sich ihrer Umwelt angepasst. Dabei haben sie die größte Oberfläche im menschlichen Körper entwickelt, die mit der Außenwelt in Kontakt ist. Unsere Lunge existiert dabei in innerer Homöostase trotz ständiger Exposition von tausenden exogener Chemikalien, Partikeln und Mikroorganismen in der Atemluft. Wie bereits für den Darm und die Haut beschrieben, lebt auch auf der Lungenepitheloberfläche eine hohe Diversität von Mikroorgansimen in Interaktion mit ihrem Wirt und ist damit ein Bindeglied zwischen unserer Lunge und der Außenwelt. Allerdings können Ungleichgewichte zwischen gutartigen und pathogenen Mikroben dieses komplexe biologische System zu akuten als auch chronischen Erkrankungen verändern. Durch empirische Untersuchungen wurde festgestellt, dass das humane Mikrobiom in seiner Diversität aktiv mit dem Immunsystem des Wirts interagiert.

Dieses Projekt hatte als Ziel, die Effekte von zwei bakteriellen Signalmolekülen auf die Entzündungsdynamik der Mäuselunge zu untersuchen. Dabei wurde auf folgende Funktionen fokussiert: die Differenzierung von T-Helfer-Zellen (T_h), die Differenzierung von Alveolarmakrophagen, und die Wundheilung während einer Entzündungsantwort. Einerseits waren es Quorum sensing-Signalstoffe vom *N*-Acyl-homoserinlacton (AHL)-Typ (w.z.B. 3-oxo-C_{12}-HSL) des Gram-negativen pathogenen Bakteriums *Pseudomonas aeruginosa* (PAO1-Stamm), sowie andererseits D-tryptophan (D-Trp), welches vom Gram-positiven probiotischen Bakterium *Lactobacillus casei* gebildet wird. Beiden werden potenziell therapeutische Wechselwirkungen mit dem Immunsystem des Wirts zugeschrieben.

Zunächst wurden die Effekte verschiedener AHL-Strukturen auf die Differenzierung von T-Helferzellen (T_h), besonders im Bezug auf die T_h17- und T_h2-Zelldifferenzierung, untersucht. 3-oxo-C_{12}-HSL induzierte eine erhöhte Interleukin 17 (IL-17) Produktion in T_h17 Zellen, während 3-oxo-C_4-HSL und C_{12}-HSL keine Stimulierung zeigten. Im Gegensatz konnte 3-oxo-C_{12}-HSL die Interleukin 4 (IL-4) Produktion der T_h2 Zellen nicht induzieren. IL-17, hauptsächlich produziert von T_h-

17 Zellen, ist ein entzündungsförderndes Zytokin, welches für die Zytokin-getriebene Anlockung von Immunzellen in Richtung der Entzündung verantwortlich ist. Auf der anderen Seite steht IL-4, welches von T_h2-Zellen produziert wird, und eine Schlüsselfunktion in der Regulation der adaptiven Immunantwort hat. IL-4 ist verantwortlich für die Rekrutierung von M2-Makrophagen, welche wiederum die Entzündung herunterregulieren und dabei zur Wundheilung beitragen. Zusammen zeigen die Ergebnisse für AHL, dass 3-oxo-C_{12}-HSL durch die erhöhte Stimulation der IL-17 Produktion zur Entzündungsreaktion beitragen kann.

Die primäre Immunantwort während einer bakteriellen Entzündung wird durch gewebespezifische alveolare Makrophagen (AM) ausgeführt. Um den Effekt von AHL auf AM zu untersuchen, wurden zunächst M0-naive AM (MH-S Zelllinie) durch Lipopolysaccharid (LPS) zu M1-Makrophagen (M1-AM) stimuliert und simultan mit AHLs behandelt (60 μM). Interessanterweise wurde die Expression und Sekretion der Zytokine Tumornekrose-Faktor α (TNFα) und IL-1β erhöht durch vor allem 3-oxo-C_{12}-HSL. Dies weist darauf hin, dass AHLs eine Rolle in der Verstärkung M1-AM Immunantwort spielen. Zusätzlich induzierte auch D-Trp eine gesteigerte TNFα Sekretion; dies deutet ebenfalls auf eine Rolle von D-Trp in der Verstärkung der entzündlichen Immunantwort durch M1-AM hin. Auf der anderen Seite induzierten sowohl 3-oxo-C12-HSL als auch D-Trp die alternative AM Polarisierung (M2-Polarisierung), welche durch die Expression der M2-Marker Arginase 1 (Arg1) und Mannose-Rezeptor C-Typ 1 (Mrc1) gekennzeichnet war. Diese Ergebnisse deuten darauf hin, dass die M2-Polarisierung durch AHL und D-Trp verstärkt wird und dass 3-oxo-C_{12}-HSL und D-Trp dadurch eventuell M2-abhängige Reparaturmechanismen während der Entzündungsauflösung vorantreiben.

Um den Einfluss auf Reparaturmechanismen zu untersuchen, wurde ein Ko-Kultursystem verwendet, welches aus alveolaren Typ-2 Zellen (AECII; LA-4 und MLE-12 Zelllinien) und AM (MH-S) bestand. Die Behandlung der Ko-Kultur aus AECII und AM mit AHL führte zur Reduktion von TNFα, IL1β und Nitric-Oxide Synthase 2 (Nos2), die als M1 Entzündungsmarker gelten. Zusätzlich wurde die Expression des M2-charakterisierenden Gens Arg1 erhöht. Auf der anderen Seite

blockierten sowohl 3-oxo-C_{12}-HSL als auch D-Trp, obwohl letzteres zu einem geringeren Grad, die *in vitro* Wundheilung der Epithelzellen. Diese Ergebnisse waren unabhängig von der Stimulation durch LPS. Des Weiteren wurde ein *in vivo* Modell für akute Lungenschädigung (ALI) etabliert, bei dem die Lungen von BALB/c Mäusen mit LPS behandelt wurden. Die Behandlung mit AHL (1200 μM, äquivalent zu einer starken lokalen PAO1 Infektion) konnte die Rekrutierung/Anzahl an polymorphonuklearen Neutrophilen (PMN) in den Atemwegen nicht reduzieren. Allerdings gelang dies durch Behandlung mit D-Trp. Es konnte gezeigt werden, dass die Behandlung mit D-Trp die Produktion des Chemokin (C-X-C motiv) Liganden 1 CXCL1 in der BAL reduzierte. Die Analyse der mRNA der gesamten Lunge ergab eine Reduktion des PMN-Markers CD11b. Diese Resultate unterstreichen die entzündungshemmende Wirkung von D-Trp in Lungenschädigungen.

D-Trp ist auch bekannt als Agonist des Aryl-Hydrocarbon-Rezeptors (AhR). Die Bindung von D-Trp an AhR führt zur Translokation von AhR in den Zellnukleus. Zahlreiche Mechanismen sind beschrieben, die nach Aktivierung von AhR initiiert werden. Darunter befindet sich das Enzym Indoleamine 2,3-Dioxygenase 1 (IDO1), welches D-Trp zu Kynurenine katabolisiert, sowie das Zytochrom P4501-1A (CYP1A1), welches in den xenobiotischen Metabolismus involviert ist. Expressionsanalysen in aus Knochenmark stammenden Makrophagen (BMDM) von $AhR^{+/-}$ und $AhR^{-/-}$ Mäusen (AhR^{tm1Bra}) zeigten, dass die Expression von IDO1 und CYP1A1 von D-Trp abhängig waren (100 μM) sowie von der Anwesenheit von AhR, nicht jedoch von der Anwesenheit von L-Trp. Um die Funktion von AhR in der Immunantwort der Lunge zu untersuchen, wurden die Expression von IL-6 und Arg1 in $AhR^{-/-}$ BMDM-Mäusen untersucht. Die zuvor gezeigte entzündungshemmende Wirkung von D-Trp war auch in den $AhR^{-/-}$ Zellen präsent. Die mRNA Expression von AhR wurde durch D-Trp verstärkt. Dies läßt eine von D-Trp oder dessen Metaboliten abhängige Rückkopplungsschleife vermuten. Die gesteigerte metabolische Aktivität von D-Trp ist konsistent mit der Regulation der Immunantwort durch Entzündungs-stimulierte AM. Daher trägt D-Trp potenziell zu einer verstärkten oder schnelleren Auflösung der Immunantwort bei.

Zusammenfassend konnte in dieser Arbeit gezeigt werden, dass nicht AHL, sondern eher D-Trp ein potentielles Therapeutikum in der Atemwegsmedizin werden könnte. Durch seine rezeptorspezifischen, immunmodulatorischen und entzündungshemmenden Funktionen in Makrophagen sowie auch in alveolaren Makrophagen könnte D-Trp zu einer Verminderung der Entzündung in der Lunge beitragen bzw. die Auflösung der Entzündung unterstützen.

INTRODUCTION

1. Breathing the world

1.1. The lung biology and function

Mammals and other air-breathing animals transport the oxygen of the air to their bloodstream and organs through the respiration of the lung. Healthy human individuals breathe around 10000 L of air per day. The carbon dioxide generated by the organisms is afterwards released from the bloodstream back to the atmosphere during the expiration. Several key anatomical elements are needed to operate the lung function and maintain its integrity. The lung carries out two main physiological tasks; conducting the airflow and performing the gas exchanges.

The upper respiratory tract (nose, pharynx and larynx and trachea), down to the bronchi and bronchioles subdivisions, guides the air to the lower respiratory tract (terminal bronchioles and alveoli). Exogenous particles are retained away from the alveolar sac, where the gas exchange takes place. Each subunit has a different role and carries a different set of specialized cells to fulfill its function. The lung alveolar duct combined with the alveoli consists of an extraordinary surface of approximately 75 m^2 [1]. 90% of the gas exchange occurs at the surface of the alveoli.

1.2. The microbes, friends and foes

The outside world is not only a vector of gases and food, but also the home of a high diversity of microorganisms. This study focuses on bacteria, which are ubiquitous on earth: from the soils to the oceans and the air. They are present everywhere and form complex communities adhering to surfaces in biofilm structures. More than 10000 species have been discovered, even though the actual diversity is postulated to be between 5 and 10 million [2]. Bacteria can be beneficial to higher organisms as well as harmful or even detrimental.

Different bacteria can be beneficial or harmful for humans. Bacteria are divided into two super families depending on the staining of their cell wall (Gram-staining): the

Gram-negative and the Gram-positive bacteria. On one hand, the Gram-positive bacteria (*i.e. Bacillus*, *Listeria*, *Staphylococcus*, *Lactobacillus*) have a thick peptidoglycan layer – containing also D-amino acids – coupled to a thin plasma membrane. In contrast, Gram-negative bacteria (*i.e. Escherichia coli*, *Pseudomonas aeruginosa*), have a more complex cell envelope consisting of a much thinner peptidoglycan layer coupled to a lipopolysaccharide (LPS) decorated outer membrane, separated by a periplasm from the plasma membrane (Figure 1).

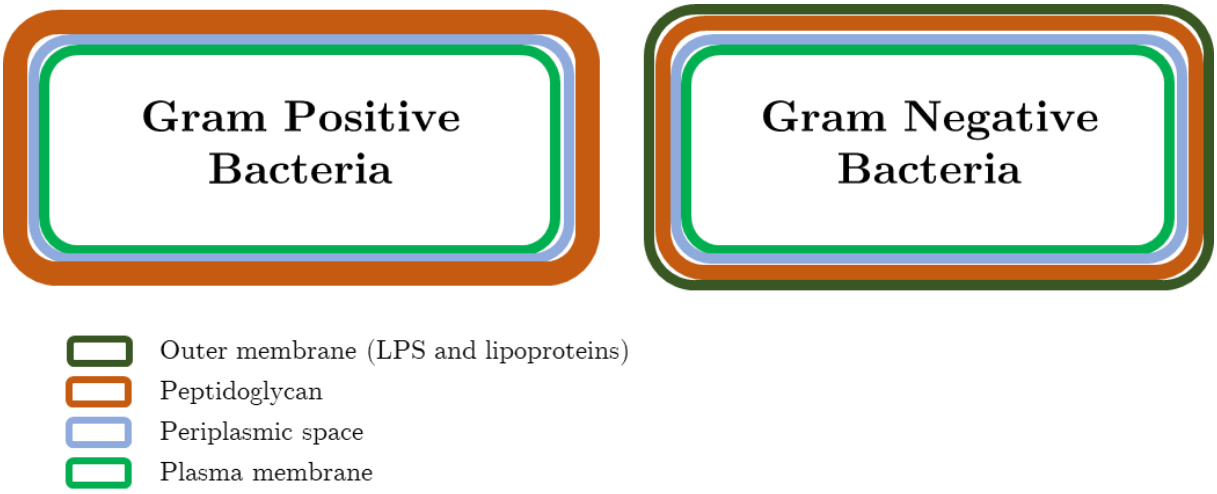

Figure 1. Gram-positive and -negative cell wall structure. The membrane structure allows the classification between these two super families.

2. The immunology of the lung

Bacteria and humans have evolved jointly to a unique symbiotic holobiont [3]. The skin and the gut microbiota act as a protecting living barrier for the eukaryotic organism against pathogenic microbes. However, the lung surface structures need to be cleared of microbial biofilms to allow an efficient gas exchange. Since the air contains aerosolized potentially harmful particles and microbes, the immune system must continuously undertake defense measures to keep the organisms' homeostasis. Therefore, humans possess complex immune responses, which can be divided into two categories: the innate and the adaptive immune system.

2.1. Innate response

The innate immune system consists of a variety of non-specific immune cells, constantly surveilling the body, ready to be activated within the first minutes after a tissue injury or a cell infection is detected [4]. This evolutionary defense mechanism relies on the recognition of pathogen-associated molecular patterns (PAMPs) or host-derived damage-associated molecular patterns (DAMPs) [5]. The recognition of these patterns will trigger a fast onset of inflammation, characterized by the recruitment of leucocyte through chemical mediators (cytokines), the activation of the complement cascade, and the identification of the pathogen leading to the antigen presentation by the antigen presenting cells (APCs). Most innate leukocytes are issued from the bone marrow [6], where after a process of maturation [7–9] they are released to the bloodstream [10]: the mast cells, the phagocytes (*i.e.* macrophages, neutrophils and dendritic cells), the natural killer cells and the basophils and eosinophils. In this study, the main focus is on the innate immune response of the lung resident macrophages, called alveolar macrophages (AMs).

The innate immune system is fast and efficient, however it is not designed to retain any information on the pathogens, nor provide long-lasting immunity to the host [11].

2.2. Adaptive/acquired response

The adaptive immunity is triggered after antigen presenting cells (APC) had contact with a given antigen. These highly specialized cells were generated during the last infection and will be reactivated in the aim of the pathogen containment of destruction. The lymphocyte B (LBs) and T (LTs) are the main effectors of this specific and acquired response. Like most lymphocytes after their generation, LTs and LBs circulate in the bloodstream in the search of an activated APC. Upon stimulation by the antigen, LTs and LBs will undergo a phase of maturation and replication. LTs will either become T helper (T_h), secreting cytokines to attract phagocytes, or T cytotoxic (T_c), tracking and killing infected cells. Activated B cells differentiate into plasma cells and will in turn produce pathogen specific antibodies,

directed to the source of the infection. After total removal of the pathogen causing the infection, the antigen pattern will be conserved as part of the immune memory. The speed of resolution is critical, since the continuation of homeostasis is the basis of the organism's healthy state. The lingering inflammation of an organ leads to scaring and remodeling, possibly impacting its functions. In this work, the focus is on the lung immune response and particularly of its epithelium; the lung's surface and vulnerable barrier to the outside world.

3. The lung epithelial barrier/epithelium

The lungs structure relies on a complex assembly of cells, forming a huge interface with the outside world (ca. 100 m^2 in humans). In this study, the importance is made not on the primary respiratory function of the lung parenchyma but on its ability to respond to the continuous flow of microbes (pathogens or saprophytes) reaching its surface. Among all the cell types present in the lung, four are lung specific: the AEC (Alveolar epithelial type I and II), the club cells and the ciliated bronchiolar cells (Figure 2). The lung consists of three distinct regions, populated by its own set of cells. From the trachea to the bronchus, the cells are predominantly ciliated cells – which motion sweeps mucus and dirt up out of the lungs – and goblet cells producing the protective mucus lining the organ. These cells allow the clearance of the lung from dust and pathogens above the size of 3 µm through its so-called mucociliary escalator [12]. Further down in the bronchioles, ciliated cells become scarcer and goblet cells are replaced by club cells, protecting the bronchiolar epithelium by its surfactant secretion. Finally, down in the alveoli, there is no mucus lining, nor ciliated cells. Small particles (< 3 µm) and pathogens have no mechanical way to be expectorated or eliminated and end up "sitting" in the alveoli, potentially harming the epithelium. As previously explained, the respiratory, alveolar surface consists of two types of pneumocytes. The AECI are the specialized cells responsible for the oxygen/carbon dioxide gas exchange considering its thickness, comprised between 0.2 and 2.5 µm, and covering 95-98% of the lung epithelium surface [13]. The AECII are more versatile and contribute to the secretion of pulmonary surfactant, reducing

surface tension as well as the replacement of AECI cells after cell damage. Inflammatory cytokine sensitivity and secretion from AECII also suggest that AECII contribute to the inflammatory response in the lung [14,15]. If the epithelium is not able to fully fulfill its barrier role, lung inflammation is the consequence.

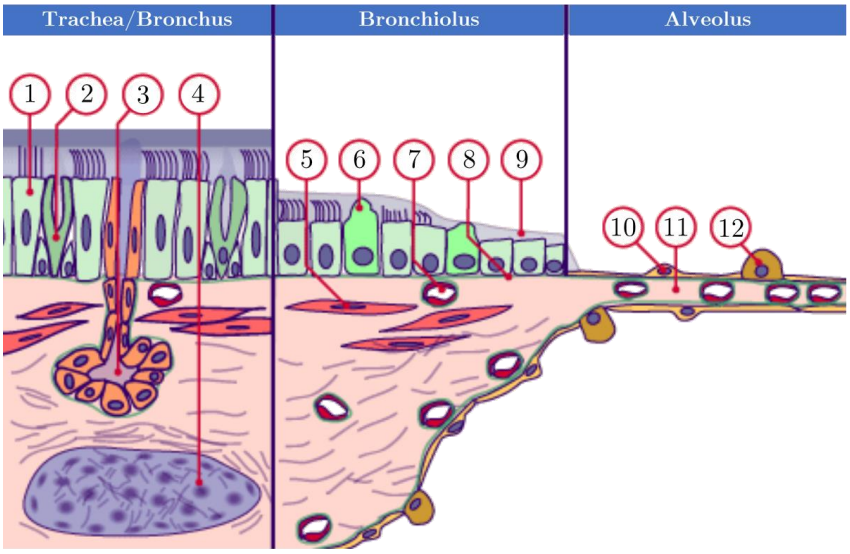

1. Ciliated cell
2. Goblet cell
3. Gland
4. Cartilage
5. Smooth muscle cell
6. Club cell
7. Capillary
8. Basal membrane
9. Surfactant
10. Alveolar epithelial cell type 1
11. Alveolar septum
12. Alveolar epithelial cell type 2

Figure 2. Overview of the pulmonary airways. The airways harbor various cell types, helping the lung clearance at all levels. Adapted from [16].

4. Macrophages development and origin

Monocytes are blood circulating leukocytes until their recruitment to a tissue and their differentiation into macrophages. In vertebrates, they are issued and generated continuously during the whole lifetime by bone marrow stem cells [17,18]. As previously explained, the macrophages play a critical role in the host defense systems. Chemotaxis will guide the monocyte precursors to the site of damage, where they will be differentiated into specialized macrophages depending to the targeted organ. The macrophages will undergo a final polarization, following a specific pathway, subdividing them into two different populations: M1 (classical) or M2 (alternative) macrophages (Figure 3).

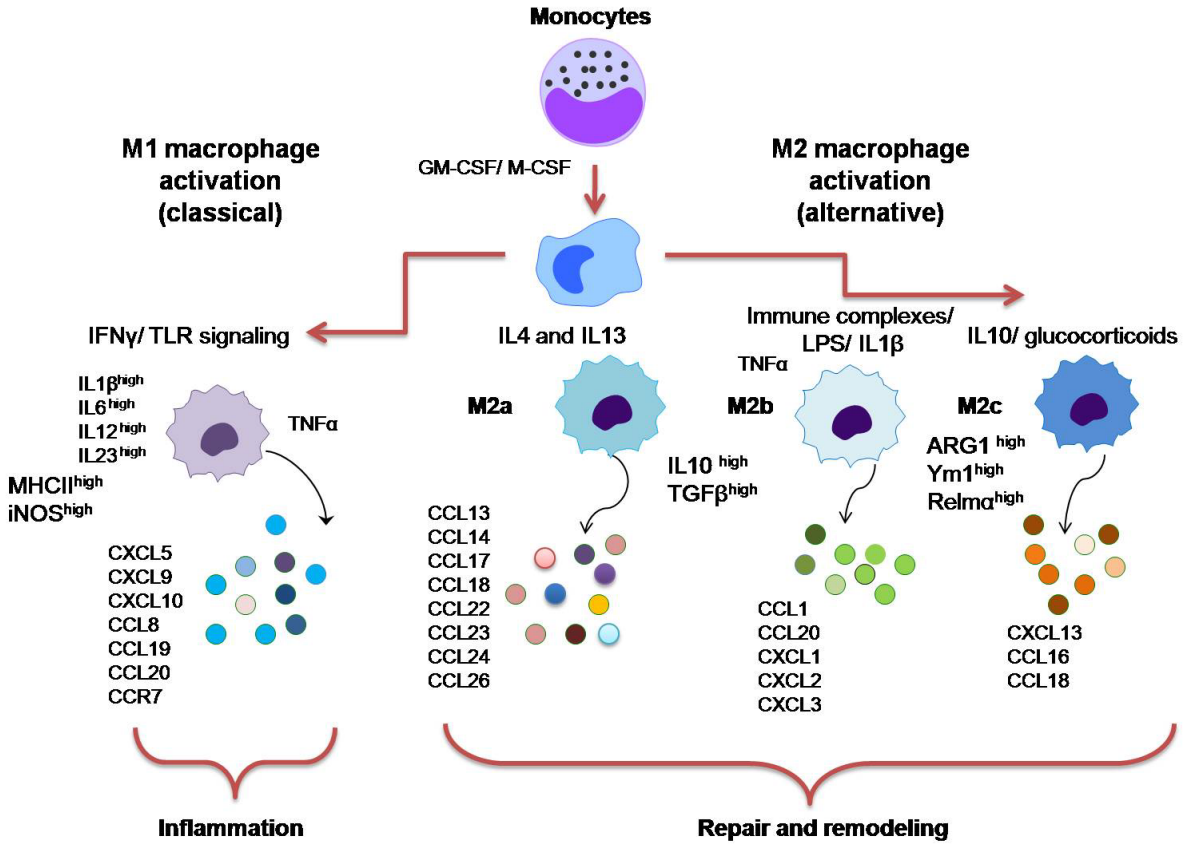

Figure 3. Schematic representation of M1 (classical) and M2 (alternative) macrophage polarization [19]. After activation and polarization, the AM will support either inflammation or repair and remodeling.

4.1. Macrophages polarization and functions

4.1.1. M1: The classical activation

Blood monocytes can be activated by macrophage colony stimulating factors (M-CSF) to induce their differentiation in mature macrophages [20]. The differentiation of macrophages encompasses a spectrum of regulated genes. Macrophages are heterogeneous and possess particular plastic cellular phenotypes, finally allowing them to adopt their functionality to the respective surrounding environment. With respect to the activation state of macrophages, the ("classical") M1 polarization describes AM involved in antimicrobial function [21–23]. As a phagocyte, its role will be mainly to recognize, engulf and digest pathogens, dead and dying cells (Figure 4). This function is part of the innate immune system, meaning it is non-selective, and fast working. Indeed, the first macrophages are recruited on the inflammation site in a matter of minutes. The M1 macrophages will produce high levels of T_h1 chemoattractant IFNγ, reinforced by its own feedback loop, involving the master cytokine TNFα, IL-6 and IL-12. Generally, LPS sensing through Toll-Like Receptor 4 (TLR4) results in this inflammatory cascade, where enhanced phagocytosis, nitric oxide synthase (NOS2) and interleukin 1 β (IL-1β) secretion lead to further macrophage and neutrophil recruitment. The M1 macrophages are also antigen presenting cells and help creating the bridge between innate and adaptive immunity; the display of the antigen on the membrane will activate Th cell which in turn will activate B cells, allowing selective target of the antigen by antibodies. Here, a variety of intracellular and extracellular markers are considered (inflammatory chemokines) as well as surface markers to characterize the AM polarization through several stimuli.

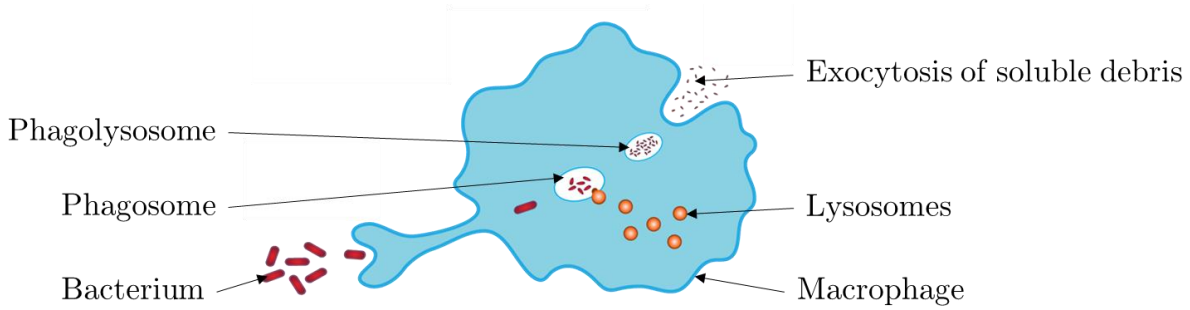

Figure 4. Overview of the phagocytosis. Bacterium are engulfed and digested by the macrophage via phagocytosis. Remains of the bacterium are excreted and/or presented at the surface of the macrophage. Adapted from [24].

4.1.2. M2(a-b-c): The alternative activation

At the cornerstone of immunity, macrophages are extremely versatile and dynamic in their pathogen responses. In the same way, M1 macrophages are polarized within the T_h1 response. M2 macrophages (or alternatively activated macrophages) participate in the resolution of the inflammation [23,25], where they are involved in wound healing, repair and remodeling, when the organism returns to its homeostasis. They fundamentally work to reestablish homeostasis [26] by secreting anti-inflammatory cytokines (*i.e.* IL-10) and clearing the tissues from apoptotic neutrophils. M2 macrophages are themselves subdivided in three subtypes [27]; M2a (IL-4 and/or IL-13 stimulated macrophages), M2b (immune complexes, LPS and IL-1β activated) or M2c (IL-10, transforming growth factor β (TGF-β) or glucocorticoid activated) (Figure 3) [7,28]. Like M1 macrophages, M2 macrophages polarization is associated with distinctive gene signatures.

M2a macrophages are activated by IL-4/13, mainly produced by T_h2 cells. Following IL-4/13 binding, a downregulation of pro-inflammatory mediators (IL-6, IL-8, and IL-12) is observed, in addition to an upregulation of C-type membrane lectins (*i.e.* MRC1), and scavenger receptors (LDL oxidation), which in turn activate Arginase 1 production, effectively blocking NOS2 expression.

M2b cells, activated by opsonized complexes (Fc antibody receptor binding) and LPS/IL-1β through TLR4 signaling, not unlike M1 macrophages. They are

characterized by high IL-10 and low IL-12 production. However, M2b produce also a significant number of inflammatory cytokines such as TNFα, IL-1β and IL-6.

M2c comprise cells stimulated with IL-10, TGF-β, or glucocorticoids, this subtype is often referred to as deactivated or anti-inflammatory helps to decrease further the inflammation and improve tissue repair and remodeling by producing large amounts of IL-10 and TGF-β. During the inflammation resolution phase, a nuclear hormone, the "Peroxisome Proliferator Activated Receptors γ" (PPARγ) plays a key role in numerous immune cells, including macrophages, lymphocytes, and dendritic cells [29] by inhibiting inflammatory signaling through NF-κB, favoring the alternative polarization of macrophages.

4.2. Alveolar macrophages: Guardians of the lung homeostasis

Macrophages are specialized hematopoietic cells, and, in the lung, the AM represent more than 95% of the resident leukocytes in the alveoli of a healthy human individual. They migrate shortly after birth to the lungs and originate from fetal monocytes [30] after GM-CSF differentiation [31]. It is understood that they are not recruited from circulating monocytes like most tissue macrophages, generated from a common bone marrow progenitor [32]. The AM reside on the lung epithelium at the interface between the environment and the host [33,34]. Thus the AM are in the lung frontline during bacterial infections and the first responders during inflammation [35]. The AM participate in several key functions allowing the lung homeostasis, such as phagocytosis of pathogens, clearance of apoptotic and necrotic cells; repair and remodeling during the resolution phase of the inflammation; and T_h cells response promotion [36]. Macrophages polarize into different subtypes depending on the stimulus and the response needed [37], each subtype being specialized in a distinct response function. Naive (or unpolarized) AM are recognized by distinctive markers on their surface, making them distinguishable from interstitial macrophages or other resident macrophages [34,38]. The markers CD11c, CD11b, SIGLEC-F or MRC1 are expressed on the AM at different levels during inflammation or quiescence of the lung [34,39] and can be used to discriminate the mouse pulmonary macrophages.

5. T_h cells: role and differentiation

T helper (T_h) $CD4^+$ cells play an important role in the adaptive immune system. They help the other lymphocyte to increase or decrease their activity during the different phases of the immune response. Through their cytokine secretion, they regulate B cells maturation, cytotoxic T cells activation and macrophages phagocytosis. T cells acquire maturity in the thymus, prior to migrating to the body. Naive T cells are presenting their first antigen during an immune response by a professional APC. Following this encounter, and after a two steps verification, T cells differentiate into one of many different subsets. During this study, the focus was on

two T_h cells "couples": the first discovered T_h1/T_h2 subset [40] as well as the T_h17/Regulatory T cells (T_{regs}) subset more recently highlighted [41]. The return to homeostasis after an immune response is guaranteed by regulation of the balance between the pro-inflammatory and anti-inflammatory T cells.

5.1. T_h1/T_h2 paradigm

The T_h1/T_h2 paradigm is used to explain the complementary roles of these cells. T_h1 cells are triggered and efficient in the event of a replication of intracellular pathogens, whereas T_h2 are specified against parasites and help tissue repair. Upon antigen presentation, the autocrine IL-12 secretion, which is reinforced by an auto feedback loop, leads to the differentiation of T_h0 cells into T_h1 or T_h2, whether a cellular or humoral response is needed. T_h1 cell's effector cytokines are interferon gamma (IFNγ) and IL-2, controlled by their key respective transcription factors T-bet and "Signal Transducer and Activator of Transcription 4" (STAT4) [42]. IFNγ is used by T_h1 cells to activate macrophages' phagocytosis, and digestion and to kill intracellular pathogens through NOx radical production [43].

On the other hand, T_h2 cells are triggered by IL-4 and IL-2 through STAT6 and GATA3 transcription factors signaling [44]. T_h2 will then secrete a variety of cytokines (IL-4, IL-5, IL-9, IL-10, IL-13 and IL-25). IL-4 will increase T_h2 differentiation due to its positive feedback loop, stimulating in turn B cells and IgE production. IL-10 secretion will reduce IL-2 and IFNγ production in other T_h cells.

5.2. T_h17/T_{regs} paradigm

The T_h1/T_h2 paradigm, first proposed by Mosmann and Coffman [45], opened the door to modern immunology. However, this model was incomplete [46]. Other T cells are also responsible for the regulation of the immune system; T_h17 and T_{regs} are issued from a developmentally distinct lineage from $T_h1/2$ cells. T_h17 cells are associated with pathogens clearance as part of the adaptive immune system. Their phenotype is acquired after IL-23 stimulation and characterized by their IL-17 cytokine production. This protein is notably involved in many inflammatory

responses. However, uncontrolled or persistent immune responses are difficult issues for the organism, causing inflammatory or autoimmune diseases. Regulatory T cells (T_{regs}) tackle this by being a crucial mediator in controlling immunity and self-tolerance. T_{regs} function is regulated by the transcription factor Foxp3 [47,48] leading to the suppression of T cell proliferation, and the inactivation of dendritic cells (DCs) [49,50].

The immune response is tightly regulated with positive and negative feedback loops, allowing a tailored reaction by the organism before and long after an injury.

6. Lung injury and inflammation

The inflammation is one of the first biological manifestation of the innate immune system when subjected to an injury or an infection. It includes, as described previously, an activation of complement, as well as a leucocyte recruitment and the antigen presentation from the professional APCs.

Two types of injuries are generally described; acute and chronic. Together they cover the inflammation spectrum. Chronic Obstructive Pulmonary Disease (COPD), asthma and Idiopathic Pulmonary Fibrosis (IPF) are part of the chronic lung diseases. A bacterial infection, or a contact with pollutants initiate an acute response in the form of an inflammation. The consequences of "Acute Lung Injury" (ALI) will be further discussed here. The speed of the organism's response is the key, relying mostly on innate immunity reactions. One prominent pro-inflammatory signaling pathway is for example the nuclear factor kappa-light-chain-enhancer of activated B cells (NF-ϰB) cascade, which is known to be triggered by the activation of LPS/TLR4 and/or IFNγ receptors. Subsequently, this leads to the production and expression of pro-inflammatory cytokines such as TNFα, IL-1β, IL-6 and IL-12. After phosphorylation and translocation of the transcription factor subunits, the following nucleus transfer will induce DNA binding and the expression of M1 macrophages' "signature genes" Nos2 and Tnf (Figure 3).

After the inflammation response, different actors restore the homeostasis. IL-4 and IL-13 are binding on their receptors at M2 macrophages, which leads to the

expression of M2 "signature genes", such as Arg1 and Mrc1 downstream of the JAK/STAT-6 axis (Figure 3 and Figure 5).

During this whole study, the inflammation was triggered solely by LPS, a well described model of acute inflammation [51,52]. It allowed a fast onset, typically within half an hour and a fast resolution within 48-72h during *in vitro* as well as *in vivo* experiments.

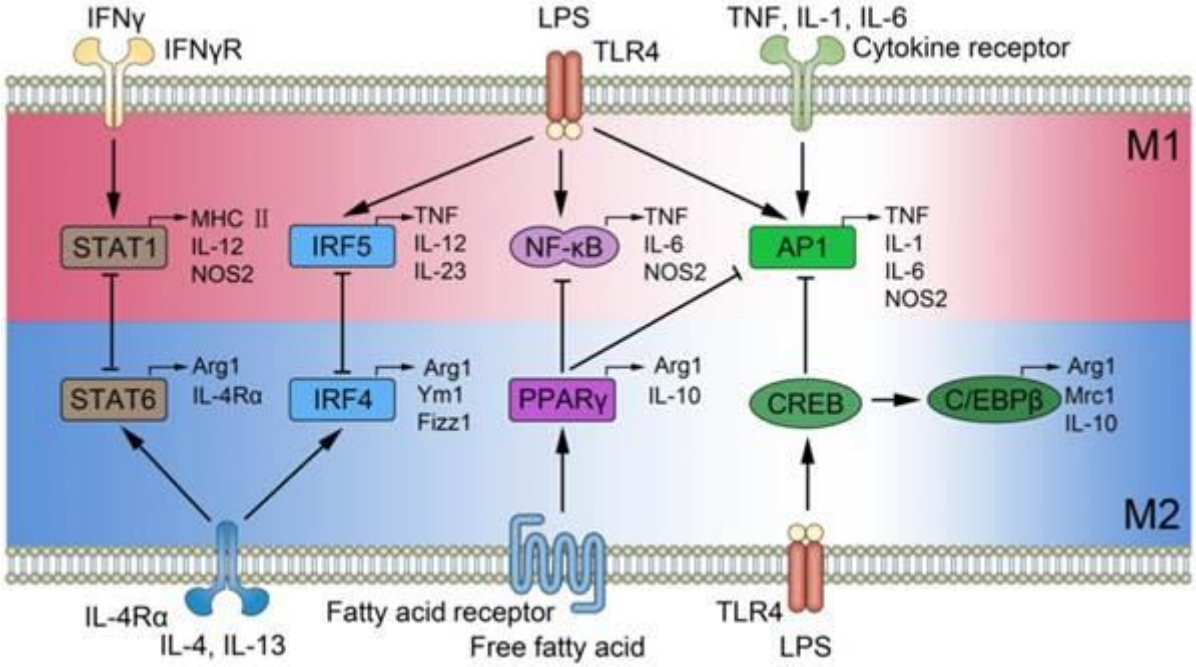

Figure 5. Signaling pathways of macrophage polarization [53]. Illustration of M1 and M2 signaling pathways interconnection, showing both the initiation and the resolution of an inflammation.

NOS2: Nitric oxide synthase 2 (NOS2) catalyzes L-arginine to produce nitric oxide (NO). NO is one of the major resources of oxidative stress.

Signal transducer and activator of transcription 1 (STAT1), Interferon regulatory factor 5 (IRF5), Nuclear factor kappa-light-chain-enhancer of activated B cells (NF-κB), and Activator protein 1 (AP-1), are transcription factors playing keys roles in many gene expressions that cause survival of the cell, viability or pathogen response. They are the central regulators of the inflammatory response.

Signal transducer and activator of transcription 6 (STAT6), Interferon regulatory factor 4 (IRF4), Peroxisome proliferator-activated receptor gamma (PPARγ), and cAMP response element-binding protein (CREB) are transcription factors involved in the regulation of many pathologic features of inflammatory responses. They include the promotion of the proliferation, survival, and regulation of T and B lymphocytes as well as specific anti-inflammatory cytokine mediated expression.

7. The Aryl hydrocarbon Receptor (AhR) and the immune system

The "Aryl hydrocarbon Receptor" (AhR), previously known as the dioxin receptor, is a ligand activated transcription factor involved in the adaptive response. It binds to a variety of ligands, its pocket fitting environmental xenobiotics (pollutants), possessing polycyclic aromatic hydrocarbon or halogenated aromatic hydrocarbon structures [54].

The immunomodulatory AhR function is versatile and depends highly on the ligand interacting with it. Duarte et al. [55] previously showed that the binding of 2,3,7,8-tetrachlorodibenzo-p-dioxin (TCDD) reduced IL-17 production by the inhibited differentiation of T_h17 cells. Other agonists, such as antiallergic drugs, have been shown to influence T_h1/T_h2 balance through AhR signaling [56].

It is now well established that the host-microbiome mutualism is a key to the organism's overall fitness [57]. This project is focused on the crosstalk effect of bacterial molecules with the immune system during homeostasis and inflammation. The immunomodulatory role of the T_h1/T_h2 and T_h17/T_{regs} balances as well as their roles in wound healing [58] was studied to get insights into possible modulations of underlying mechanisms by bacterial signaling compounds.

8. The lung microbiome

Ambient air does not only carry oxygen to the body but also particles and pollutants as well as microbes. The smaller the exogenous body, the deeper it penetrates into the lung. Given the great amount of air inhaled, the cumulated concentration of the substances in the lung is not negligible and is suggested to worsen pulmonary functions, which in turn could influence other organs systemically.

Surprisingly, the lung, as one of the gate keepers of immunity, and the interaction with its microbiome have been rather poorly studied. The current microbiome research focuses more *e.g.* on the gastro-intestinal tract, the skin, the urogenital system and the upper pulmonary system. However, recent publications have been showing the important role played by microbes (bacteria, fungi, viruses and phages)

on the dynamics of lung diseases (*i.e.* asthma [59], transplantations [60], cystic fibrosis [61]) as well as in the homeostasis of healthy individuals. The lung microbiome is unique to the individual; it is diverse, and varies over time [62,63]. It consists mostly in *Proteobacteria*, *Firmicutes*, *Bacteroidetes*, and *Actinobacteria* in healthy individuals [64]. However, the dual role played by these commensal bacteria and their interaction with the host immune system remains poorly understood. A potential therapeutic effect of probiotic bacteria and their signaling molecules was hypothesized and already partly uncovered for immune diseases including chronic and acute lung diseases [63–68].

Within the biofilms formed by bacteria, cellular communication networks are created. The molecules involved are either N-Acyl homoserine lactones of Gram-negative bacteria, and *e.g.* D-amino acids of Gram-positive bacteria. The cross talk between pathogenic bacteria and the immune system via the epithelium appeared to be critical for patients with lung diseases [69], where quorum sensing molecules such as the 3-oxo-C_{12}-HSL autoinducer seem to be key players in the severity of the disease by modulating various immune responses. On the other hand, the role of D-tryptophan of probiotic *Lactobacilli* in beneficial interactions is just getting started to be understood [67].

8.1. *Pseudomonas aeruginosa* and the quorum sensing compounds N-Acyl homoserine lactones

Pseudomonas aeruginosa is a Gram-negative opportunistic pathogen, well known to worsen lung function and mortality in patients with cystic fibrosis [69]. In addition, it is also recognized as a relevant pathogen during acute exacerbations of "Chronic Obstructive Pulmonary Disease" (COPD). Its pathogenicity is controlled through the production of quorum sensing molecules [70] such as the "N-Acyl homoserine lactones" (AHL), which control transcription of specific virulence genes. The quorum sensing (QS) is the auto-regulation phenomenon [71] used by bacteria to enable self and neighbor communication. The expression of the *Pseudomonas aeruginosa* 3-oxo-

C_{12}-HSL autoinducer is controlled through two [transcriptional regulation protein/autoinducer enzyme] couples: [RhlR/RhlI] and [LasR/LasI] [72,73]. The AHL-signaling compounds were shown to directly interfere with the host's immune responses [74–76].

Understanding the crosstalk of AHL signal molecules with barrier organs and the immune system could enable the development of immune modulatory strategies [77] for treatment of inflammatory lung diseases [78].

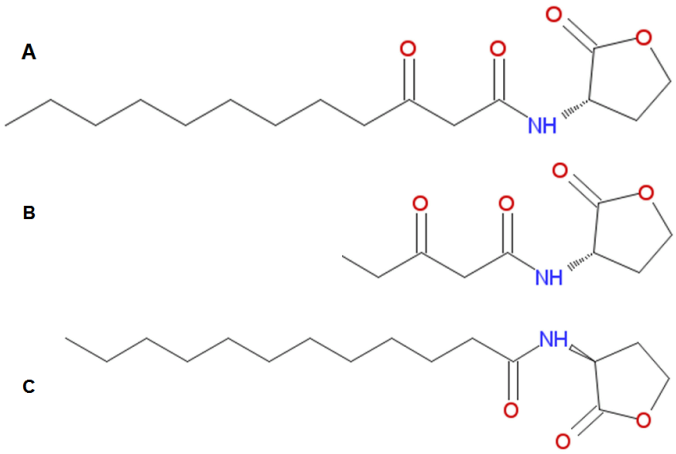

Figure 6. N-Acyl homoserine lactones. (A) 3-oxo-C_{12}-HSL, found in *e.g. Pseudomonas aeruginosa*, *Pseudomonas putida*, *Yersinia enterocolitica* **(B) 3-oxo-C_4-HSL,** synthetic AHL possessing the 3-oxo moiety and a short alkyl chain **(C) C_{12}-HSL**, found in the *Acidithiobacillus ferrooxidans, Sinorhizobium meliloti*, do not possess the 3-oxo moiety.

Early studies have linked the 3-oxo-C_{12}-HSL auto-inducer to cell apoptosis and cytotoxicity. Shiner et al. [79] showed that 3-oxo-C_{12}-HSL (100 µM) induced apoptosis in murine fibroblasts, and in human mesenchymal stem cells [80]. Tateda et al. described the cytotoxicity of 3-oxo-C_{12}-HSL towards murine bone-marine derived macrophages, neutrophils and monocytic cell lines [81]. Furthermore, Vikström et al. indicated that the 3-oxo-C_{12}-HSL triggered the alteration of junction protein causing a disruption in epithelial barrier function and integrity [82,83].

Since more than ten years, the immunomodulatory effects of quorum sensing have been studied. Cytokine signaling can be altered by 3-oxo-C_{12}-HSL. Smith et al. [84] discovered that 3-oxo-C_{12}-HSL increased both IL-8 production and expression in in human epithelial and fibroblast cells, whereas IL-2 secretion was inhibited [74].

Recruitment of immune cells (such as neutrophils and macrophages) and growth of cell population are also affected by 3-oxo-C_{12}-HSL treatment [85,86]. T cell proliferation [74] and T_h1/T_h2 cells differentiation were inhibited with a 3-oxo-C_{12}-HSL concentration as low as 18 μM [87]. These results extend the findings of Zimmermann et al. [75,88], describing an increased chemotaxis and phagocytosis of neutrophils after 3-oxo-C_{12}-HSL treatment. Kravchenko et al. explained the macrophages immunomodulation by the disruption of an TLR-independent NF-κB signaling [89,90]. This effect may be related to the ability of 3-oxo-C_{12}-HSL to function as a PPARγ agonist [76,91]. However, the immune mechanisms involved after 3-oxo-C_{12}-HSL exposition as well as the target receptor within host cells are not yet fully resolved. However, evidence from Maurer et al. recently suggested that 3-oxo-C_{12}-HSL activates the expression of the surface receptor T2R38 [92].

In this study, 3-oxo-C_4-HSL and C_{12}-HSL act as controls for 3-oxo-C_{12}-HSL which is immunologically active. They mimic the 3-oxo moiety and the alkyl chain length of the 3-oxo-C_{12}-HSL, while both possessing the lactone ring (Figure 6). Indeed, it is speculated that only the combination of the oxo moiety with the lactone ring enables an immunomodulatory function. The three lactones are degraded into biologically inactive opened ring structure at neutral pH or slightly alkaline solution, with a half-life of approximately 10 hours [78]. In plants having only an innate immune system, AHLs interfere with several biological systems, inhibiting or promoting root growth, as well as priming resistance against pathogens [93,94].

8.2. The inflammatory response triggered by microbes

Gram-negative bacteria's outer cell wall contains to an important part LPS, phospholipids and proteins. The endotoxin LPS is one of the most described "Pathogen Associated Molecular Pattern" (PAMP): it activates several "Antigen Presenting Cells" APCs such as monocytes, macrophages, DCs and B cells, and is predominantly responsible for the inflammatory response during bacterial infection [95]. In mammals, pathogens are first recognized by the innate immune system through several mechanisms including specific recognition and signal transduction,

followed by the adaptive immune system. The classical pathways include different strategies used to fight back infection and restore homeostasis. “Toll-Like Receptors” (TLRs) are the most studied classes of “Pattern Recognition Receptors” (PRRs); they possess a ligand binding domain able to recognize a variety of pathogens, such as bacteria, fungi or viruses. 10 subtypes or TLRs have been described, each specializing in a type of PAMPs [5]. The “Retinoid Acid-Inducible Gene I (RIG-I)-Like Receptors” (RLRs) and “Nucleotide-Binding Oligomerization Domain (NOD)-Like Receptors” (NLRs) are PRRs involved in the intracellular immune activation and the recognition of foreign nucleotides. The activation of the PRRs drives the NF- κB dependent inflammatory cascade, leading to production and release of the pro-inflammatory master cytokines tumor necrosis factor alpha (TNFα), and interleukin 1 beta (IL-1ß) from the cell, effectively inducing neutrophil maturation and chemotaxis.

The *Pseudomonas aeruginosa* 3-oxo-C_{12}-HSL autoinducer has been shown among other effects to accelerate apoptosis in macrophages and neutrophils [81] and inhibit DNA binding to the PPARγ. These interferences of the immune responses result from the upstream activation of T2R38 receptor and inhibition of NF-κB pathways [96].

8.3. *Lactobacillus casei* and D-tryptophan

Kepert et al. [67], analyzed immunomodulatory effects on dendritic cell maturation in the supernatant of probiotic Gram-positive *Lactobacillus* spp., *Lactobacillus rhamnosus GG* and *Lactobacillus casei W56* shared the secretion of the unusual amino acid D-tryptophan (D-Trp). After purification, MS- and NMR-confirmation analysis, D-Trp was confirmed as newly identified immunomodulatory probiotic substance [67].

Both L-tryptophan (Figure 7) and D-tryptophan (D-Trp) are amino acids of bacterial/fungal origin secreted by several probiotic bacterial strains [67]. Catabolizing enzymes (*e.g.* indoleamine-2,3-dioxygenase - IDO) participating in Trp degradation, are found in cells of the immune system. It is not clear yet, which role D/L-Trp metabolites play in detail [66,97]. However, evidence are in favor of either a suppressing effect of T-cell proliferation by these metabolites, or of a more general

suppression of immune cells through pro-apoptotic mechanisms [97]. Interestingly, it was discovered that the IDO enzyme catabolizes L-Trp as well as D-Trp [98].

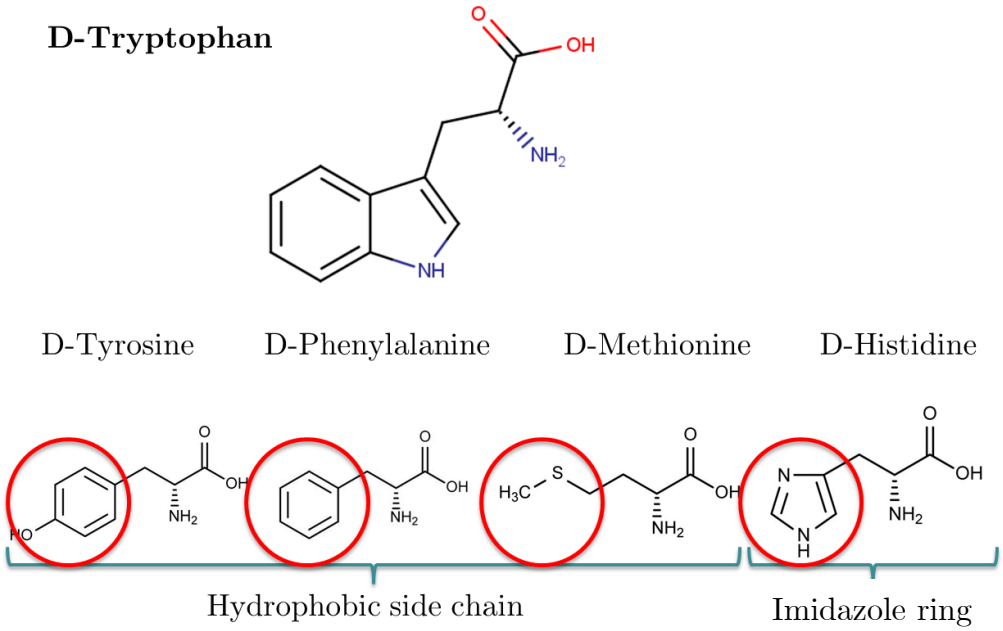

Figure 7. D-tryptophan structure and similarities to other D-amino acids.

9. Project outline and hypotheses

In this project, the two aspects of the immunity were treated:

- innate immunity by the study of macrophages activation upon AHL treatment
- adaptive immunity and the differentiation of $T_h2/17$, considering their relevance in asthma [99].

Specific AM polarization, upon *e.g.* AHL and D-Trp application, could play a key role in the epithelium defense and homeostasis [100,101]. D-Trp could induce immune tolerance, possibly driving similar modulatory effects compared to AHL [97,102,103], although the structures differ considerably.

There is overwhelming evidence for the importance of the crosstalk between microbiome and its host. From the plants to the mammals, these important relations have been unevenly studied. Indeed, the mutualism of microbes with human cells in

the gut is well described. However, the lung microbiome in its interaction with alveolar immunity remains greatly unexplored.

This study investigated, how two types of molecules, AHL and D-tryptophan produced from Gram-negative and Gram-positive bacteria, respectively, interact with the lung structure, integrity, and immunology. T_h17/T_h2 differentiation, AM polarization, responses in wound healing, *in vitro* and *in vivo* acute lung injury, and the associated response pathways were examined in the alveolar compartment.

MATERIALS AND METHODS

1. Materials

1.1. Mice

The mice used for the study on the AHL effects on T_h cells (wild type Balb/c genetic background) were kept and bred at the Institut für Molekulare Immunologie (IMI), Helmholtz Zentrum München.

The mice used in the ALI *in vivo* studies were wild-type C57BL/6J genetic background and were imported from Charles River Laboratories, and then kept at the institute of Lung Biology and Disease (iLBD), Helmholtz Zentrum München, Neuherberg, according to the national and institutional guidelines. Mice were female and aged from 8 to 16 weeks. After sacrifice, BALF, BAL cells, spleen and lungs were snap frozen and stored.

$AhR^{-/-}$ and $AhR^{-/+}$ (C57BL/6 Ahr^{tm1Bra}) mice were bred and kept under the supervision of the Dr. Ohnmacht in the Center of Allergy and Environment (ZAUM), Helmholtz Zentrum München, Neuherberg. The mice used were mixed males and females aged from 25 to 30 weeks.

1.2. Kits

Name	Company
LightCycler® 480 SYBR Green I Master (2X conc.)	Life Science
Superscript™ II Reverse Transcriptase kit	Invitrogen
Duo set ELISA kit (CXCL1, TNFα, IL-1β, CXCL5, GM-CSF)	R&D Systems
RNeasy Mini Kit	Qiagen
Giemsa and May Grünwald solutions kit	Sigma-Aldrich
RNaseOUT™ Recombinant Ribonuclease Inhibitor	Invitrogen

dNTP Mix (10 mM each)	Fermentas

1.3. Chemicals

Name	Company
3-oxo-dodecanoyle homoserine lactone	Sigma-Aldrich
3-oxo-butanoyle homoserine lactone	University of Nottingham
Dodecanoyle homoserine lactone	University of Nottingham
D-F, D-H, D-M, D-P, D-Y, D-W, L-W	Sigma-Aldrich
Acetonitrile	Sigma-Aldrich
Rosiglitazone	Sigma-Aldrich
Probenecid	Sigma-Aldrich
Dimethyl sulfoxide	Sigma-Aldrich
Entellan® mounting medium	Merck Millipore

1.4. Recombinant proteins and antibodies

Name	Company
Recombinant murine IFNγ	Immunotools
Recombinant murine IL-4 IL-2, IL-6, IL-13, IL-23	Immunotools
Lipopolysaccharides (LPS) from *E. coli*	Sigma-Aldrich
Anti-mouse CD3	BD Bioscience
Anti-mouse CD28	BD Bioscience
Anti-mouse IFNγ	BD Bioscience
Mouse TGFβ	BD Bioscience

1.5. Buffers and solutions

Buffer/Solution	Concentration	Chemical
Wash buffer (PBS-T)	1X 0.05%	PBS Tween 20
PBS buffer (10X)	137 mM 2.7 mM 10 mM 2 mM	NaCl KCl Na_2HPO_4 KH_2PO_4
TBE buffer (10X)	890 mM 890 mM 20 mM	Tris base Boric acid EDTA (pH=8.0)
MH-S medium	1X 10% 1% 2 mM 50 μM	RPMI-1640 medium FBS Penicillin/streptomycin Glutamine β-mercaptoethanol
LA-4 medium	1X 15% 1% 2 mM 1%	HAM-12 medium FBS Penicillin/streptomycin Glutamine Non-essential amino acids
MLE-12 medium	1X 10% 1% 2 mM	RPMI-1640 medium FBS Penicillin/streptomycin Glutamine
FACS Buffer	1X 1%	PBS BSA

RIPA buffer (1X)	20 mM 150 mM 1 mM 1 mM 1% 1% 2.5 mM 1 mM 1 mM 1μg/mL	Tris-HCl (pH 7.5) NaCl Na_2EDTA EGTA NP-40 sodium deoxycholate sodium pyrophosphate β-glycerophosphate Na_3VO_4 Leupeptin
loading buffer (2X)	100 mM 4% 0.2% 20%	Tris pH=6.8 SDS Bromophenol blue Glycerin
Electrophoresis (5X running buffer)	15.1 g 94 g 50 mL	Tris Glycin 10% SDS
Transfer buffer(1X)	3.02 g 14.4 g 200 mL	Tris pH=8.5 H_2O Methanol
10% PAGE (4 gels) Resolving	15.9 mL 13.3 mL 10.0 mL 400 μL 400 μL 16 μL	H_2O 30% Acrylamid 1.5 M Tris pH=8.8 10% SDS#10% APS TEMED

10% PAGE (4 gels) Stacking	13.6 mL 3.4 mL 2.5 mL 200 µL 200 µL 20 µL	H_2O 30% Acrylamid 1 M Tris pH=6.8 10% SDS 10%APS TEMED
Block buffer (ELISA)	1 g 100 mL	BSA 1X PBS
Stop solution (ELISA)	0.2 M	H_2SO_4
RT-PCR Mix	0.1 M 10 mM 1 µL 0.01 mM	RNase free H2O 5x First Strand Buffer 10x DTT 20x 4dNTPmix RNAse inhibitor 40 U/µL Superscript II RT 200 U/µL Random Nonamers

1.6. Primer sequences

Target gene	Acc. No.	Forward primer (5'-3')	Reverse primer (5'-3')
Actb	NM_007393	TCCATCATGAAGTGTGACGT	GAGCAATGATCTTGATCTTCAT
Arg1	NM_007482	GGAACCCAGAGAGAGCATGA	TTTTTCCAGCAGACCAGCTT
Ccl17	NM_011332	TTGTGTTCGCCTGTAGTGCATA	CAGGAAGTTGGTGAGCTGGTAA
Il6	NM_031168	GCCAGAGTCCTTCAGAGAG	AGACTCTCTCCCTTCTGAGC
Il1b	NM_008361	CAACCAACAAGTGATATTCTCCATG	GATCCACACTCTCCAGCTGCA
Il12b	NM_008352	GGAAGCACGGCAGCAGAATA	AACTTGAGGGAGAAGTAGGAAGG

Irf4	NM_013674	AAAGGCAAGTTCCGAGAAGGG	CTCGACCAATTCCTCAAAGTCA
Irf5	NM_012057	GCCACCTCAGCCGTACAAG	CTCCCAGAACGTAATCATCAGG
Mrc1	NM_008625	CATGAGGCTTCTCCTGCTTCT	TTGCCGTCTGAACTGAGATGG
Nfkb1	NM_008689.2	AGGAAGAAAATGGCGGAGTT	GCATAAGCTTCTGGCGTTTC
Nos2	NM_010927	CCTGTGAGACCTTTGATG	CCTATATTGCTGTGGCTC
Rela	NM_009045	CTTGGCAACAGCACAGACC	GAGAAGTCCATGTCCGCAAT
Retnla	NM_020509	CGAGTAAGCACAGGCAGT	CCAGCTAACTATCCCTCCAC
Tnf	NM_013693	CACCACGCTCTTCTGTCT	GGCTACAGGCTTGTCACTC
Il4ra	NM_001008700	TCTGCATCCCGTTGTTTTGC	GCACCTGTGCATCCTGAATG
Psmd11	NM_178616	GAATGGGCCAAATCAGAGAA	TGTACTTCCACCAAAAGGGC
Psme1	NM_011189	AGGCTTCCACACGCAGATCT	ACCAGCTGCCGATAGTCACC
Psme2	NM_001029855	CCAGATCCTCCACCCAAGGA	CCGGGAGGTAGCCACACTTA
Psme3	NM_011192	TAGCCACGATGGACTGGATG	CACAAACACCTTGGTTCCTTGAA
Psma3	NM_011184.4	TGAAGAAGGCTCCAATAAACGTCT	AACGAGCATCTGCCAGCAA
Psmb5	NM_011186.1	TGCTCGCTAACATGGTGTATCAGTA	GGCCTCTCTTATCCCAGCCA
Psmb6	NM_008946.4	AGACGCTGTCACTTACCAACTTGG	AAGAGACTGGCGGCTGTGTG
Psmb7	NM_011187.1	TGCCTTATGTCACCATGGGTTC	TTCCTCCTCCATATCTGGCCTAA
Psmb8	NM_010724	TGCTTATGCTACCCACAGAGACAA	TTCACTTTCACCCAACCGTC
Psmb9	NM_013585	GTACCGTGAGGACTTGTTAGCGC	GGCTGTCGAATTAGCATCCCT
Psmb10	NM_013640	GAAGACCGGTTCCAGCCAA	CACTCAGGATCCCTGCTGTGAT
Csf-2	NM_009969	GCCATCAAAGAAGCCCTG	GCGGGTCTGCACACATGTTAAA
Lcn2	NM_008491	GAAGAACCAAGGAGCTGT	TCAATGCATTGGTCGGTG
Tgfb	NM_001013025	TGACGTCACTGGAGTTGTACG	GGTTCATGTCATGGATGGTGC
Ccl2	NM_011331	CTTCTGGGCCTGCTGTTCA	CCAGCCTACTCATTGGGATCA

Cx3cl1	NM_009142	GCGACAAGATGACCTCAC	CCAGGTGTCACATTGTCC
Cxcl1	NM_203320	CCGAAGTCATAGCCACAC	GTGCCATCAGAGCAGTCT
Cxcl5	NM_002994	CCCTACGGTGGAAGTCAT	CTTCACTGGGGTCAGAGT
Cxcl2	NM_002089	TCCAGAGCTTGAGTGTGACG	TCCAGGTCAGTTAGCCTTGC
Cxcl9	NM_008599	GGAGTTCGAGGAACCCTA	GGGATTTGTAGTGGATCG
Pparg	NM_001127330	GTAGAAGCCGTGCAAGAG	GAGGAACTCCCTGGTCAT
Cxcr2	NM_009909	AGCAAACACCTCTACTACCCTCTA	GGGCTGCATCAATTCAAATACCA
Cd36	NM_001159555	TGGAGATTACTTTTTCAGTGCAGAA	TCCAGCCAATGCCTTTGC

2. Methods

2.1. Alveolar macrophages (AM) cell line culture

Murine alveolar macrophages cell line (MH-S) is derived from Balb/c mice and was purchased from American Type Culture Collection. Cells were grown to confluence in MH-S medium (RPMI-1640 medium supplemented with 10 % fetal bovine serum (Biochrom) and 0.05 mM β-mercaptoethanol and 100 U/ml Penicillin and 100 µg/ml Streptomycin (Gibco) at 37°C and 5 % CO_2). When confluence was reached, the cells were washed twice in pre-warmed PBS at 37°C, and then 1 mL of trypsin-EDTA (Sigma-Aldrich) per 25 cm^2 of culture was added to the flask. Cells were incubated at 37°C, 5% CO_2 for 5 min. After complete detachment, the trypsin was inactivated by fresh pre-warmed MH-S medium. The cells were resuspended and collected and centrifuged (1200 rpm, 5 min, RT). Cells were then seeded in a new flask after a 1:5 dilution or used directly for experiments. The cells were plated according to the table below. MH-S cells were split twice a week.

Culture plate	Surface area (cm^2)	Cells at confluency
6-well	9	$1.2x10^6$
12-well	4	$0.4x10^6$
24-well	2	$0.2x10^6$

Table 1. Cell culture experiment preparation. Relation between well plates, and cell density.

2.2. Alveolar epithelial cell type 2 (AECII)

Murine pneumocytes type 2 cell line (LA-4) is derived from A/He mice lung adenoma and was purchased from American Type Culture Collection. The subculture procedure is the same as described previously, with the culture media changed to the LA-4 culture media.

2.3. Alveolar macrophages polarization

AM were polarized *in vitro* towards the M1 phenotype with LPS (1 μg/mL, Sigma) and/or IFNγ (20 ng/mL, Immunotool) or towards the M2 phenotype with IL-4 (20 ng/mL, Immunotool) treatment for up to 72 h. Unpolarized AM (M0) served as controls. Polarization was validated via quantitative RT PCR for M1 markers (Tnf, Il1b, and Nos2) and M2 markers (Arg1, Cxcr2, and Il10r) [104,105]. Cell culture supernatants were collected for γlammatory cytokines measurement. Adherent AMs were washed twice with PBS and harvested for mRNA isolation (Qiagen) and measurement of mRNA expression levels (Light Cycler 480, Roche).

2.4. N-Acyl homoserine lactones (AHL) treatment

Bacteria produce AHL in a continuous manner to determine their neighboring bacterial concentration (e.g. quorum sensing). To mimic this biological process, cells were treated simultaneously with 3-oxo-C_{12}-HSL, C_{12}-HSL, 3-oxo-C_4-HSL, or vehicle (0.6% (n=2) and 1% (n=1) DMSO) was added. The concentration of AHL used in

the media was 60 µM according to previous studies [78,106], which had been shown to be of biological relevance. Cells and supernatants were harvested after 6h (n=1), 24h (n=3), or 72h (n=1) of treatment.

2.5. AECII/AM single well coculture

LA-4 (or MLE-12) cells were seeded on the first day, following the density recommended in Table 1. After incubating overnight in the standard conditions, MH-S were added on the top of the LA-4 monolayer respecting a final cell ratio of 1:3 (MH-S:LA-4) in a 1:1 medium mix. After another overnight incubation, the cells were treated.

2.6. AECII/AM/*Pseudomonas aeruginosa* (PAO1) transwell culture

Murine cells were grown on the bottom well following the same procedure as explained in 2.5. PAO1 were cultivated for the last 24h in the same 1:1 media as the murine cells at the concentration 10^6 CFU/mL. $0.5x10^6$ PAO1 were added on the transwell (Becton Dickinson Labware) above the AECII/AM layer. QS-molecules treatment was added in the transwell to allow molecular diffusion to the murine cell layer in the bottom well.

2.7. AECII/PAO1 supernatant culture wound healing assay

Murine AECII (LA-4) were plated on 24-well plates and then let at rest overnight. The cells were scratched, gently rinsed with PBS and covered by 1 mL of PAO1 bacterial free supernatant/LA-4 medium (1:1). The cells were incubated 24h under normal conditions as previously described in 2.1. The area of the wound was measured by light microscopy directly after its creation and 24h after.

2.8. Intratracheal instillation

2.8.1. Acute Lung Injury (ALI)

ALI is modeled by the inhalation of a suspension of LPS particles (2 µg/mL, 50 µL) in the mouse trachea to create an acute inflammation of the lungs characterized by leucocytes infiltration, increased blood barrier permeability and massive cytokine release. To assess the therapeutic anti-inflammatory potential of AHL and D-Trp during an ALI, 8 weeks old C57BL/6J mice were anesthetized with MMF (2.5 µL/g) and intratracheally instilled. The lungs and BALF were harvested for analysis after 24 or 48h after initial LPS instillation. The mice were then woken up with MMF antagonist (10 µL/g) and let to rest for 6 hours.

2.8.2. D-Trp/AHL Treatments

The mice were anesthetized following the same protocol as in 2.8.1 and then treated with 50 µL PBS, AHL (300-1200 µM dissolved in ACN and diluted in PBS) or D-Trp (100 µM-50 mM dissolved and diluted in PBS). The mice were then woken up with MMF antagonist (15 µL/g) and let to rest. 24h later, the lungs were washed to collect the BALF and cells, and the lungs were harvested.

2.9. BAL analysis

2.9.1. Cytospins slides generation

BAL cells were centrifuged and resuspended in 1 mL of cold PBS. The cells concentration was obtained counting the cells with a *Neubauer* counting chamber. A variable volume (100-200 µL) containing 30 000 cells is then loaded on the Cytospin. The cells are centrifuged on the Cytospin 400rpm 6 min at 400 rpm. The slides are then dried at room temperature for an hour. The slides are then either frozen at -80°C or stained directly.

2.9.2. May-Grünwald-Giemsa staining

A dilution in water 1:5 of Giemsa solution is prepared. The dried Cytospin slides are soaked consecutively 10 min in May-Grünwald solution, then 2 min in water, followed by 15 min in diluted Giemsa and finally in water for an additional 2 min. The slides are then dried for one hour and then covered with Entellan® and mounted with cover slips. The total number of cells visible on the slide is then counted with the help of a microscope (bright field).

2.10. Enzyme-Linked Immunosorbent Assay (ELISA)

Cell supernatant or BAL cytokine content was snap-frozen and kept at -80°C until analysis. Concentrations were measured via spectrophotometry (Tecan-Magellan™) using ELISA kits (Duoset Detection Kit; R&D Systems) according to the manufacturer's instruction. The standard curve was set using dilutions of the recombinant protein of interest. The detection limits were comprised between 3.9 and 60 pg/mL depending on the assay.

2.11. Cell viability assay with Water Soluble Tetrazolium salt (WST)

The WST-1 kit used contains a light sensitive electron-coupling reagent diluted in PBS. The principle of the assay is the reduction of the tetrazolium salt to formazan by metabolic active cells [107]. More viable cells directly translate to more activity of the mitochondrial succinate dehydrogenase; which leads to an increase of the dye formazan. The quantification of the dye is measured by light spectrometry.

The procedure was performed in 96-well plates. The wells were plated in advance with a cell concentration of 250 000 cells per well. At the time of the experiment, a final volume of 100 µL of reagent diluted to its working dilution (1:10) is added to the cells and incubated 15 min at 37°C. The absorbance of the samples was measured against a background control as blank using a microplate reader at λ=450 nm.

2.12. RNA isolation

The RNA isolation from cell lysate was conducted according to the RNeasy Mini Kit instruction manual (Qiagen). The RNA quality and concentration were controlled at 260 nm by spectrophotometric analysis (Nanodrop 2000, Thermo Scientific).

2.13. Reverse Transcription of total mRNA

The reverse transcription was conducted using 1 µg of mRNA. The cDNA synthesis was performed following the Invitrogen guidelines (cf. Buffers and solutions). 10 µL of mRNA template and 1 µL of Nonamers were heated 5 min at 70°C then cooled on ice for 5 min. The RT-PCR mix was then added to the samples and incubated 1 hour at 42°C. The enzyme was inactivated in a final step (15 min at 70°C). The samples were then diluted down 1:5 before -20°C storage.

2.14. Transcriptome analysis – Quantitative PCR

cDNA synthesis was conducted following the Invitrogen guidelines. mRNA quantification was measured by real time quantitative PCR (qPCR) (Roche, LightCycler®) after 45 cycles using the TaqMan SYBR green PCR master mix. The used primer sets are summarized in Methods 1.6. The fold change in expression of each target gene relative to Hypoxanthine-guanine phosphoribosyl transferase (Hprt, murine cells) was calculated based on the threshold cycle (Ct) where the Normalized Relative Quantity (NRQ) is expressed: $2^{-\Delta Ct}$, where $\Delta Ct = Ct_{target\ gene} - Ct_{Hprt}$.

2.15. Lung homogenate preparation

After dissection, the lung lobes were snap frozen in liquid nitrogen, then powdered using a micro-dismembrator (Sartorius). The lung homogenate was then dissolved in RIPA for protein analysis or in Qiazol® for mRNA isolation.

2.16. T_h cells isolation and differentiation

Naive $CD4^+$ T cells were harvested from Balb/c mice spleen (6-8 weeks, WT, Institute for Molecular Immunology), and isolated via $CD4^+$ positive selection or negative depletion with MACS® magnetic beads technology (Miltenyi Biotec). They were differentiated to T_h2 cells using IL-2/-4 or T_h17 cells using IL-6/-23 and TGFβ1 in a medium containing the anti-CD3/CD28/IFNγ antibodies. Differentiation was confirmed via qPCR (Gata3 for T_h2 and Rorc for T_h17). T_h2 and T_h17 cells were cultivated for 72h and 96h respectively with *P. aeruginosa's* active AHL (3-oxo-C_{12}-HSL) or controls (3-oxo-C_4-HSL, C_{12}-HSL, and DMSO) at concentrations ranging from 5 to 100 µM.

2.17. FACS analysis

2.17.1. IL-4/17

The primary T_h cells previously and freshly isolated were activated with PMA (50 ng/mL)/Ionomycin (1 µg/mL) during 5h (37°C, 5% CO_2). CD4 external receptors were stained first by anti-CD4 Ab and incubated 25 min at 4°C. The cells were then fixed with cytofix/cytoperm™ (BD Biosciences) following the manufacturer's instructions. Internal IL-4/IL-17 staining was performed with IL-4/IL-17 Ab and PermWash™ (BD Biosciences). The cells were then incubated 30 min at 4°C. After centrifugation, the supernatant was discarded, and the stained cells were kept in FACS buffer for a maximum of one week before FACS analysis (BD FACSCanto).

2.17.2. Annexin V-PI

Isolated cells were incubated (15 min, dark, RT) with binding buffer and AB Annexin V-FITC. After centrifugation and supernatant removal, PI in FACS buffer was added to the cells immediately prior to FACS analysis.

RESULTS: EFFECT OF BACTERIAL METABOLITES ON LUNG EPITHELIUM AND IMMUNITY

In this manuscript, bacterial metabolites are subdivided in two distinct categories, whether they consist of N-Acyl homoserine lactone compounds originating from Gram-negative bacteria or the amino-acid D-tryptophan originating from the Gram-positive bacteria *Lactobacillus casei*.

I- EFFECT OF N-ACYL HOMOSERINE LACTONE COMPOUNDS OF GRAM-NEGATIVE BACTERIA ON LUNG EPITHELIUM AND IMMUNITY

1. The quorum sensing molecule AHL modulates T_h cell differentiation

1.1. 3-oxo-C_{12}-HSL increased IL-17 accumulation in T_h17 cells

T helper cells 2 and 17 essentially participate in the etiology of atopic and non-atopic forms of asthma [99]. This study asked whether any of the 3 AHLs affect Th cell function or activation, which might in turn improve host's health. FACS analysis ($CD4^+/IL\text{-}17^+$) of pre-differentiated and isolated T_h17 cells, treated with 3-oxo-C_{12}-HSL (100 µM) showed a 2.1 and 1.5-fold increase in IL-17 production after 48 and 96h respectively (Figure 8). It is important to note that, using our protocol, T_h17 differentiation can take up to 5 days [108]. During the stimulation of naïve T cells, TGF-β as well as IL-21 are required for the induction and the differentiation of T_h17 cells. Furthermore, the T_h17 lineage (IL-17 producing cells), was shown to exclusively drive TGF-β-treated T cells to become T_h17 cells [109–111]. However, the 3-oxo-C_{12}-

HSL did not reduce T_h17 cell subset differentiation as previously described [87,112], but instead enhanced it without contact with an antigen presenting cell. Here the differentiation was only driven by cytokine and antibody stimulation (Table 2).

		Differentiation cocktail						
T_h17	24h-72h	**RPMI Medium**	**α-CD3** (4 µg/mL)	**α-CD28** (30 ng/mL)	**IL-6** (20 ng/mL)	**IL-23** (10 ng/mL)	**TGF-β1** (5 ng/mL)	**α-IFNγ** (10 µg/mL)

Table 2. Murine T_h17 cell differentiation protocol from isolated primary naïve T cells

Among the three AHLs used, only 3-oxo-C_{12}-HSL which contained a lactone ring, an oxo-group and a long alkyl chain, increased T_h17 differentiation (Figure 6). The C_{12}-HSL lacked the oxo function and the 3-oxo-C_4-HSL had a short alkyl chain. Therefore, all three functional groups were needed to increase the T_h17 differentiation.

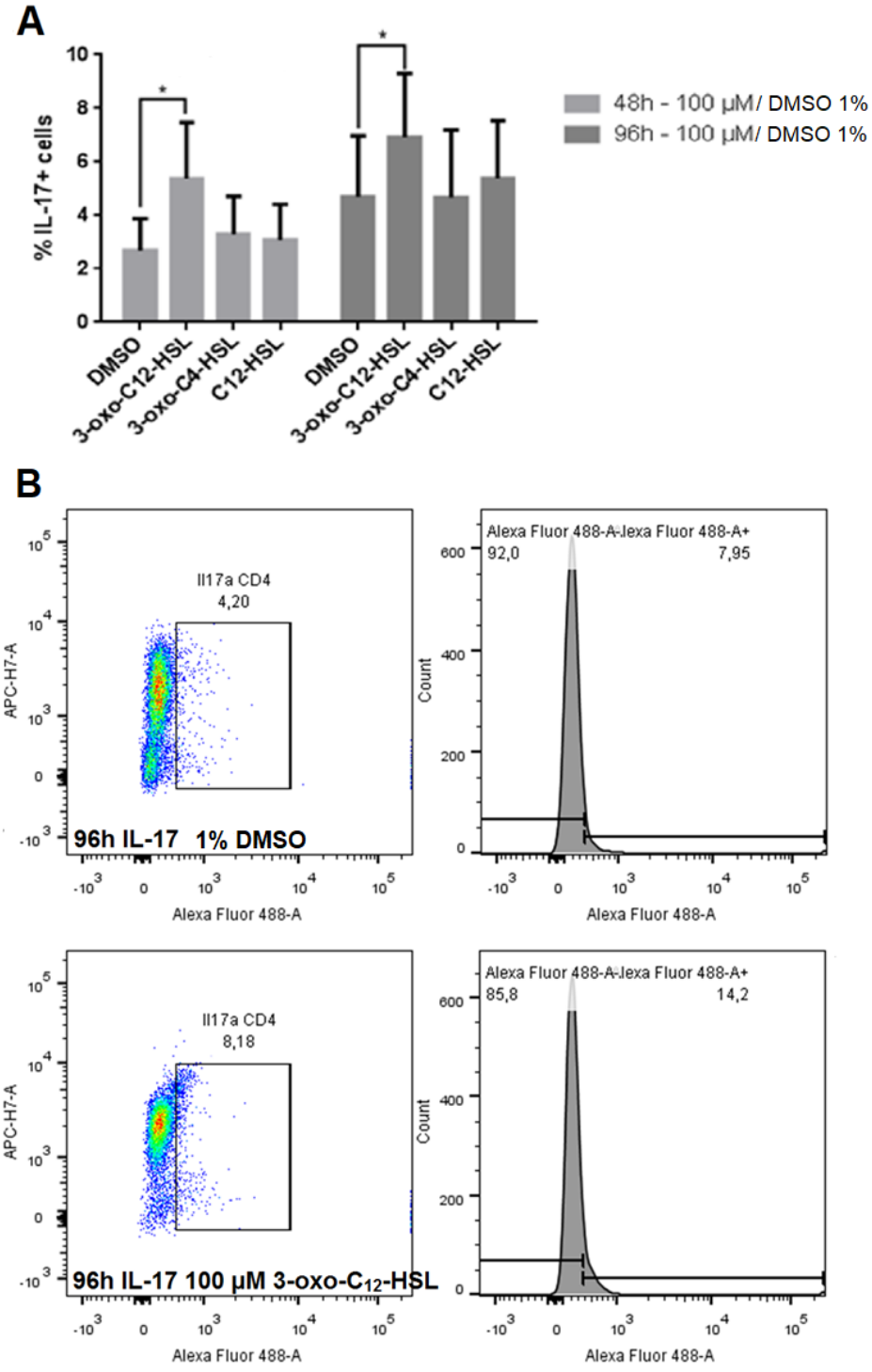

Figure 8. 3-oxo-C_{12}-HSL treatment increases T_h17 differentiation.FACS analysis of wild type mouse primary spleen $CD4^+$ T_h cells, isolated with magnetic beads and simultaneously polarized into T_h17 and treated with AHL. (A) Quantification of 3 independent experiments were the percentage of $IL\text{-}17^+$ cells among all cells is shown. (B) The dot plots (X-axis: $IL\text{-}17^+$ and Y-axis: $CD4^+$) and histograms (X-axis: $IL\text{-}17^+$ and Y-axis: cell count) are representing the gating of T_h17 cells identified as both $CD4^+$ and $IL\text{-}17^+$. FACS representative dot blot of 3 experiments. (DMSO 1%, n=3, values represent the mean ± SEM, *: $p<0.05$)

1.2. 3-oxo-C_{12}-HSL did not influence T_h2 cells polarization

T_h2 cell differentiation was not modulated by 3-oxo-C_{12}-HSL treatment at any concentration or time point investigated. However, the 3-oxo-C_{12}-HSL alkyl analogue C_{12}-HSL (50 µM) slightly reduced IL-4 production after 48h, showing that substitution of the alkyl chain had some role during T_h2 differentiation (Figure 9). However, compared to the results obtained with IL-17^+ cells (Figure 8), this slight reduction caused by C_{12}-HSL suggests more a minor side effect and does not appear to be biologically relevant towards T_h2 cells differentiation.

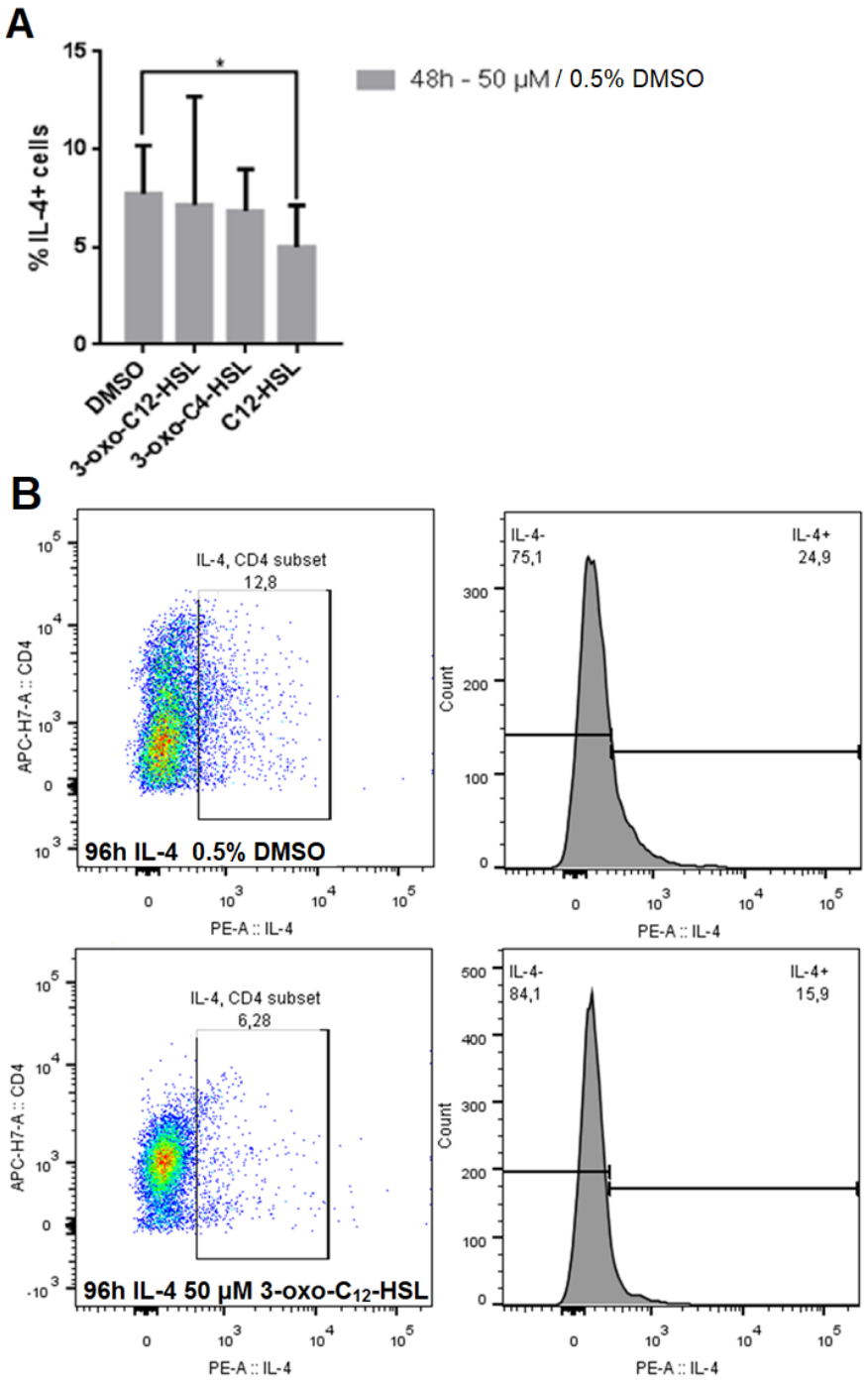

Figure 9. C_{12}-HSL treatment decreases T_h2 differentiation. FACS analysis of wild type mouse primary spleen $CD4^+$ T_h cells, isolated with magnetic beads and simultaneously polarized into T_h2 and treated with AHL. (A) Quantification of 3 independent experiments were the percentage of $IL\text{-}4^+$ cells among all cells is shown. (B) The dot plots (X-axis: $IL\text{-}4^+$ and Y-axis: $CD4^+$) and histograms (X-axis: $IL\text{-}4^+$ and Y-axis: cell count) are representing the gating of T_h2 cells identified as both $CD4^+$ and $IL\text{-}4^+$. FACS representative dot blot of 3 experiments. (DMSO 0.5%, n=3, values represent the mean ± SEM, *: $p<0.05$)

2. Bacterial AHL-compounds influence the innate inflammatory response

The immunologic activity of "Alveolar Macrophages" (AM) provides the first line of defense against microbial invasion in the lower respiratory tract. The clearance capacity of AM further protects the fragile alveolar surface from deposited debris and inhaled particles. Therefore, the well-balanced plasticity of AMs is crucial for the maintenance of respiratory health. "Naïve" macrophages, M0 were polarized with LPS/IFNγ into pro-inflammatory M1 macrophages (classical activation) or with IL-4 in anti-inflammatory M2 macrophages (alternative activation). M1 AMs do not only fight invading pathogens, but may also contribute to tissue damage when they become hyperresponsive, possibly leading to uncontrolled release of pro-inflammatory mediators that exacerbate acute tissue injury of infected airways [113]. In a similar manner, M2 polarized AM key functions include resolution of airway inflammation, pulmonary wound healing and anti-parasitic responses [114]. However, disproportionate M2 activity can also contribute to the pathology of chronic lung diseases characterized by an excessive T_h2 response, as evidenced for allergic asthma or tissue remodeling for pulmonary fibrosis [115].

2.1. AHL reduces alveolar macrophages pro-inflammatory gene expression upon M1 polarization

The polarization protocol significantly regulated the expression levels of certain M1 and M2 markers depending on the type of stimulation. After 24h, LPS/IFNγ alone induced Tnf mRNA expression by 35 folds, whereas in combination with the 3-oxo-C_{12}-HSL, Tnf expression was reduced to 14 folds. Similarly, mRNAs for IL-1β (Il1b) and IL-10 (Il10) demonstrated a 1060-fold increase and a decrease to 1.65-fold after LPS/IFNγ treatment and a 500 and 1.10-fold decrease after AHL stimulation, respectively (Figure 10). Current data suggest that AHL treatment of LPS-treated AM limits TNFα, IL-1β and IL-10 cytokine production [78], thus modulating their inflammatory immune role. Interestingly, these results were in favor of a global AHL

response and not only from the 3-oxo-C_{12}-HSL. Since only 3-oxo-C_{12}-HSL is of biological relevance, it became clear that the genetic regulations were driven by a common feature; indeed, all three tested molecules share the lactone ring.

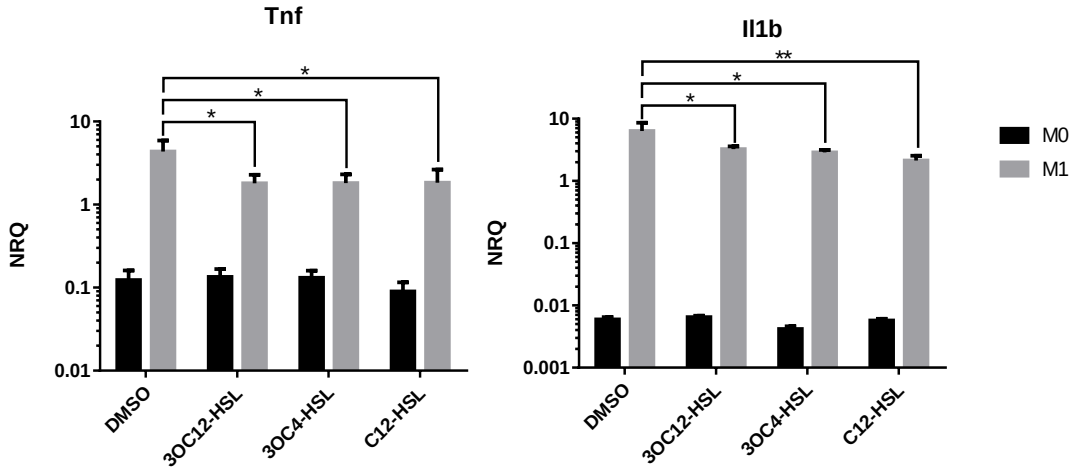

Figure 10. AHL treatment reduces LPS/IFNγ induced Tnf and Il1b mRNA expression in AM. MH-S cells were analyzed 24h after AHL (60 µM)/LPS (1 µg/mL) treatment for mRNA expression relative to Hprt.
M0: no polarization; M1: LPS(+)/IFNγ(+). (1% DMSO, n=3, values represent the mean ± SEM, *: $p<0.05$, **: $p<0.01$)

2.2. AHL signaling increases *in vitro* inflammatory cytokine production.

To investigate whether mRNA expression is translated to protein expression *in vitro*, cell supernatants were analyzed to detect the relevant M1 cytokines secretion after LPS, or AHL treatment. The protein detection was realized via a protein immunosorbent assay (ELISA). TNFα and IL-1β's pathways of cytokine expression rely both on inflammatory transcription factors (nuclear factor kappa-light-chain-enhancer of activated B cells) NF-κB and Activator protein 1 (AP-1) and their related signaling. In addition IL-1b protein maturation depends on the cleavage of the inactive Pro-IL-1b by Caspase 1/Interleukin-1 converting enzyme, a unique two-signal mechanism allowing a tight regulation of the release of mature IL-1β, the pro-

inflammatory master cytokine [116]. This additional step between transcription and extracellular release can also explain potential differences between mRNA regulation observed via qPCR and protein secretion. In a similar way, TNFα needs to be cleaved by the metalloprotease ADAM17/tumor necrosis factor-α-converting enzyme before release of the transmembrane protein expressed cytokine into the intracellular space. The results showed a 1.4-fold increase of TNFα in the supernatant of the AM treated with AHL whereas baseline levels of M0 AM were not affected. Furthermore, it is noticeable that the dimethyl sulfoxide (DMSO) vehicle control also led to a reduction of TNFα and IL-1β release by the AM. Interestingly, the data obtained do not confirm qPCR findings (Figure 11) where a moderate decrease of Tnf, and Il1b was observed. This can be explained by the fact that gene expression analysis and protein analysis were performed at the same time point. Protein release is downstream from mRNA expression and translation, and it is likely that the latter already passed its maximum at the time of analysis. Indeed, Tnf regulations are notoriously fast and can return to baseline level within a day [117]. Thus, obtaining the maximum of TNFα secretion and mRNA expression at the same time is not feasible.

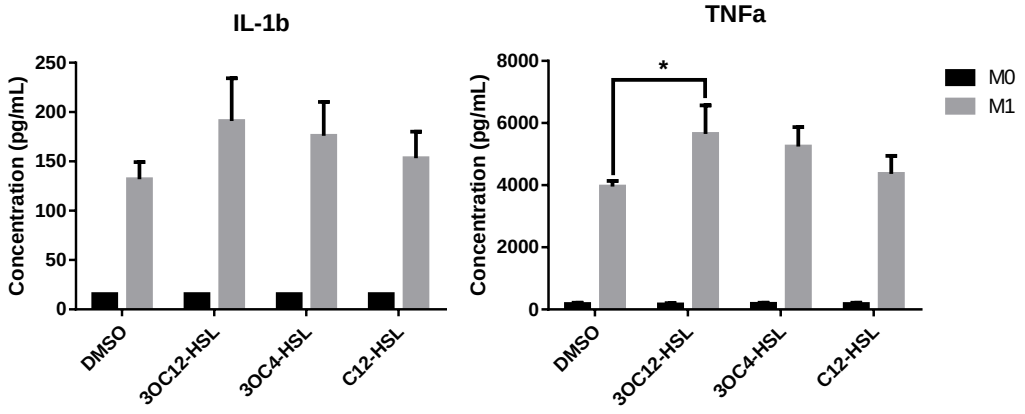

Figure 11. 3-oxo-C_{12}-HSL treatment increases LPS/IFNγ induced IL-1b and TNFα release. MH-S cell supernatants were analyzed 24h after AHL (60 μM)/LPS (1 μg/mL) treatment. ELISA assay.
M0: no polarization; M1: LPS(+)/IFNγ(+). (1% DMSO, n=3, values represent the mean ± SEM, *: $p<0.05$)

2.3. *In vitro* AHL supports M2 polarization

AHLs triggered the pro-inflammatory cytokine TNFα secretion, hence showing that they both increase M1 polarization when LPS treated. Here, in the aim of showing a possible anti-inflammatory potency of AHLs, M2 polarization upon AHL treatment was measured. To this end, the gene expression of Arginase 1 (Arg1) and Mannose Receptor C-Type 1 (Mrc1), previously described as classic M2 markers [118], were measured.

Arg1 and to some extent also Il1b displayed significant higher levels of mRNA levels compared to the vehicle control (DMSO) in the M2 polarized group. A moderate decrease of Il10 mRNA expression was also observed in the M2 polarized group (Figure 12). As for the M1 polarization, the changes in gene expression were not only limited to the 3-oxo-C_{12}-HSL but also concerned the cell treated with 3-oxo-C_4-HSL. This confirms previous results obtained for the T_h cells, suggesting an obligate involvement of the lactone ring and the presence of a 3-oxo group in the pro-inflammatory role of AHLs in the Th cell and the AM activities.

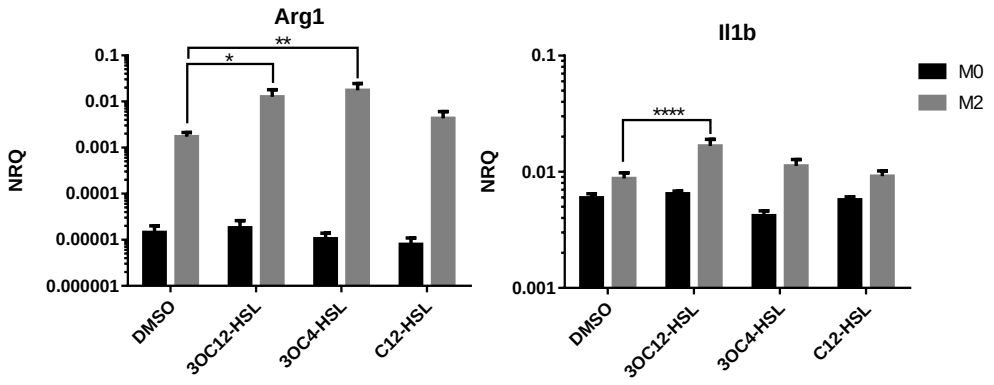

Figure 12. 3-oxo-C_{12}-HSL and 3-oxo-C_4-HSL treatment increases IL-4 induced Arg1 and Il1b mRNA levels in AM. MH-S cells were analyzed 24h after AHL (60 µM)/IL-4 (20 ng/mL) treatment for mRNA expression relative to Hprt.
M0: no polarization; M2: IL-4(+). (1 % DMSO, n=3, values represent the mean ± SEM, *: $p<0.05$)

2.4. Dimethyl sulfoxide influences AM polarization

AHLs are organic molecules, and precipitate in aqueous medium even at low concentration, essentially because of their hydrophobic alkyl chain. AHLs need to be dissolved in the cell medium to further interact with them. There is no consensus, what is the best solvent for this group of molecules. The solvent must be non-interacting with the molecule it transports for stability reasons and relatively inert to the molecule's target.

As previously explained, dimethyl sulfoxide (to concentration up to 1%) was described as a solvent of choice for its biocompatibility and low toxicity [119] in drug testing assays particularly when facing solubility issues, dissolving easily polar and non-polar molecules. Considering its high diluent power towards AHL and its relative innocuity towards mammalian cells, DMSO was thought at first to be the vehicle of choice for the AHL delivery. However, the data showed that even low concentrations of DMSO could alter gene and protein expression (Figure 22). Meanwhile, Elisia et al. demonstrated in 2016 the anti-inflammatory effects of the DMSO *ex vivo*; 0.5% of DMSO in the cell medium was sufficient to reduce TNFα secretion by a factor of 1.8 [120]. This confirms previous results of this study. Some concerns were also raised concerning the toxicity of the substance for AM. The acetonitrile (ACN) showed a better biocompatibility than DMSO as an AHL solvent (Figure 13) and was then used during the following experiments. A metabolic activity assay was performed, assessing the viability of the AM facing a DMSO or an ACN dose response. AM showed a greater viability from 0.1% to 10% ACN treatment, with at least 60% cell viability after 24h. On the other hand, as confirmed by other recent findings [120], DMSO treated AM displayed a greater mortality for higher doses. The 3-oxo-C_{12}-HSL (dissolved in DMSO) displayed the same viability trend as the DMSO alone on the cells, bringing to the conclusion that DMSO had more effect on the cell viability than the AHL alone. Remarkably, the viability exceeds 100%, this is explained by the high mitosis rate of MH-S cells. Thus, in our system, ACN (0.2%) was more tolerated than DMSO (1%) by the AM. Consequently, for the following experiments, ACN (0.2%) was confirmed as vehicle solvent.

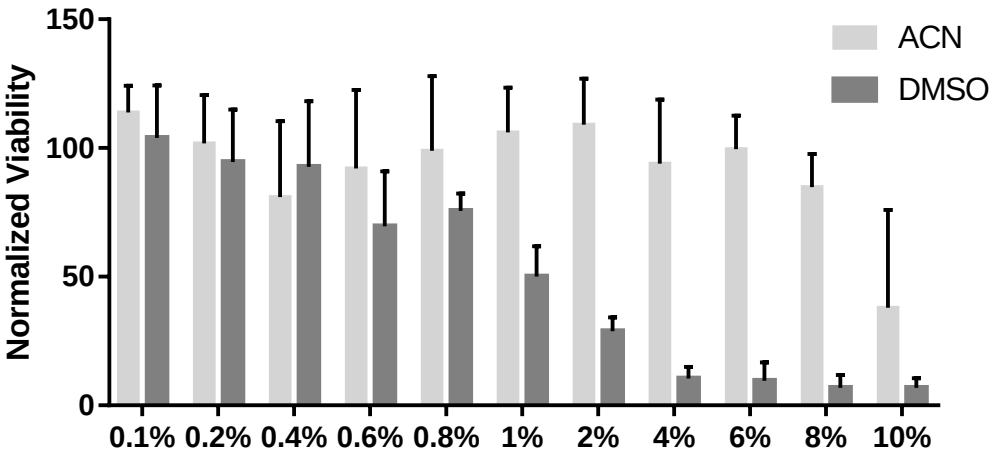

Figure 13. Naive AM (M0) show a greater viability on a wide range of concentrations when treated with ACN. Naive MH-S cells were incubated 24h with DMSO or ACN treatment. WST-1 assay assessed cell viability via metabolic activity. The results obtained are normalized to untreated AM. (n=3)

3. AHL treatment on AEC/AM coculture reduces M1 inflammatory gene expression

The epithelial cells are the first lining of the lung epithelium. They fulfill several roles, from surfactant production to cell repair, and even immune functions [121,122]. Alveolar epithelial cells type 2 (AECII) constitute most of the respiratory surface area potentially interacting with QS molecules. AM/AEC interactions are responsible for the epithelium integrity and immunity and might also contribute for AM activation. Also, it has been shown that AM/AECII crosstalk during ALI was promoting TNFα mediated AECII proliferation via autocrine GM-CSF secretion [123].

An AM/AECII coculture model was used to investigate AHL effects on AM polarization (MATERIALS AND METHODS, 2.5). AECII and AM were introduced successively in the medium cocultured overnight. AHLs (60 µM) and polarization medium (20 ng/mL IL-4 or 1 µg/mL LPS) were then applied to the cells simultaneously.

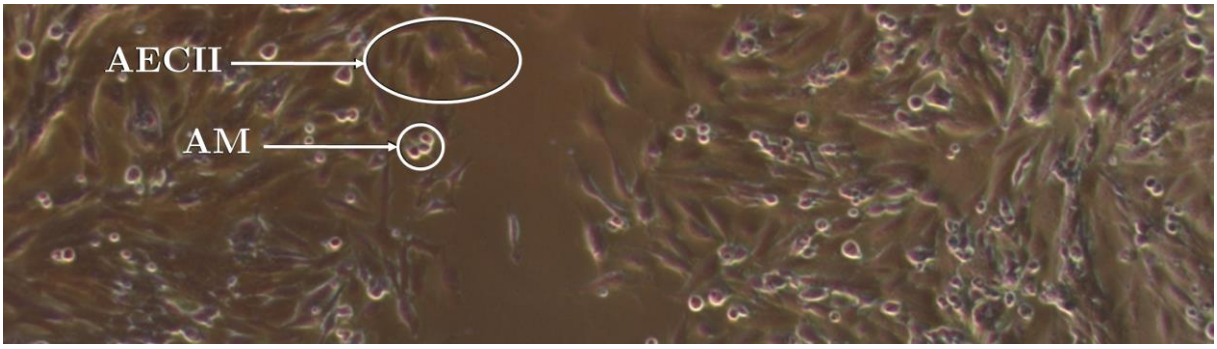

Figure 14. Light microscopy of murine AECII (LA-4)/AM (MH-S) coculture 48h after plate seeding. LA-4/MH-S were respectively seeded at a 24h interval and were incubated at 37°C, 5% CO_2. MH-S are notably smaller and rounder than the elongated LA-4 cells.

AHL treatment on AM/AEC coculture reduced Nos2, Tnf and Il1b expression by more than 2 folds after 3-oxo-C_{12}-HSL (60 µM) and LPS treatment (Figure 15), consistent with the previous data (Figure 10) on AM monocultures.

Rosiglitazone (RGZ) is an anti-inflammatory drug [124] from the Thiazolidinedione family, particularly studied as a ligand to the PPARγ receptor and its effects on epithelial wound healing and lung repair [125]. It has been shown by Xu et al. that RGZ treatment was impairing M1 polarization and more specifically TNFα expression [126]. Here, RGZ was used as a positive control of wound repair, since PPARγ activation by RGZ impairs the NF-κB pathway, reducing the M1 overall polarization. A robust increase in Arg1 levels in the M2 polarized group was also observed (Figure 15 B) as well as a 120-fold increase after IL-4 stimulation, compared to a 20-fold increase for the ACN vehicle control. This was a strong confirmation of the anti-inflammatory promoting effect of RGZ and 3-oxo-C_{12}-HSL towards M2 polarization. These results are consistent with previous findings on gene regulations and

polarization of AM culture caused by AHLS. The presence of epithelial cells rose the background mRNA level of TNFα, reinforcing their immune role. This confirms previous findings of Thorley et al. [127], describing the active role of AECII during the immune response consisting in the expression of TLR4 and TNF-α. In essence, these results agree with Pechkovsky et al. [128], showing that AECII cell lines promoted NOS2 expression in LPS or IFNγ treated AM.

Interestingly, the 3-oxo-C_{12}-HSL was the only AHL which had a significant effect on the inflammatory genes tested. Therefore, this suggests a more complex mechanism linked to this specific AHL structure.

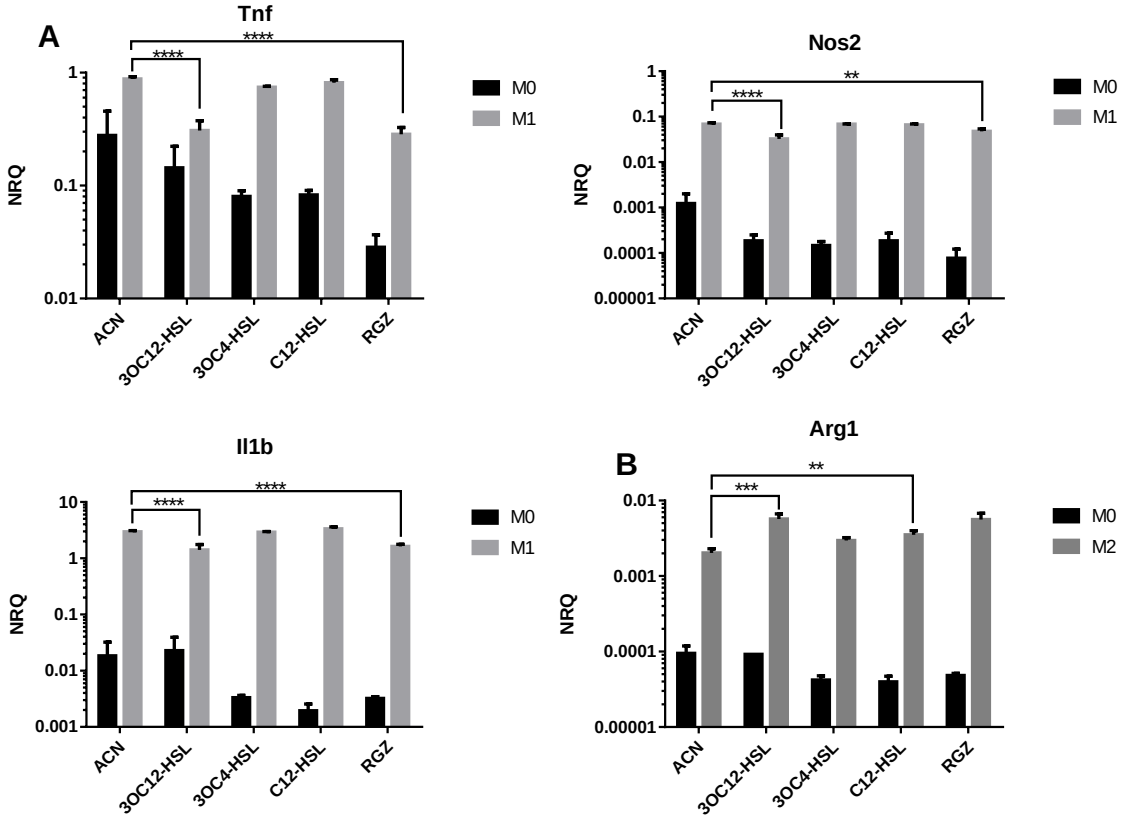

Figure 15. 3-oxo-C_{12}-HSL (60 μM) treatment reduces (A) LPS induced Tnf, Nos2 and Il1b mRNA expression in AM/AECII coculture as well as increases (B) IL-4 induced Arg1 expression. MH-S/LA-4 cells were analyzed 24h after AHL/polarization treatment for mRNA expression relative to Hprt.
M0: no polarization; M1: LPS(+)/IFNγ(+); M2: IL-4(+). (ACN 0.2%, n=3, values represent the mean ± SEM, **: $p<0.01$, ***: $p<0.001$, ****: $p<0.0001$)

4. AHL-molecules impaired epithelial barrier function and wound healing is independent to LPS induced acute inflammatory effect

Respiratory diseases are a global burden [129], all of them lead to a certain extend of destruction or modification of lung structures. The alveolar epithelium represents the largest surface area of our body that is continual interacting with the ambient environment, and frequently subject to pathogen attacks [130]. Adults lungs are capable of moderate self-repair [131], however, extensive damage lead to loss of lung function and in some cases, death. Thus, the lung epithelial barrier repair after an injury is vital [132]. AECII cells had been shown to play a central role during alveolar repair [10] and innate immunity. It was hypothesized that AM and AECII worked conjointly towards epithelial repair. For this purpose, a coculture wound repair assay was set to investigate the effect of inflammation, AHLs, and cell types on wound healing. The model used was simulating an acute lung injury. This translated *in vitro* to a longitudinal cut through the cell bi-layer submerged in medium (MATERIALS AND METHODS, 2.8.1). AECII and AM were cocultured and treated with AHL under pro-inflammatory or normal conditions (Table 3).

#	AECII (LA-4/MLE-12)	AM (MH-S)	LPS (1μg/mL)	AHL (60 μM)	Impact of?
1	+	-	-	-	Coculture
2	+	+	-	-	
3	+	+	+	-	Inflammation
4	+	+	-	+	AHL
5	+	+	+	+	AHL and inflammation

Table 3. Summary of coculture conditions in epithelial immunity assays.

To measure the rate and efficiency of wound repair [133], two types of AECII (LA-4 and MLE-12) were monitored for 48h. LA-4 and MLE-12 are two commonly used murine AECII cell lines; expressing most but not all the features of primary cells [134]. Testing various cell lines avoids to limit the results to only one cell line phenotype. LA-4 cells are issued from urethan-induced mouse lung adenoma. They are not tumorigenic but produce and release a C-type RNA virus into the culture medium [135]. MLE-12 cells are distal respiratory epithelial cell lines transformed by the oncogene SV40 Large T Antigen [136]. The responsiveness of AECII towards LPS (to simulate an acute lung inflammation) is subject to controversy [121,127].

An acute inflammation assay was performed consisting in AHL/LPS co-stimulation on an AECII monolayer. The monolayer of the control group was completely repaired 48h after the scratch (100% cell density), thus 48h was decided as the endpoint. The 3-oxo-C_{12}-HSL treatment resulted in optically greater mortality (*i.e.* greater cell detachment from the well) and fewer repair of the wound for both cell lines (Figure 16 and Figure 17). These findings did not support a pro-resolving effect of the AHL on inflammation. A similar previous work on Caco-2 cells showed that the 3-oxo-C_{12}-HSL was disrupting tight junctions of the intestinal wall [83]. These results could be extended to other epithelial cell lines such as LA-4. Interestingly, the same results were observed in the presence and the absence of LPS treatment (Figure 16), indicating that the epithelial repair is not TLR4 dependent in our setup. The presence of AM in the coculture experiment did not have a beneficial effect on the repair (Figure 17).

Remarkably, wound closure impairment was only observed for the cells stimulated with the 3-oxo-C_{12}-HSL (Figure 17). This may be explained by the presence of a specific receptor for 3-oxo-C_{12}-HSL on AECII [96]. RGZ did not increase the repair speed of the AECII monolayer; this could be due to its poor solubility in ACN, as some fine crystalline precipitate was observed in the well.

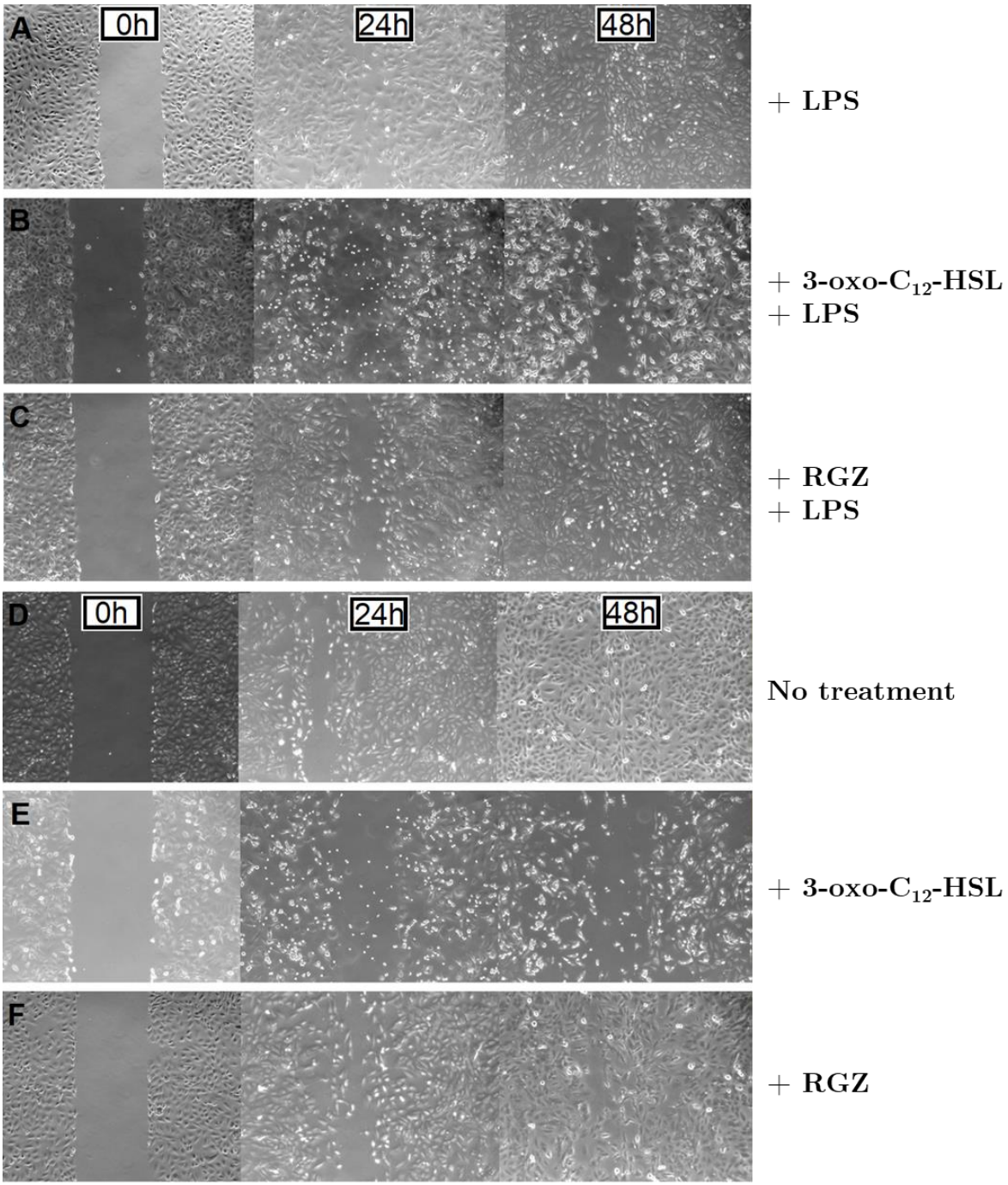

Figure 16. 3-oxo-C_{12}-HSL impairs wound repair of AECII monolayer. Light microscopy of LA-4 cells cultivated from 0 to 48h after scratch and (**A**) LPS (1 mg/mL), (**B**) 3-oxo-C_{12}-HSL (60 µM)/LPS (1 mg/mL), (**C**) RGZ (60 µM)/LPS (1 mg/mL), (**D**) no treatment control, (**E**) 3-oxo-C_{12}-HSL (60 µM), and (**F**) RGZ (60 µM). Wound surfaces were determined 0 and 24 hours after wounding.

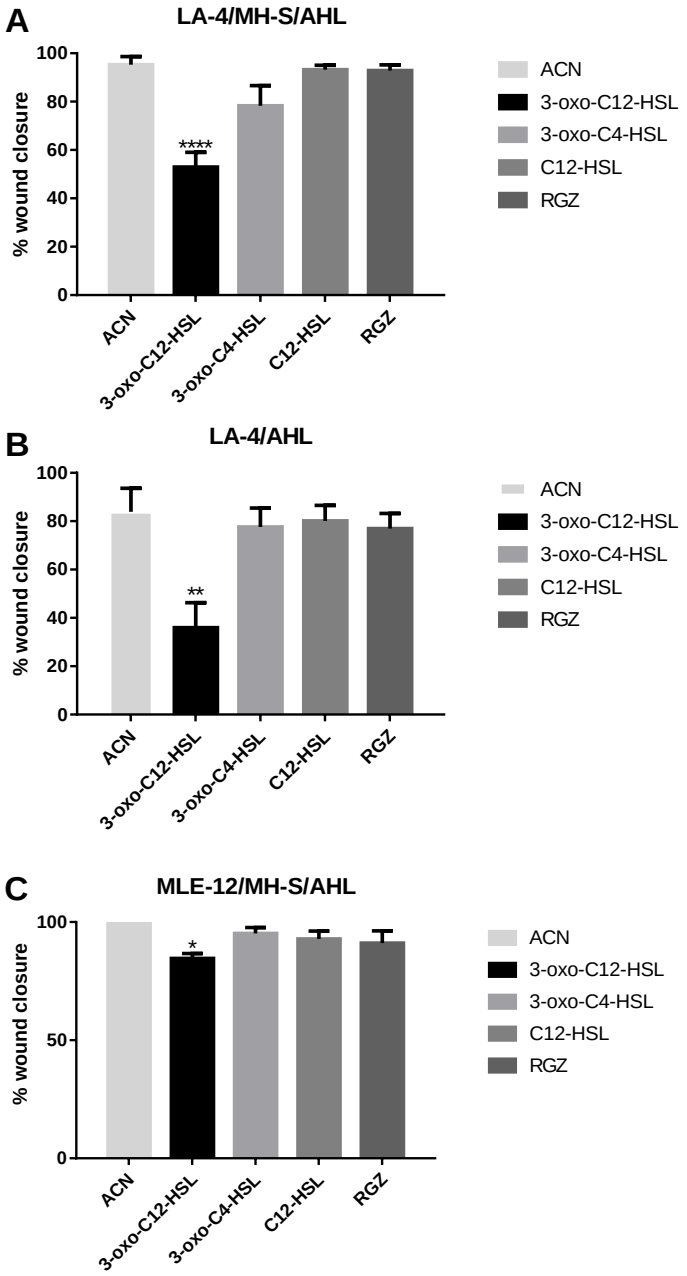

Figure 17. 3-oxo-C_{12}-HSL selectively impairs wound closure of AECII monolayer and AECII/AM coculture. (**A**) LA-4/MH-S (**B**) LA-4 (**C**) MLE-12/MH-S cells were cultivated from 0 to 24h after simultaneous scratch and treatment with ACN (0.6%)/3-oxo-C_{12}-HSL (60 µM)/3-oxo-C_4-HSL (60 µM)/C_{12}-HSL (60 µM)/RGZ (60 µM). Wound widths were determined 0 and 24 hours after wounding. (n=7, values represent the mean ± SEM, *: $p<0.05$)

5. *P. aeruginosa* PAO1 supernatant impairs epithelial wound healing independently to 3-oxo-C_{12}-HSL

Initial hypotheses and results postulated the AHL as the mediator of wound repair impairment and mRNA pro-inflammatory gene deregulator. However, *Pseudomonas aeruginosa* signaling consists in more than just AHL-dependent virulence regulating, QS-systems. PAO1 QS systems are also controlled by the *pqsA-E* operon for the biosynthesis of 2-alkyl-4(1H)-quinolone (AQ) molecules [137]. AQ signaling is not part of the scope of this study. PAO1 consists in two AHL dependent quorum-sensing virulence systems (Las and Rhl); LasI being responsible for the synthesis of the autoinducer 3-oxo-C_{12}-HSL, and RhlI directing the synthesis of the C_4-HSL [138]. To investigate the selective effect of the 3-oxo-C_{12}-HSL on the epithelium, in addition to the wild type strain, two PAO1 mutant strains were used; Las KO and Rhl KO, silencing their respective autoinducers. The mutant strains were obtained by the team of the Dr. Rothballer (Molecular Microbial Ecology, Helmholtz Zentrum München) from the construct developed by Wilder et al. [139]. The supernatant from the wild and mutant strains were sterile filtered and used to treat AECII/AM cultures ongoing a wound healing assay. Prior to the experiment, wild type PAO1 supernatant was analyzed and a 3-oxo-C_{12}-HSL concentration of 17 µM was measured. Consistently with these findings, LA-4 cells were treated with 20 µM 3-oxo-C_{12}-HSL in a 1:1 PAO1:LA-4 medium.

In a previous study, Wu et al. showed that PAO1 cell-free supernatant had the same effect on AECII (A549 cell line) as LPS (200 ng/mL) treatment [140] which lead to 25% of cell death. Here, as explained above, LPS did not significantly influence the wound repair of LA-4 or MLE-12 cells. However, all the PAO1 supernatants resulted in the almost complete destruction of the epithelial cell layer surrounding the wound. This deleterious effect on wound healing was stronger than any other 3-oxo-C_{12}-HSL concentration (Figure 18). The wounded area ended being unquantifiable for both mutant bacterial strains. Thus, this suggested that the wound healing dynamics were not modified by 3-oxo-C_{12}-HSL and depended on other factors present in WT/KO PAO1 supernatant of *Las* KO and *Rhl* KO mutants of PAO1.

Indeed, cytotoxic and degradative bacterial enzymes can survive sterile filtration and can cause DNA damage as well as cell death [141] Yet, the results (Figure 18) suggest a threshold between 20 and 60 µM where 3-oxo-C_{12}-HSL alone actively impairs the epithelial repair.

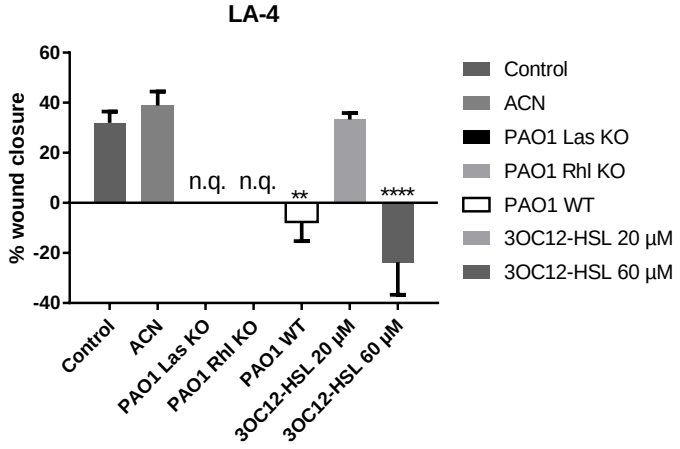

Figure 18. PAO1 supernatant and 3-oxo-C_{12}-HSL impairs epithelial wound closure of AECII monolayer. LA-4 cells were cultivated from 0 to 24h after simultaneous scratch and treatment with ACN (0.6%)/PAO1 Las KO supernatant/PAO1 Rhl KO supernatant/PAO1 WT supernatant/3-oxo-C_{12}-HSL (20-60 µM). Wound widths were determined 0 and 24 hours after wounding. (n=3, values represent the mean ± SEM, **: $p<0.01$, ****: $p<0.0001$, n.q.: non-quantifiable due to massive cell death). NB: The medium used was a 1:1 mixture LA-4 medium (HAM):PAO1 medium (MOPS), this explain the subpar repair of the wound for the untreated group.

Pseudomonas aeruginosa is a common opportunistic pathogen and is responsible for chronic as well as acute infections. *In vivo*, the bacterial contamination can lead to local high levels of AHL and other bacterial secretion in the supernatant, resulting in cell death during biofilm development [142]. However, these effects were more dramatic *in vitro* where the generally toxic bacteria-free supernatant induced the epithelial death. Therefore, this *in vitro* model is not supporting any effects of AHLs on wound healing. In the aim of using 3-oxo-C_{12}-HSL therapeutically against inflammation, this study further pursued the underlying mechanisms of the modulation of the inflammation by investigating the effects of acute injuries *in vivo*. Various models of acute lung injuries exist, each with their pros and cons [143]. In the following animal experiment, the acute lung injury was performed via LPS

intratracheal instillation. This invasive method allows further observations of biological changes, like changes in protein secretion, as well as pathological changes, such as neutrophilic alveolar infiltrates. The application of a precise volume of the LPS solution allows a good reproducibility and a non-fibrotic repair phase [144], together with a measurable alveolar neutrophil recruitment.

6. *In vivo* Acute Lung Injury (ALI) can be modulated by bacterial effectors

ALI is an inflammatory model developed to recreate inflammation *in vivo* or *in vitro* without the risk of putting in contact live pathogens in the organism of interest [10,145], with a quick onset (typically less than half an hour), followed by a total resolution of the inflammation (at least 95%) within 72 hours [146]. In this study, LPS was applied intratracheally to 6-8-week-old female C57BL/6J mice, either half an hour prior, or six hours prior to the bacterial molecule treatment. C57BL/6J is a common inbred mouse strain, widely used in pulmonary studies. However, it differs from the other widely used strain BALB/c by its higher T_h2 response in the lungs and overall higher cytokine release upon antigen sensitization [147].

LPS is known to activate the NF-κB pathway through TLR4 signaling, thereby classically polarizing AM and driving pro-inflammatory cytokine release, which in turn induces inflammatory cells recruitment [100]. The inflammation in the lung can be quantified by various techniques [148]. Here, the main focus was on cell number and population, Broncho-alveolar lavage (BAL) protein concentration and mRNA levels of inflammatory markers in whole lung homogenates.

7. Application of QS-molecules failed to reduce LPS induced neutrophil recruitment

AHL were instilled intratracheally and tested for pro-inflammatory or toxicity potency, as it would interfere with the LPS induced ALI (Figure 19). No dose response was observed between 300 and 1200 µM in the AHL treated mice. 24h after AHL treatment, BAL sampling showed no significant difference in PMN numbers between the PBS and AHL instilled mice (<10%). These results suggest that AHL or ACN alone do not trigger any acute inflammation upon treatment with doses up to 1200 µM.

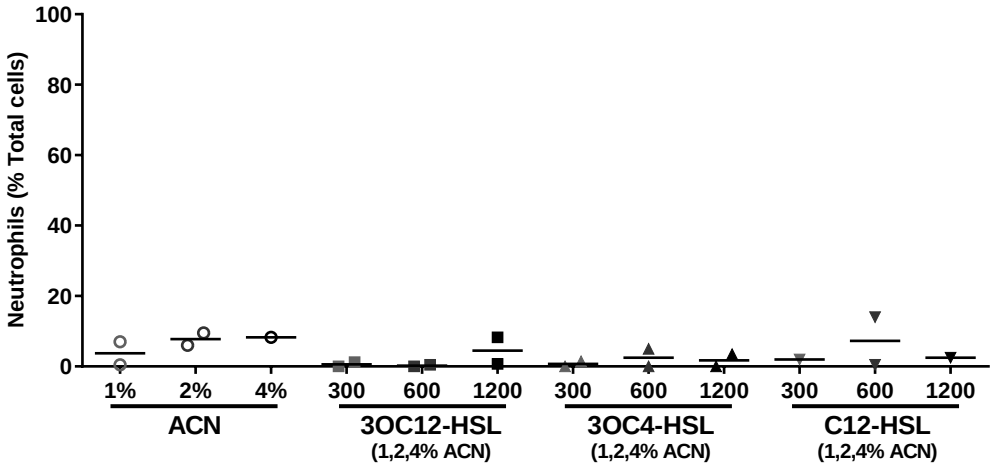

Figure 19. No inflammation is observed after AHL instillation up to 1200 µM. AHL or ACN were instilled into the lungs of mice at concentrations up to 1200 µM. This did not trigger BAL neutrophil recruitment (neutrophils < 10% total cells). BAL was harvested after 24h and cells counted manually after May-Grünwald-Giemsa staining (n=2/condition).

Neutrophils migrate to the lung alveoli during an ALI. Thus, a neutrophil count is a robust indicator of the inflammatory state [149–151] of a lung as well as the lung fluid composition. To test the eventual inflammatory dynamics of AHL *in vivo*, mice were instilled a first time with LPS and 6 hours later with AHL. This protocol enabled us to monitor the therapeutic effect of AHL on ALI, as a reduction of cytokine concentration or cell number would indicate a reduced response on the inflammation process. The mice were treated with the highest doses of AHL and

ACN not triggering an inflammation to purposely hit the maximum efficiency against the LPS induced inflammation. However, no reduction in neutrophil numbers reduction was observed in the BAL upon the AHL treatment, even for doses as high as 1200 µM (Figure 20). These results showed that a direct effect from QS molecules against acute inflammation cannot be found in this experimental system. On the other hand, AHLs have been shown to participate to PMN recruiting [75]. Recent studies [67] discovered that probiotic bacteria release molecules which may allow a quicker resolution of the inflammation.

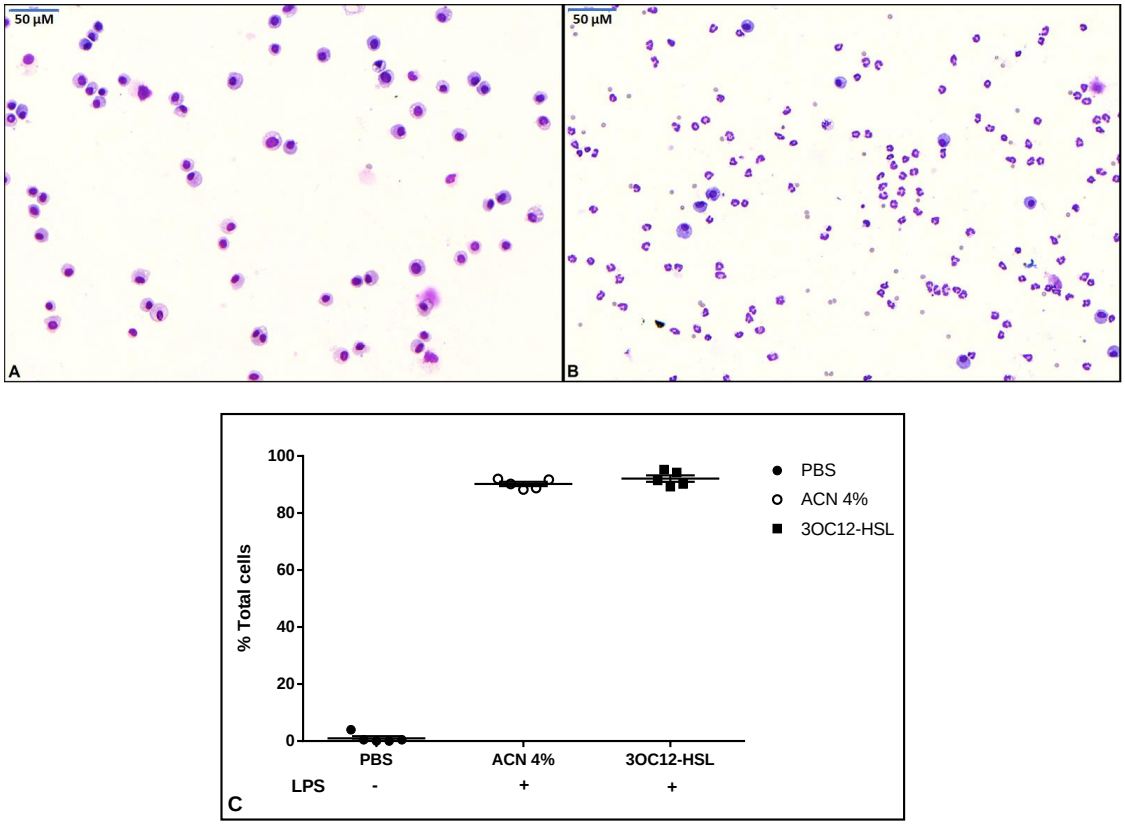

Figure 20. BAL neutrophils recruitment after LPS instillation is not affected by 3-oxo-C_{12}-HSL. (**A**) May-Grünwald-Giemsa staining of control (PBS) and (**B**) inflamed (LPS) lung. (**C**) 3-oxo-C_{12}-HSL (1200 μ M), ACN (4%) or control (PBS) were co-instilled with LPS (6h delay). BAL was harvested 24h later and cells were counted manually (n=5).

II- EFFECT OF D-TRP OF PROBIOTIC GRAM-POSITIVE BACTERIA ON LUNG EPITHELIUM AND IMMUNITY

1. Probiotic bacterial molecules modulate the innate pulmonary response

Following the previous results showing that the AHL structure was affecting macrophages polarization [78] and T_h cells differentiation [112], it was hypothesized that other bacterial small molecules could modulate the immune response too. It has been shown recently by Kepert et al. [67] that supernatant from Gram-positive probiotic bacteria strains (*e.g. Lactobacillus casei*) decreased Chemokine (C-C motif) ligand 17 (CCL17) cytokine secretion in human Hodgkin lymphoma cell line as well as T_h2 response in mice. The active molecule was identified as D-tryptophan (D-Trp), while L-Trp and other amino acids were immunologically inactive. The D-Trp relative innocuity [152], specificity and affordable price could lead to acute or chronic inflammation treatment. Here D-Trp effects were compared with the previously described AHL-effects on AM polarization, wound healing and inflammation resolution.

2. *In vitro* D-Trp impairs M1 macrophages inflammatory phenotype

Various D-amino acids were used as controls, chosen for their chemical similarities (*i.e.* acidity; aromaticity) with D-Trp: Tyr, Phe, Met, His, and Pro (Figure 7). None of them displayed a significant effect on AM polarization (Suppl. Fig. 6). The LPS/IFNγ stimulation effectively drove the M1 polarization (Figure 21). D-Trp alone did not induce a biologically significant expression of Tnf, Il1b or Nos2 (NRQ<0.1). After 24h of D-Trp/LPS treatment, Tnf and Il1b showed reduced expression, ranging from 3.6 to 3.8 folds respectively and Nos2 was only non-significantly reduced at 1.7-fold (Figure 21) compared to the DMSO vehicle control (1%). Furthermore, the

effects on Tnf were observed for doses as low as 10 μM D-Trp. These results suggested that D-Trp impairs M1 polarization of AM *in vitro* via the downregulation of key inflammatory genes. It is important to notice the biological effect induced of DMSO alone. This biologically compatible chemical was used in numerous previous studies as a vehicle agent [153,154], chosen for its relative inertia towards organisms. Furthermore, the DMSO M0 control was cut down compared to the Non-Template-Control (NTC, media only control) by 90 folds. After these findings were reproduced and confirmed, it became urgent to reflect and rely on a different vehicle control, as detailed in 2.4.

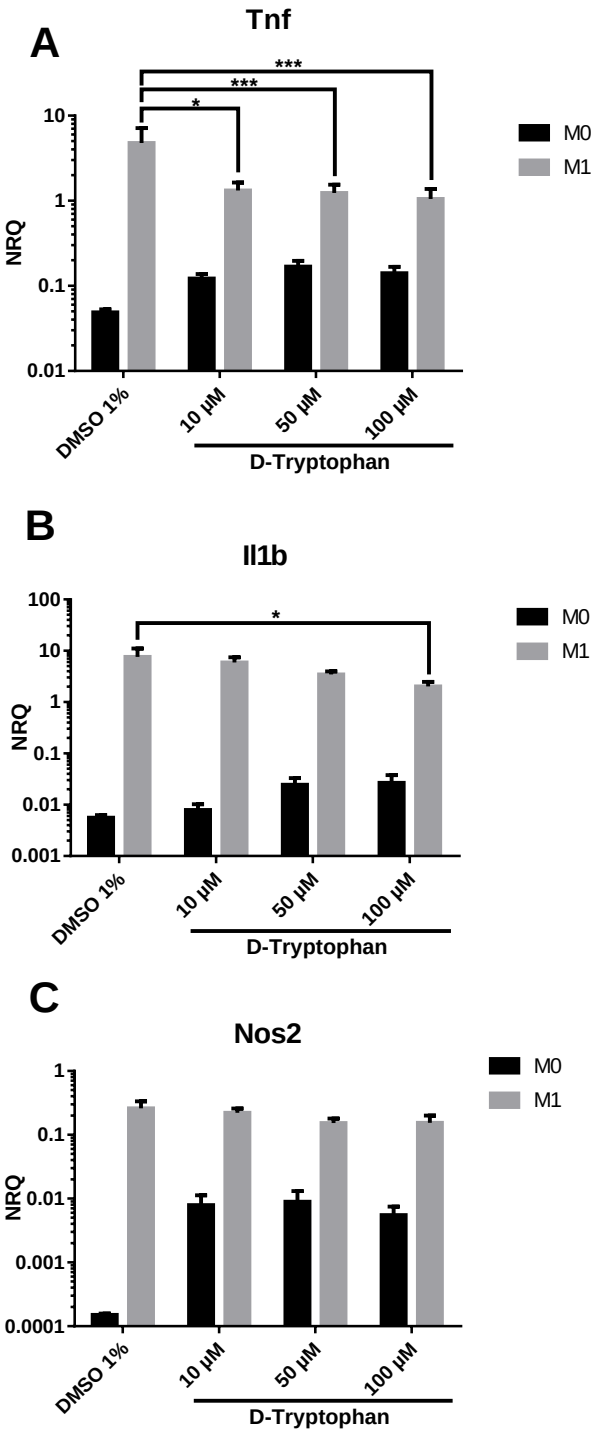

Figure 21. D-Trp effects on LPS/IFNγ induction of Tnf (A), Il1b (B) and Nos2 (C) mRNA expression in AM. MH-S cells were analyzed 24h after AHL/LPS treatment for mRNA expression relative to Hprt.
M0: no polarization; M1: LPS(+)/IFNγ(+). (n=3, values represent the mean ± SEM, *: $p<0.05$, ***: $p<0.001$)

Alike to the results observed with the AHL, the amount of protein secretion subsequent to the LPS/D-Trp treatment was measured. The data showed that LPS treatment together with a low dose of D-Trp (10 μM) increased the extracellular amount of TNFα by 1.5-fold (Figure 22). This effect was however lost with higher doses of D-Trp. As for the results obtained in Figure 11, it is likely that the reasons for the discrepancies observed between the gene expression and the protein secretion are found in the simultaneous sampling of both the genetic material and the cell supernatant. Indeed, gene expression and protein release do not occur at the same time.

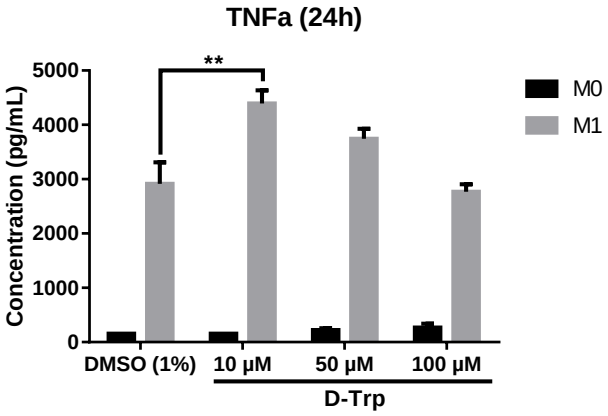

Figure 22. D-Trp treatment increases LPS/IFNγ induced TNFα release in M1.

MH-S cells supernatant was analyzed 24h after D-Trp/LPS treatment. M0: no polarization; M1: LPS(+)/IFNγ(+). ELISA assay. (n=3, values represent the mean ± SEM, ***: $p<0.001$)

3. *In vitro* D-Trp stimulates M2 polarization

Low doses of D-Trp triggered the pro-inflammatory cytokine TNFα secretion, hence showing the potency of this amino acid to increase LPS stimulated M1 polarization. Next, this study aimed to confirm whether not only the M1 but also the M2 polarization could be altered by the D-Trp cotreatment. To this end, Arg1, Mrc1 and Il10 gene expression, previously described as classic M2 markers [118], were measured. Arg1 and, to some extent also Il1b, displayed significant higher levels of mRNA levels compared to the vehicle control in the M2 polarized group. A moderate decrease of

Il10 mRNA expression was also observed in the M2 polarized group (Figure 12). Arg1 and Mrc1 displayed higher levels of mRNA expression when treated with D-Trp in the M2 polarized group. These findings indicate a shift towards M2 polarization after D-Trp treatment *in vitro*, illustrating a reinforced anti-inflammatory phenotype in the presence of both D-Trp and IL-4, at concentrations as low as 10 µM. The results corroborated the hypothesis that D-Trp induces an immune tolerance where the effects were driven towards the suppression of T cells proliferation as described in previous studies [102]. This could be explained by D-Trp modulating Mrc1 expression through the IDO enzyme [155].

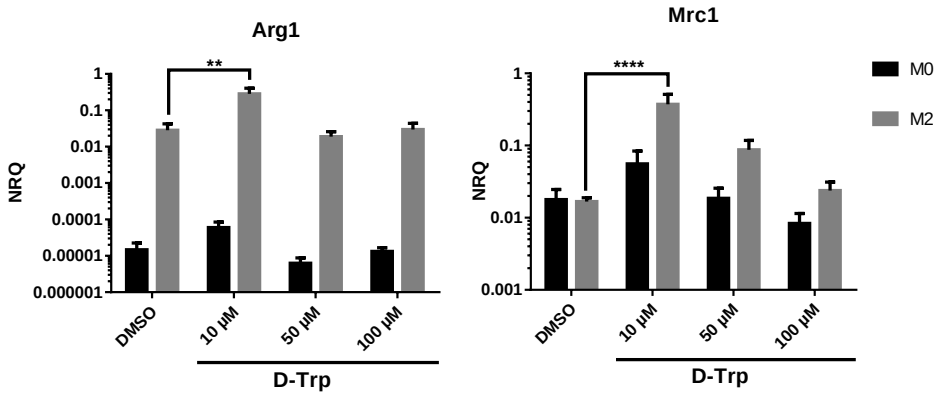

Figure 23. D-Trp treatment increases IL-4 induced Arg1, and Mrc1 mRNA levels in AM. MH-S were analyzed 24h after AHL/LPS treatment for mRNA expression relative to Hprt.
M0: no polarization; M2: IL-4(+). (n=3, values represent the mean ± SEM, **: $p<0.01$, ****: $p<0.0001$)

4. High concentration of D-Trp drives M1 polarization in AEC/AM cocultures

Considering the highest D-Trp concentration tested in cocultures of AM with alveolar cells type 2 (AECII) (100 µM), the results showed that without other stimuli, unpolarized AM increased their Tnf and Il1b expression by 4 and 11 folds respectively (Figure 24 A). This effect was not seen for AM monocultures. This suggest that AECII in collaboration with AM recognize high amounts of D-Trp and increase pro-inflammatory genes expression. However, this effect is lost under low D-Trp

concentrations, where Tnf and Il1b level are comparable with the control after LPS stimulation.

Surprisingly, no significant effect was observed on the Arg1 mRNA expression level, representative of the AM alternative polarization (Figure 24 B). Indeed, it has previously been shown during *in vitro* studies that consecutively to AM apoptosis and TNFα secretion, AECII were producing IL-6, which in turn increased M2 related gene expression [14,156].

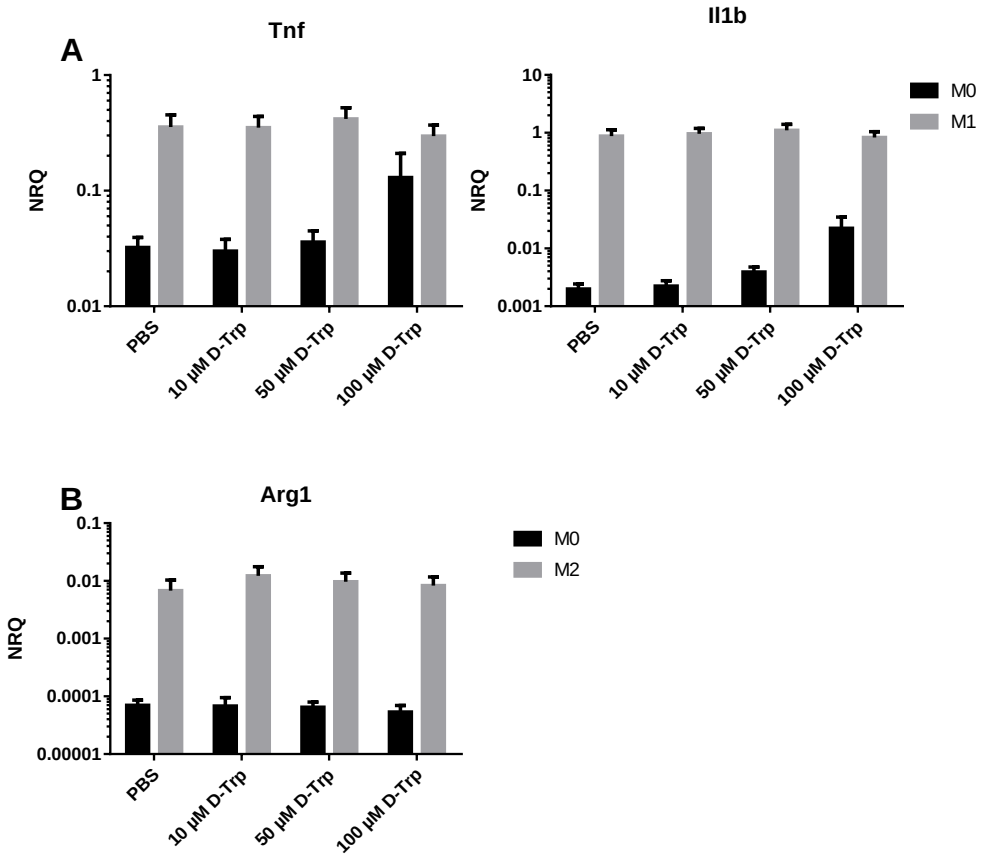

Figure 24. 100 µM D-Trp treatment promoted (A) Tnf and Il1b mRNA expression for M0 AM, and (B) did not influence IL-4 induced Arg1 level in AM/AECII coculture. MH-S/LA-4 cells were analyzed 24h after D-Trp/LPS treatment for mRNA expression relative to Hprt.
M0: no polarization; M1: LPS(+); M2 : IL-4(+). (n=3, values represent the mean ± SEM)

5. Wound healing efficiency is mildly reduced by D-Trp treatment on AECII monolayer

Racemic (D-/L-) Trp has been shown to help wound healing of skin related injuries [157,158]; however, its effect on the lung epithelium had not been studied yet. Two AECII cell lines (LA-4 and MLE-12) were selected to assess the possible cell specificity of D-Trp. The results showed that similar to the previous AHL experiments, D-Trp did not promote epithelial wound healing on AECII/AM cocultures. The data even showed a minor reduction in wound healing for both cell lines LA-4 and MLE-12 after 24h D-Trp treatment (100 µM and 10 µM respectively). In comparison to the AHL effects on wound healing, D-Trp had a rather low biological impact on the repair process (Figure 17 and Figure 25) with an average repair above 75% for all conditions. In total, D-Trp did not support AECII/AM repair in our model of lung epithelium physical injury. The mechanical stress obtained during the injury likely promoted the AM to a M1 polarization, increasing TNFα release and subsequently TGF-β1 production. The TNFα increase due to the exogenous D-Trp (Figure 22) created a cytokine rich environment, potentially contributing to a dysregulated epithelial wound repair [159].

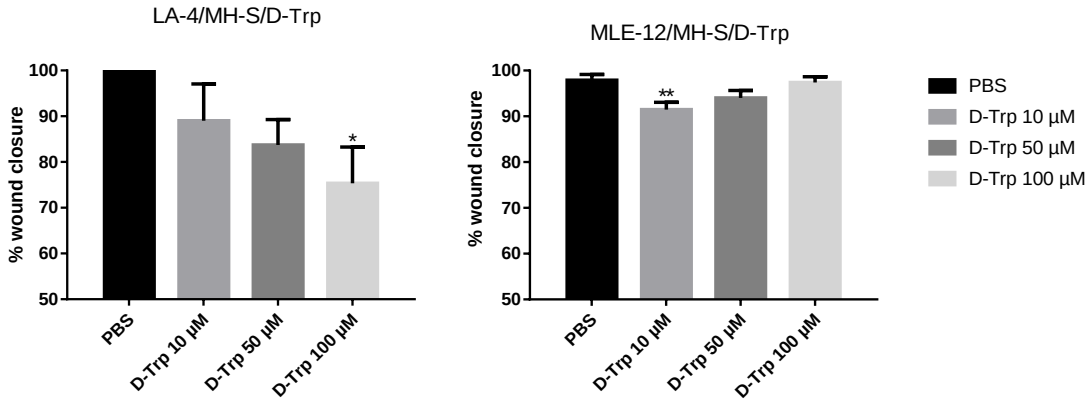

Figure 25. D-Trp mildly impairs wound closure of AECII monolayer and AECII/AM coculture. LA-4/MLE-12/MH-S cells were cultivated from 0 to 24h after simultaneous scratch and treatment with PBS or D-Trp (10-50-100 µM). Wound widths were determined 0 and 24 hours after wounding. (n=3, values represent the mean ± SEM, *: $p<0.05$)

6. D-Trp moderately limits neutrophil (PMN) recruitment after acute lung injury (ALI)

The probiotic by-product D-Trp, as presented before, displays a distinctive structure compared to the AHL and possesses also a mode of action independent of TLRs. In this study, D-Trp has been shown to induce various pro- and anti-inflammatory signals *in vitro*. To further investigate its potential anti-inflammatory effects, a similar protocol as used with the AHL was set. Firstly, a gradient of D-Trp was tested to determine the best concentration to use, aiming for a robust therapeutic effect, considering the limits of an intratracheal application, as well as the potential toxicity of D-Trp (Figure 26). No significant PMN recruitment was observed for D-Trp concentrations up to 1 mM. The local concentration is expected to be much lower than 1 mM due to dilution effect in mucus [160].

During the course of acute lung injury (ALI), the D-Trp treatment time of instillation can be crucial. Since the potency of the amino acid is unknown, D-Trp can be used in the early onset of the inflammation, a few hours later, or during its peak. The LPS induced inflammation is peaking between 8 and 24h [161,162]. Hence, the treatment should be administered before this window. Two possible mode of actions of the D-Trp treatment are hypothesized. On one hand, D-Trp could carry anti-inflammatory properties, reducing the level of inflammation at peak time (8-24h). Alternatively, D-Trp could support a pro-resolving effect, playing a role after the inflammatory peak (24-48h). Analyzing BAL content before and after the peak would allow to assess the resolution kinetics and give evidence towards a possible mode of action.

To cover two time points, a simultaneous as well as a 6h delayed application was chosen for the D-Trp treatment. Indeed, the tracheal treatment is a semi-invasive technique; in regard of the animals' stress level and to minimize unwanted interactions, the mice should also benefit from a resting time between the anesthesia.

After the establishment of an ALI, the 6h delay between LPS and D-Trp application was crucial to obtain a biologically relevant effect on PMN recruitment (Table 4). These results gave evidence for an anti-inflammatory mode of action. Also, the time course of the ALI revealed that the peak of the inflammation likely occurred before

24h (Figure 27). Furthermore, simultaneous treatments did not influence PMN numbers in the BAL, making a preventive treatment against ALI unlikely to have positive responses. A larger scale experiment confirmed the previous results: when D-Trp treatment occurred 24h after ALI, the total number of BAL cells and PMN were significantly reduced (Figure 28). A higher cell number reflects a stronger inflammation, characterized by a higher vessel permeability correlated with a higher cytokine concentration.

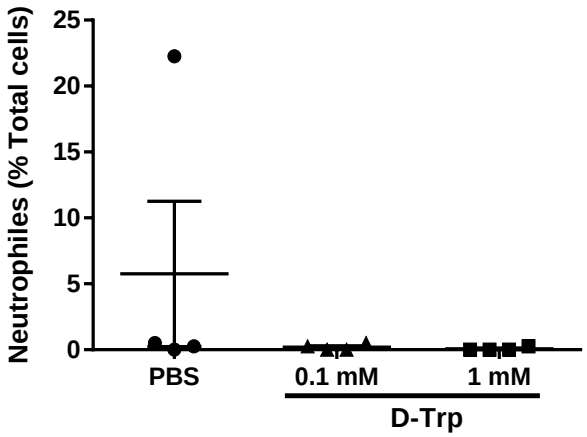

Figure 26. Intratracheal application of D-Trp does not trigger PMN at concentrations up to 1 mM. Percentage of PMN in BAL 24h after D-tryptophan application. 0 to 1 mM (50 µl) D-Trp were applied *in vivo* intratracheally. BAL was harvested after 24h and cells were counted manually (n=4/condition). NB: The PBS control reaching 22% PMN can be explained by the invasive treatment method where small lesions in the trachea can appear during the intubation, creating a small inflammation on its own.

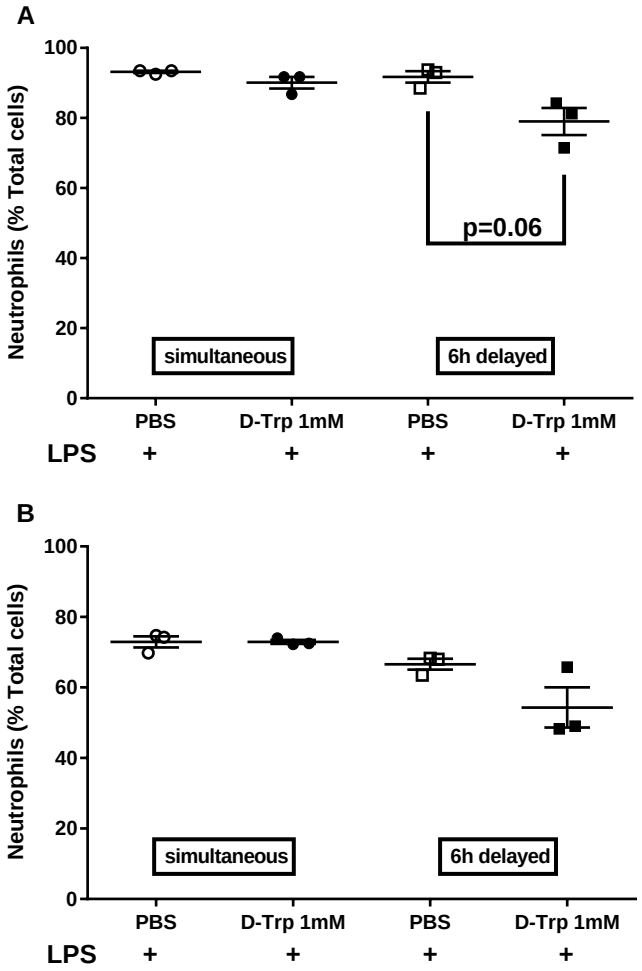

Figure 27. D-Trp reduces neutrophils recruitment when applied 6h after LPS.

Percentage of PMN in BAL 24/48h after LPS with or without D-Trp treatment (simultaneous or 6h delayed). (A) 24h (B) 48h after LPS treatment. (n=3/condition)

		SIMULTANEOUS		6h DELAYED	
		PBS	D-Trp 1mM	PBS	D-Trp 1mM
24h	**PMN (% total cells)**	93,17	90,08	91,75	79,00
48h		72,92	72,92	66,58	54,33
	PMN reduction	**22%**	**19%**	**27%**	**31% (p=0.06)**

Table 4. Summary data of neutrophils presence in BAL after LPS induced ALI.

Percentage of PMN in BAL 24/48h after LPS with or without D-Trp treatment (simultaneous or 6h delayed), (n=3/condition)

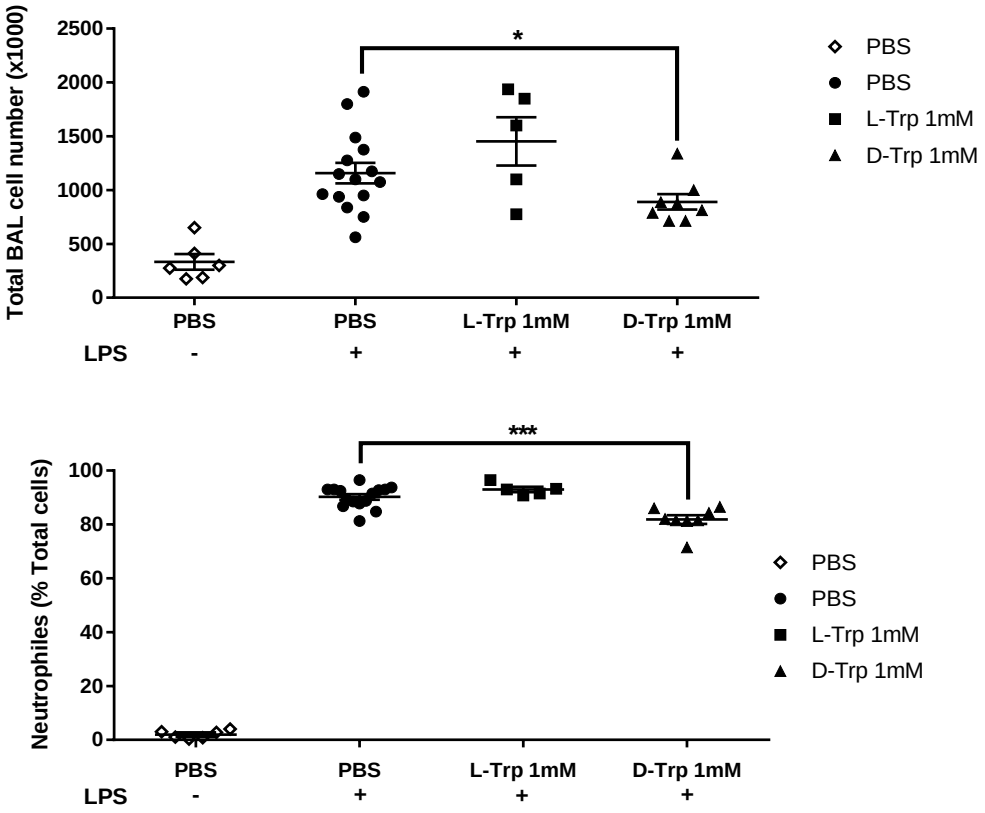

Figure 28. D-Trp, but not L-Trp treatment reduced BAL PMN numbers 24h after ALI. BAL cell-count 24h after D-Trp (1 mM, 6h delayed) intratracheal instillation (n=6-15). (*: $p<0.05$, ***: $p<0.001$, unpaired t test with Welch correction)

7. CCL17 concentration declines in BAL after ALI and D-Trp treatment

BAL cytokine analysis and quantification were performed to assess the onset of inflammation and to understand at which level D-Trp interferes with the epithelium. Following the results showing a lower BAL cell count by D-Trp treatment, a mild reduction of the total BAL protein was observed (Figure 29). ELISA immunoassays and Bradford protein assay were then conducted to characterize the BAL constitution during the resolution of ALI. Protein candidates were chosen considering their relevance on immune cells during ALI. The chemokine (C-X-C motif) ligand 1 (CXCL1) is a major cytokine involved in triggering PMN recruitment, mediated by both TNFα and NF-ϰB signaling [163] (Suppl. Fig. 8; CCL17 is implicated in effector/memory T_h1 lymphocytes attraction and is elevated at several inflammatory conditions [164–166]). Furthermore, several D-Trp containing probiotic supernatants have been shown to decrease CCL17 expression (human Hodgkin lymphoma KM-H2 cells), as well as reducing costimulatory molecules of LPS-stimulated human dendritic cells [67]. To extend Kepert et al. results to lung injuries, CCL17 concentration was measured. D-Trp treatment 6h after LPS instillation significantly reduced CCL17 expression (5 mM) in the BAL 24h after LPS instillation, as previously described *in vitro* [67]. Also, a trend towards reduced CXCL1 expression was observed after D-Trp instillation (Figure 30). The 5 mM dosage was provided in order to validate the mice tolerance for a high dosage of D-Trp in an injured environment. Altogether these results confirm that D-Trp has an active role in inflammatory protein modulation. However, the molecular cascade leading to a faster resolution of the inflammation is unclear.

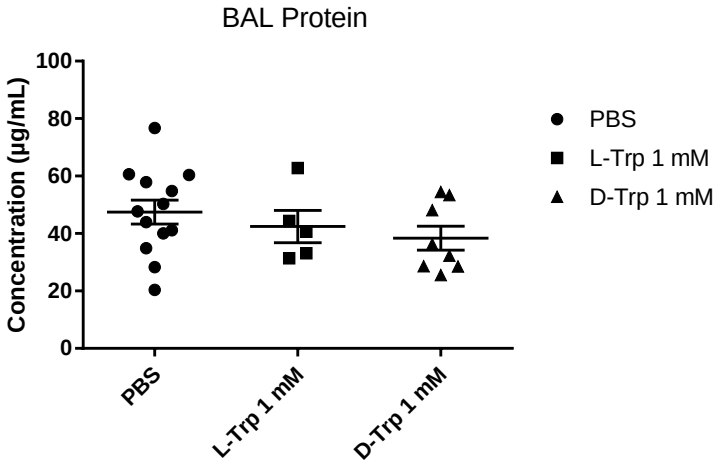

Figure 29. D-Trp treatment did only slightly influence BAL protein concentration after LPS treatment. BAL protein concentration 24h after D-Trp or L-Trp (1 mM) intratracheal application. BCA assay (n=4-15).

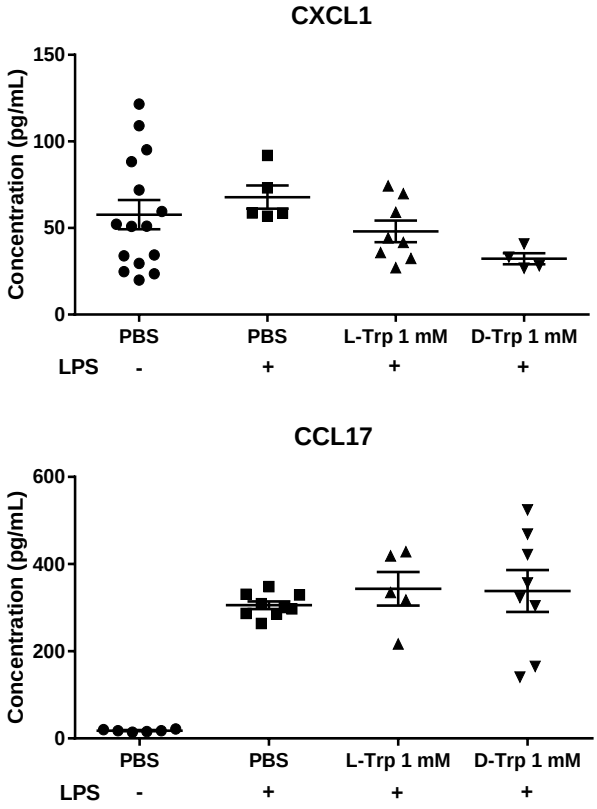

Figure 30. High concentration of D-Trp (1 mM) tend to reduce the expression of key inflammatory cytokines in the BAL. BAL cytokine concentration 24h after LPS instillation. Assessed by ELISA (n=4-15). (*: $p<0.05$, ***: $p<0.001$, unpaired t test with Welch correction)

8. D-Trp reduces mRNA expression of CD11b, Alox12 and Fpr2 in whole lung homogenate

In this study, the data showed that BAL cytokine concentration and PMN numbers were reduced after ALI and D-Trp treatment. Lower PMN numbers and a shift towards reduced inflammation or enhanced resolution can be highlighted by lung mRNA analysis.

D-Trp metabolism is brought about by intracellular and extracellular mechanisms, bringing into play its biosynthesis in microbes (Suppl. Fig. 9) and its metabolism in pro- and eukaryotes (Suppl. Fig. 10). This study focused on the latter, considering that mammalians are unable to synthesize it [66]. The previous experiments indicated that inflammatory pathways were modulated by D-Trp treatments *in vivo* leading to reduced inflammatory response or/and enhanced resolution. Indeed, evidence of changed cell populations as well as in cell number, together with reduced inflammatory cytokine concentration showed an altered composition of the BAL. However, the pathways in place responsible for PMN or AM recruitment were still unidentified. Transcript analysis from whole lung was then analyzed to gain an insight on the mechanisms leading to modulated inflammation. It was hypothesized that PMN were majorly responsible for the release on the investigated inflammatory cytokines CXCL1 and CCL17, as well as resident macrophages and recruited AM, participating both in the first response and the injury resolution. Then, the expression of a small panel of genes was studied, consisting of previously described common PMN and AM markers, as well as D-Trp receptors involved in D-Trp metabolization. Integrin alpha M (CD11b) is expressed by several leucocytes, particularly PMN ($CD11c_{low}CD11b_{high}$) [167] and inflammatory activated alveolar macrophages [167]. Its mRNA levels were reduced by a factor of 4 in D-Trp treated lungs (Figure 31), while BAL PMN numbers have been found to be reduced by 10%. This decrease in CD11b expression suggests that in addition to the contribution from a reduction in PMN numbers in the lung, persisting 24h after LPS application, also other cells such as $CD11b^{+}$ macrophages might show reduced activation upon D-Trp treatment. Serum amyloid A 3 (Saa3), a well described inflammatory factor [168],

rapidly and powerfully induced by LPS in lung macrophages, was not regulated by D-Trp. This argues that the initial response to LPS was not affected by D-Trp. To monitor the regulation of inflammation, the expression of murine 12-lipoxygenase (ALOX12) resolution protein, the analogue to the human 15-lipoxygenase (ALOX15) [169–171], was studied. In the biosynthesis of lipoxins and other pro-resolving mediators, ALOX15 has a pivotal role in the resolution of inflammatory responses [172]. Its concentration is increased in M2 macrophages after IL-13 activation due to its positive feedback loop. Altogether, ALOX12 participates in the resolution of the inflammation through the synthesis of lipoxins [173] (Suppl. Fig. 11). However, no significantly increased expression of Alox12 was observed, nor of the lipoxin receptor FPR2 [174] (Figure 31). This may be explained by the time course of the experiment: IL-13 activation and subsequent polarization of the macrophages requires previous T cell recruitment and interaction in the lung. Probably, the 24h window was too short to measure the responses.

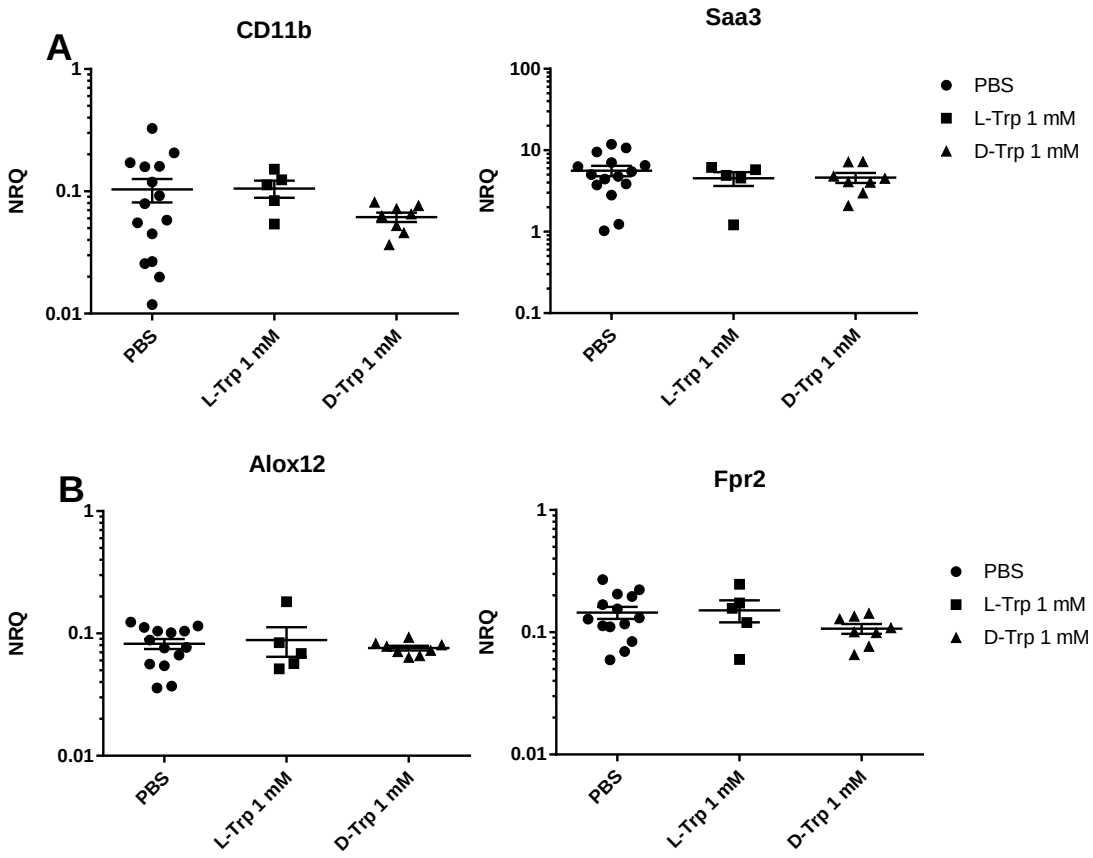

Figure 31. (A) D-Trp effect on CD11b and Saa3 expression as well as on (B) macrophages inflammation markers Alox12 and Fpr2 in whole lung homogenate 24h after LPS (t=0) and D-Trp treatment (t=6h). mRNA expression relative to Hprt (n=4-15). (*: $p<0.05$, **: $p<0.01$, unpaired t test with Welch correction).

9. IL-6 increase in AhR$^{-/-}$ M1 BMDM is reduced after D-Trp treatment.

Following earlier results showing the direct or indirect involvement of the aryl hydrocarbon receptor (AhR) on lung immunity, this study aimed to discover whether D-Trp anti-inflammatory effect is dependent on the presence of the AhR using AhR$^{-/-}$ cells. Bone marrow macrophages from AhR$^{-/-}$ (Ahr^{tm1Bra}) mice [175,176] were cultured for seven days, differentiated into AM, and polarized following the method described in MATERIALS AND METHODS (Table 5). The polarization efficiency was measured through the levels of robust AM mRNA markers and proteins.

AhR$^{-/-}$ and AhR$^{-/+}$	**PBS**	**D-Trp 50 μM**	**D-Trp 100 μM**	**L-Trp 100 μM**
LPS (1 μg/mL)	x	x	x	x
IL-4 (20 ng/mL)	x	x	x	x
No polarization	x	x	x	x

Table 5. Combination matrix of experimental planning. 24h stimulation of LPS (M1 AM), IL-4 (M2 AM) combined with D-Trp/L-Trp application).

The inflammatory cytokine IL-6 was induced to higher levels in AhR$^{-/-}$ BMDM. These results confirmed previous works [177], where the aryl hydrocarbon receptor was described as the cornerstone of the tolerance defense pathway. The early response failed unless the AhR$^{+/-}$ was activated by D-Trp (Figure 32). Furthermore, relative to PBS, high dose of D-Trp (100 μM) induced IL-6 in AhR$^{+/-}$ BMDM but was repressed in AhR$^{-/-}$ cells. These results were confirmed to a lesser extend at protein level, where supernatants of D-Trp treated AhR$^{-/-}$ cells showed slightly lower concentration of IL-6 than the PBS control cells (Figure 33). M2 marker (Mrc1 and Arg1) were increased in D-Trp/IL-4 polarized BMDM only in the AhR$^{+/-}$ genotype. It suggests that AhR plays a role in early inflammation response helping M2 polarization. All these results pointed towards AhR and NF-κB downstream signaling

leading to an increased Cytochrome P4501-1A1 (CYP1A) activity as well as xenobiotic metabolism through the kynurenine pathway.

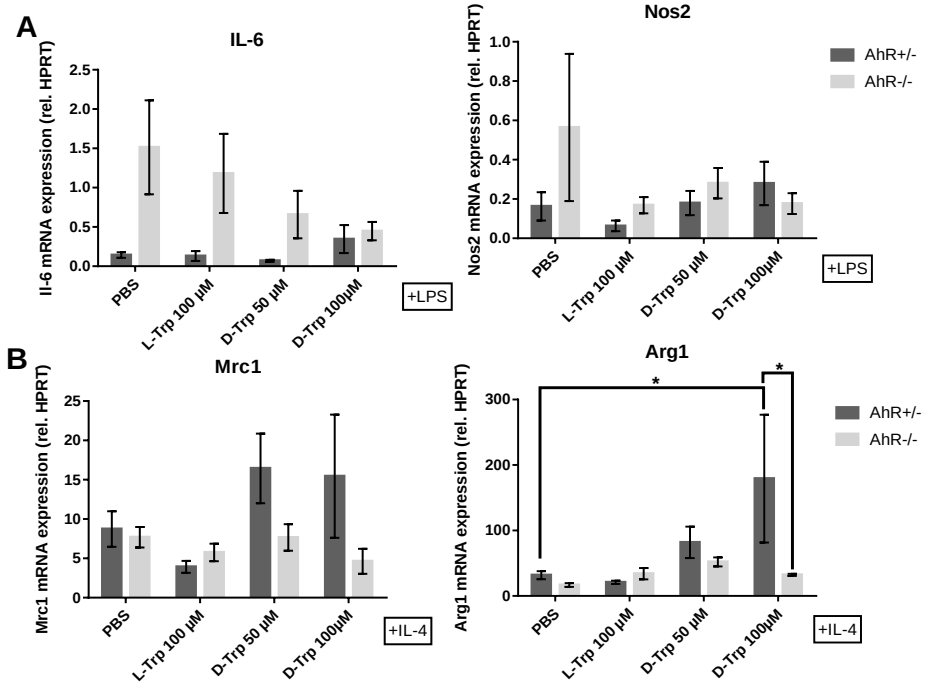

Figure 32. mRNA expression levels of inflammation markers in response to L-/D-Trp in AhR$^{-/-}$ and AhR$^{+/-}$ BMDM after (A) LPS and (B) IL-4 stimulation. AhR$^{-/-}$ BMDM display increased Il-6 and Mrc1 expression after LPS stimulation, reduced to WT level after D-Trp treatment. BMDM were incubated 24h after D-Trp or L-Trp treatment and polarization. The mRNA expression is relative to Hprt. (n=6, values represent the mean ± SEM, *: $p<0.05$)

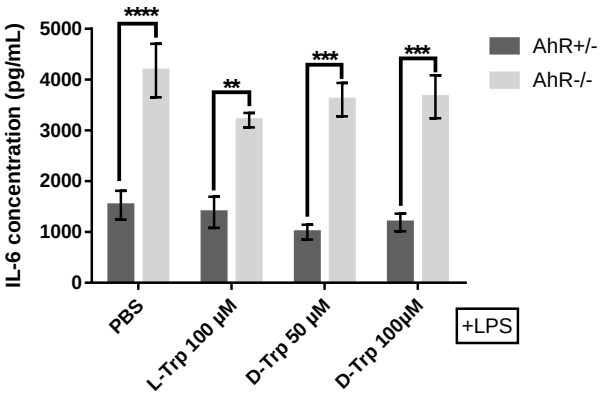

Figure 33. IL-6 concentration after L-/D-Trp treatment in AhR$^{+/-}$ and AhR$^{-/-}$ mice. AhR$^{-/-}$ BMBM showed increased IL-6 concentration after LPS stimulation. BMDM were incubated 24h after D-Trp/LPS treatment. ELISA assay (n=6, values represent the mean ± SEM, **: $p<0.01$, ***: $p<0.001$, ****: $p<0.0001$).

10. AhR signaling mediates D-Trp activity through both the kynurenine and the Cyp1a1 pathway and NF-ϰB regulation.

D-Trp and L-Trp are both agonists of the aryl hydrocarbon receptor (AhR) [178]. However, D-Trp might have a much greater affinity to the receptor (Figure 34), which could be explained by the configuration difference between the two amino acids [179]. It had been shown that AhR is involved in immune responses, and that LPS stimuli induced an AhR-dependent CYP1A1 increase [176] (Figure 35). The absence of AhR reduced mRNA expression of key proteins in the kynurenine and the NF-ϰB pathways for both LPS and IL-4 treated BMDM was tested. Furthermore, D-Trp displayed a bioactivity threshold of 100 μM, from which BMDM drastically increased Ido1 and Cyp1a1 mRNA expression. The increased activity of AhR by D-Trp binding could be part of a feedback loop involving D-Trp metabolites [180]. This increased metabolic activity of D-Trp is consistent with the regulation of immunity observed in AM through inflammation, towards an increased or faster response.

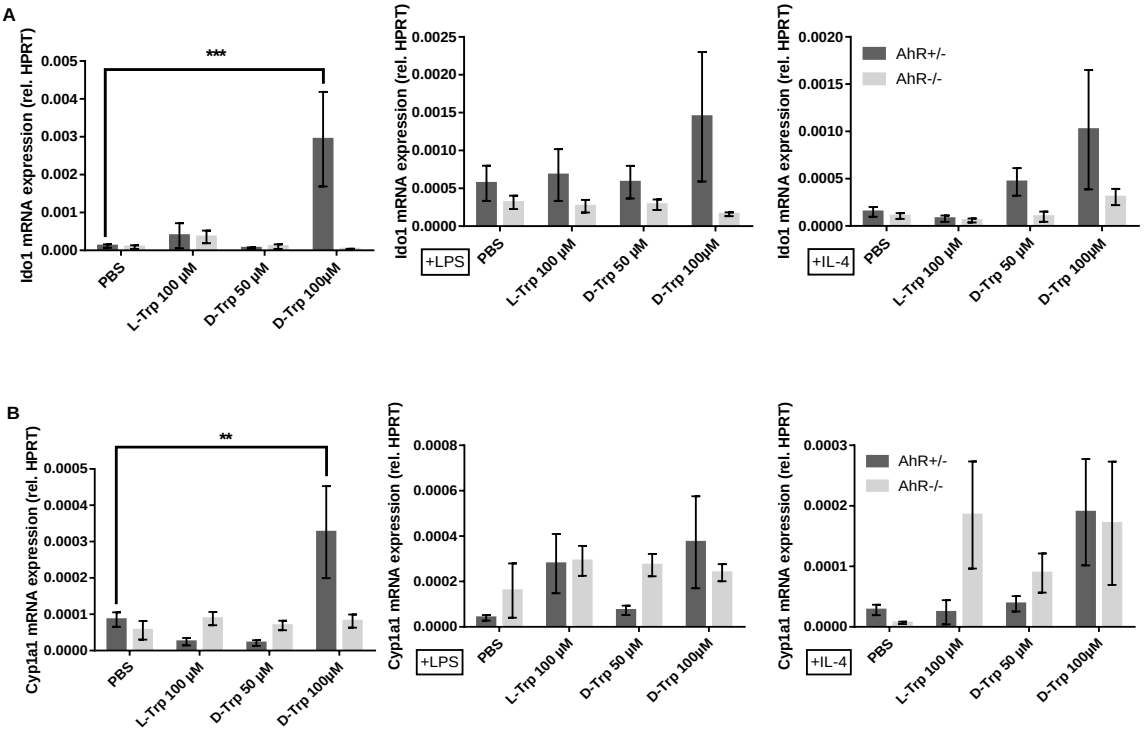

Figure 34. AhR dependent Ido1 (A) and Cyp1a1 (B) mRNA expression in AhR$^{+/-}$ and AhR$^{-/-}$ BMDM. D-Trp increases mRNA expression of Ido1 and Cyp1a1 (key AhR downstream targets) in BMDM. BMDM were incubated 24h after LPS or IL-4 treatment. The mRNA expression is relative to Hprt. (n=6, values represent the mean ± SEM, **: p<0.01, ***: p<0.001)

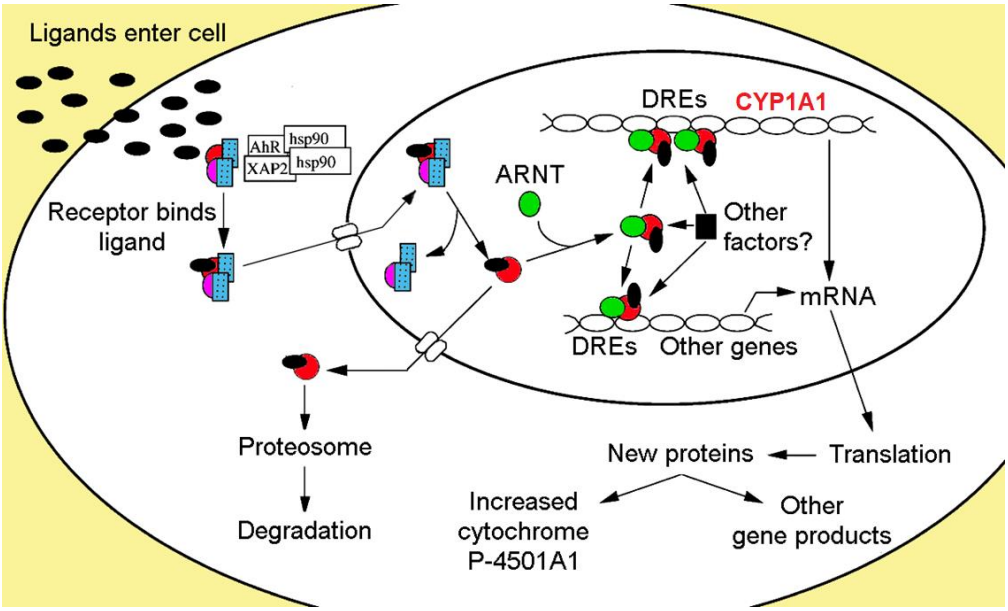

Figure 35. Molecular mechanism of activation of gene expression after AhR-ligands interaction [178]. Exogenous ligands penetrate the cell through lipid interactions and binding to the AhR.

11. D-/L-Trp impairs a key enzyme of the AhR/kynurenine pathway

Eukaryotes regulate the Trp-metabolization through different enzymes participating to the indole, kynurenine or serotonin pathway (Suppl. Fig. 10). D-/L-Trp is an agonist of the AhR-receptor, mediating immune tolerance and immunity following IDO induced D-/L-Trp catabolization through the kynurenine and AhR activation pathway (Figure 36) [181].

The focus was made on the kynurenine pathway, being downstream the recognition of D-Trp recognition by the AhR. Indeed, evidence suggests that the kynurenine pathway is participating in T-cells modulation, and more generally in mediating reduced immune response [102,176]. The first and limiting step of this pathway is the catabolization of the L-Trp and D-Trp into kynurenine by the Indoleamine 2,3-dioxygenase 1 enzyme (IDO1) [182]. Surprisingly, Ido1 expression in the whole lung was reduced after D-Trp treatment which contrast with the hypothesis that a greater Trp intake would increase the enzyme metabolic activity (Figure 37), nor was it increased consequently to a TNFα inflammatory response [79], [80]. D-Trp is more likely to be metabolized involving other enzymes also participating to the kynurenine pathways such as the tryptophan 2,3-dioxygenase 1/2 (TDO1/2) or IDO2. These findings unraveled the AhR as a key player in D-Trp mediated immunity, especially in acute inflammation.

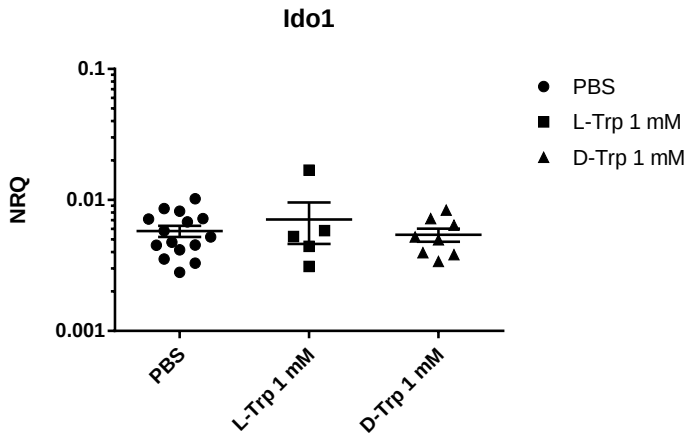

Figure 36. Ido1 mRNA expression in whole lung homogenate 24h after consecutive LPS and L-/D-Trp treatment. mRNA expression relative to Hprt (n=4-15). (**: $p<0.01$, unpaired t test with Welch correction)

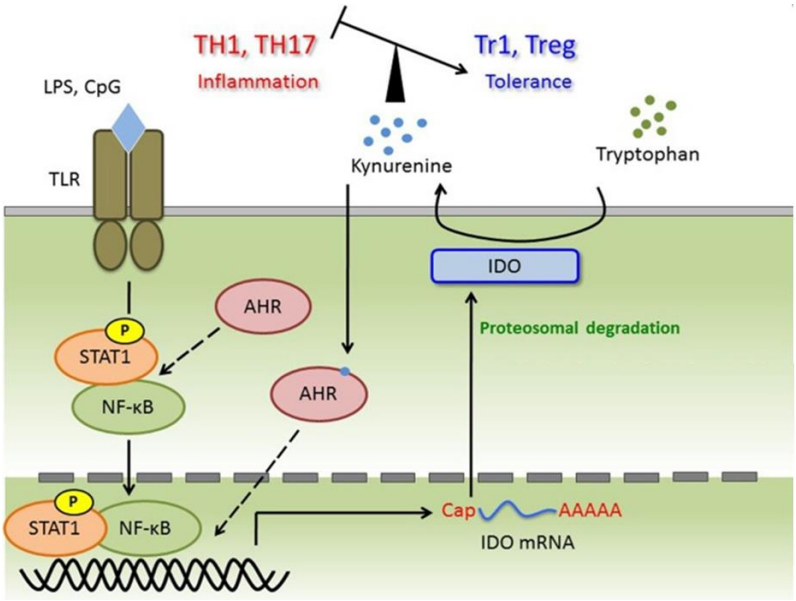

Figure 37. Toll-like receptor ligands trigger transcriptional activation of STAT-1 and NF-ϰB, and then induce IDO mRNA. Adapted from [181].

DISCUSSION

I- EFFECT OF N-ACYL HOMOSERINE LACTONE COMPOUNDS OF GRAM-NEGATIVE BACTERIA ON LUNG EPITHELIUM AND IMMUNITY

1. Quorum sensing and Pseudomonas aeruginosa

Quorum sensing (QS) signaling molecules are not necessarily limited to bacterial-bacterial signaling [183,184] but also involved in inter-kingdom communication, for example with human immune cells [185]. In that context they may not exclusively be linked to pathogenesis either considering that QS is used in plants by several probiotic bacterial species; this mechanism being the reflection of their ability to colonize various niches [70]. For example for the bacteria *Pseudomonas aeruginosa* (PAO1), the prominent QS molecule 3-oxo-dodecanoyle homoserine lactone (3-oxo-C_{12}-HSL), from the acyl-homoserine lactones (AHL) family, is secreted and recognized by a set of two major bacterial signal components: LasI/LasR and RhlI/RhlR [186]. However, 3-oxo-C_{12}-HSL can beyond bacterial interaction also modulate the immunity of the host [74–78,85] by activating non canonical immune pathways, independent from pathogen-associated molecular pattern (PAMPs) and the respective pattern recognition receptors (PRRs) [90]. 3-oxo-C_{12}-HSL controls the production of *Pseudomonas aeruginosa* virulence factors [187], giving it a selective advantage in pathogenic interactions. Besides N-Acyl-HSL, AQ-QS system exists in *P. aeruginosa*, which is able to modulate the immune response to human bronchial epithelial cells [137].

2. 3-oxo-C_{12}-HSL effect on $T_h2/17$ cells differentiation

It has been previously shown that 3-oxo-C_{12}-HSL inhibits T_h2 differentiation [77]. The differentiation of the T_h cells was assessed from their ability to produce their relevant cytokines. Interestingly, our findings suggest for the first time that C_{12}-HSL (50 µM/48h) mildly impairs IL-4 production of T_h2 cells (Figure 9). Furthermore, it has been demonstrated that IL-17 production increases rapidly after *Pseudomonas* infection [188]. In the same manner, our results illustrated an increase of IL-17 production on the T_h17 differentiated cells after 3-oxo-C_{12}-HSL stimulation (100 µM/48h and 100 µM/96h). 3-oxo-C_{12}-HSL and C_{12}-HSL possess similar molecular features (lactone ring and alkyl chain length). This could explain the comparable reactivity of the two AHL.

The results presented in this doctoral thesis suggests a shift of T_h cells differentiation towards T_h17 as well as a reduction in T_h2 differentiation. The T_h immune cells upon AHL-application present a more inflammatory phenotype. Earlier hypotheses support a ubiquitous impairing role of AHL on immune cells in both innate and adaptive immune response. However, no significant AHL-induced anti-inflammatory effect was observed, despite being discussed in previous studies [78].

3-oxo-C_{12}-HSL has the highest potency for IL-17 induction, while C_{12}-HSL has the highest potential for IL-4 repression. These findings indicate that the actions of different AHLs rely on different pathways or receptors in differentiated T cells. Consequently, the impact of AHL on T cell cytokine production suggests a complex model involving possibly other immune response cells mediating the interaction. Indeed, T cells maturation is triggered by APC/T cell co-stimulation involving T cells receptors (TCR) and the major histocompatibility complex (MHC) [189]; the APCs consisting mostly of DCs and macrophages in a lesser extent. Newly differentiated T_h cells will then in turn recruit macrophages via inflammatory cytokines (*i.e.* IFNγ) to the site of inflammation [190]. Thus, airborne bacteria encounter first AM and epithelial cells in the lungs. This may subsequently modulate T cell recruitment or function. Thus, in current experiments the focus was set on the effects of AHL on AM polarization, and epithelial barrier function.

3. 3-oxo-C_{12}-HSL modulation of AM polarization and function

In the lung, the first line of defense can be seen in the alveolar epithelium, which oversimplified consists of epithelial cells type I and type II (AECI and AECII) and alveolar macrophages (AM). AECI cells cover 98% of the alveolar surface to maintain the gas exchange between the alveoli and blood [191,192], and AECII cells secrete surfactant, maintain the fluid balance and have also been described as defender of the alveolus [193]. The tissue resident AM are known for their effective uptake of inhaled particles, to fight microbes [34], and to mediate acute lung inflammation and resolution in many disease conditions [194].

3-oxo-C_{12}-HSL through its auto-paracrine signaling [71] has been shown to reduce the expression of inflammatory cytokines in AM [78]. 3-oxo-C_{12}-HSL significantly inhibited the LPS-induced inflammatory response in macrophages by reducing the secretion of pro-inflammatory TNFα, and increasing anti-inflammatory interleukin 10 (IL-10) [78]. It was shown in this thesis work, in a novel coculture model of AM and AECII cells, that 3-oxo-C_{12}-HSL increased the polarization of M2 polarized AM (Figure 15). These findings suggested an anti-inflammatory activity of the AHL causing a M2 shifted polarization. Mechanistically, this anti-inflammatory effect can be explained by the fact that 3-oxo-C_{12}-HSL impaired the activation of NF-ϰB functions which subsequently repressed the expression of inflammatory cytokines such as TNFα [89,195]. Other findings, in contrast, suggested that through a mechanism involving inflammatory signaling of protein kinase RNA-like endoplasmic reticulum kinase (PERK) and Eukaryotic Initiation Factor 2 alpha (eI-F2α), 3-oxo-C_{12}-HSL can activate PERK phosphorylation and eI-2Fα inhibition. This subsequently reduces the nuclear factor of kappa light polypeptide gene enhancer in B-cells inhibitor alpha (IϰBα) production and activated NF-ϰB p65 production [154]. This finally increases chemokine (C-X-C motif) ligand 1 (CXCL1) and interleukin 6 (IL-6) transcription, and thus selectively induces neutrophil chemotaxis [86].

Until 2018, *in vivo* immunomodulatory effects of AHL on live animals have not been described. In this thesis, the effects of intratracheal applied AHL on an inflamed lung of C57BL/6J mice were evaluated to further identify, if AHL treatment could reduce

lung inflammation, neutrophil recruitment, and inflammatory cytokine levels. To rule out any possibility of autoinflammation, a dose response was conducted. Despite the relatively small group size (2), dose response up to 1200 µM resulted in comparable cell recruitment as in the ACN control treatment (5-10% of total cells), indicating that the AHLs alone did not induce any obvious pro- or anti-inflammatory effect (Figure 19).

An impairment of the NF-κB pathway is linked to the inhibition of the peroxisome proliferator-activated receptor gamma (PPARγ), an important anti-inflammatory antagonist of NF-κB [91]. The impairment of PPARγ results in a further decrease of downstream functions such as wound repair, homeostasis, and control of inflammatory energy [196]. Disruption of barrier integrity has been observed after 3-oxo-C_{12}-HSL treatment on Caco-2 epithelial cells, and could be prevented by inhibition of p38 p42/p44 Mitogen-activated protein kinases (MAPK) [83], reducing thereby macrophage phagocytosis [197]. Results presented in this thesis (Figure 16 and Figure 17) supported *in vitro* impairment of wound repair by 3-oxo-C_{12}-HSL application for two AECII cell lines (LA-4 and MLE-12), independently of the presence of LPS (1 µg/mL).

4. Quorum sensing receptors

3-oxo-C_{12}-HSL receptors on the host cells have been partially elucidated; one target receptor of a variety of AHLs on epithelial cells seems to be the Ras GTPase-activating-like protein IQGAP1 (IQGAP1) [86,96,198]. Other groups identified the taste receptor T2R38, present on peripheral blood neutrophils, monocytes, and lymphocytes, as responsible for the entry of AHLs into the cell [96]. When in contact with AHL, epithelial cells triggered also a cascade leading to a calcium dependent repression of NO production in AM [199]. Very recent publications link the 3-oxo-C_{12}-HSL target entry into the cell to the PPARs for human lung epithelial cells and murine fibroblasts [76,200]. Jahoor et al. argued that the proinflammatory effect of 3-oxo-C_{12}-HSL on murine fibroblasts and human lung epithelial cells could be blocked by the PPARγ agonist RGZ [76], suggesting a mutually antagonistic mode of action

of the two compounds on PPARγ. These results were corroborated *in vitro*, where RGZ pre-treatment reduced Tnf expression after 3-oxo-C_{12}-HSL stimulation (Figure 15 and Suppl. Fig. 1).

Interestingly, it has been shown that the neutrophils, monocytes and macrophages taste receptor T2R38 [92] is activated by 3-oxo-C_{12}-HSL and its surface expression [201], regulating a calcium dependent NO production [199]. This defense mechanism is hypothesized to help mucociliary clearance during airway bacterial infection. Our results showed however a decreased expression of T2R38 in M1 AM *in vitro* after 3-oxo-C_{12}-HSL treatment (Suppl. Fig. 3). This suggests that the mechanism leading to T2R38 over-expression do not rely solely on 3-oxo-C_{12}-HSL. In a preliminary array experiment, all the analyzed taste receptors showed weak baseline expression and expressed no significant difference between the M1 and M2 subtypes (Suppl. Fig. 4). Of notice, Lee et al. [199] used a higher 3-oxo-C_{12}-HSL concentration (100 µM vs. 60 µM), possibly leading to the higher gene expression effect.

II- EFFECT OF D-TRP OF PROBIOTIC GRAM-POSITIVE BACTERIA EFFECT ON LUNG EPITHELIUM AND IMMUNITY

1. D-amino acids and probiotic microbiome

The lung epithelial interface is constantly in contact with the outside worlds' microbiome (including pathogens and probiotics). A healthy individual remains in a state of homeostasis thanks to the lungs immune system. Upon a greater inflammation, the individual's immune system cascade fires up. As soon as pathogenic microorganisms and their products try to find their way infecting the hosts' body, the innate response machinery is triggered. Its main line of defense consists in phagocytes and PMN; nonspecific leucocytes aiming in killing the infection before it starts to spread [5]. This primary cell activation works simultaneously with several biological phenomena, such as increased mucus in the lungs, swelling or

redness. This study focused mostly on this acute phase and its resolution. After the threat, a quick return to the homeostasis is vital for the organism.

Mammals and in particular humans have evolved to exist and thrive in a quasi-symbiosis with a multitude of microorganisms. They cover the skin on the outside, are present in our lungs, and the digestive tract on inside surfaces. These microbes are not only mostly inoffensive, but they are commensal (*i.e.* beneficial). As such, they are non-invasive, and protect the host by competing against the proliferation of pathogenic bacteria.

Different kinds of bacteria shape the lung microbiome; pathogenic (*Moraxella catarrhalis*, *Haemophilus influenzae*, and *Streptococcus pneumoniae*) as well as commensal and even beneficial (*Bacillus*, *Lactobacillus*, *Lactococcus*, *Staphylococcus*, *Streptococcus*, and *Streptomyces*). The commensal Gram-positive bacteria *Lactobacillus casei* and other beneficial strains produce D-Trp, a D-amino acid recently discovered to be involved in various immunological processes within the colonized host [67].

L-amino acids are the most common amino acid enantiomer used by mammals [202], and are a necessity for the organism, and its immune response [203]. The amino acids are the building blocks of the immune proteins' synthesis (cytokines, and antibodies), which are responsible for T cells, B cells, and macrophages activation or proliferation. One might not expect that a single amino acid could trigger or influence an immune response on its own. However, our data presents *in vitro* as well as *in vivo* strong immunological evidences towards lung injury resolution due to D-Trp treatment.

The role of probiotic bacteria has been extensively studied in the gut [204,205], with PubMed reaching 11,990 hits as of September 2018 for the keywords "gut microbiome". "Lung microbiome" however totaled 1050 hits, and "lung microbiome immunity" a shy 206 hits (Table 6). Only one publication focused on D-Trp and its effect regarding airway diseases [67], where D-Trp, and not its L-enantiomer successfully reduced CCL17 human Hodgkin lymphoma cell line *in vitro* as well as decreased gut T_{regs} numbers and T_h2 response. The results from this study corroborate the one from Kepert et al., where other D-amino acids were found to be

immunologically inactive; particularly towards macrophage polarization (Suppl. Fig. 6).

‘Keywords	PubMed hits
Microbiome	46224
Gut microbiome	11990
Lung microbiome	1050
Gut microbiome immunity	1400
Lung microbiome immunity	206
D-Trp gut	2
D-Trp lung	10

Table 6. Comparative table of PubMed hits in September 2018 against selected keywords. Although the microbiome has been fairly studied; its relation to the lung, and to immunity remain poorly understood. The specific role of D-Trp is a very novel topic.

2. D- and L-tryptophan functions

D-Trp is a byproduct of the peptidoglycan cell wall synthesis in Gram-positive bacteria which contains several D-amino acids. However, its roles in bacterial signaling and cross signaling are still mostly unknown. In the host, the L-Trp isomer is predominant and serves as a precursor for a variety of substrates, the most known being serotonin and kynurenine (Suppl. Fig. 10). However, Trp studies used a racemic mix or L-Trp only, largely ignoring the D-enantiomer. This created an abundance of data regarding the interplay of D-/L-Trp and immunology, scarcely considering the specificity of the D-enantiomer of Trp regarding inflammation [67] or microbial properties [206].

3. D- and L- amino acids against microbes

Most L- amino acids promote to variable extents growth and formation of biofilms [207]. On the contrary, D-amino acids effects on biofilm formation did not reach a general consensus. They have been shown on one hand to inhibit *Bacillus subtilis* biofilm formation [208] or to trigger the biofilm disassembly [209]. On the other hand Kao et al. [210] did not observe any inhibitory effect of D-amino acids on *Pseudomonas aeruginosa's* moderately virulent (PAO1) and virulent (PA14) strains [211] biofilm formation, concluding that D-amino acids were not a viable treatment against *Pseudomonas aeruginosa's* infections. Brandenburg et al. [157] showed that bacterial biofilm synthesis on wounds is inhibited by D- and L-Trp. Considering these results, it appears that the great diversity of bacteria seems to respond differently upon D-Trp supplementation or treatment. Our investigation focuses primarily on the effects of D-Trp on mammalian cells described by Kepert et al. [67], and particularly on AM and epithelial cells.

Koseki et al. [212] studied the influence of L- and D-amino acids on bacterial growth *in vitro*. Interestingly, they showed that only D-Trp reduced significantly as an incompatible substrate bacterial growth of *Listeria monocytogenes*, *Salmonella enterica*, and *Escherichia coli O157:H7*. These results were in contrast with Chan et al. [213], who described that D-enantiomers showed less antimicrobial activity, although deciding racemic Trp (and Arg) as potential antimicrobial agents. D- and L-amino acids have also been used for fighting against pathogens, in the form of engineered antimicrobial peptides. Yet, Muñoz et al. [206] showed similar properties for the antimicrobial properties of the tryptophan-rich hexapeptide PAF26 for both isomers of tryptophan. In this study, alveolar macrophages (AM) Il1b, Tnf and Nos2 gene expression were compared after exposure to LPS (1 µg/mL) and several D-amino acids (D-Tyr, D-Phe, D-Met, D-His, D-Pro, and D-Trp). No significant effect of D-Tyr, D-Phe, D-Met, D-His, or D-Pro on AM polarization was found for a given amino acid concentration of 100 µM (Suppl. Fig. 6). However, D-Trp at 10 µM concentration gave a significant stimulation of Mrc1, Arg1 of M2 AM; and Il1b, Tnf of M1 AM.

4. D-Trp modulates lung immunity

Knowing that AM are the first responders in the lung [19], this study aimed to extend Kepert et al. [67] results to other immune cells, in particular AM. As a proof of concept, AM cell line MH-S were polarized (M1 vs M2) and simultaneously treated with D-Trp (10-100 µM). As detailed previously, M2 polarization was associated with the T_h2 major cytokines responses (IL-4 and IL-13), involved during the resolution of an infection or injury. Kepert et al. highlighted that on one side oral D-Trp induced gut T_{regs} recruitment and on the other side reduced T_h2 numbers and Il-4 levels in BALF. IL-4 measurements were not included in this study, considering that the focus was drawn on innate immunity. The genetic expression of M1 inflammatory as well as M2 resolution markers were measured, illustrating the fact that D-Trp was supporting IL-4 dependent M2 polarization (Figure 23) and at the same time inhibiting M1 polarization (Figure 21) *in vitro* at concentrations ranging from 10 to 100 µM, confirming our initial hypothesis.

Since D-Trp helped reducing the inflammatory response, it was suggested that this effect could be translated to a more complex model of the epithelium injury during a coculture model of wound healing. However, D-Trp did not improve wound healing in the AECII monolayer culture system. On a singular note, high concentrations of D-Trp (100 µM) on AECII/AM coculture triggered M0 AM to express key M1 genes Il1b and Tnf. It could be explained as a toxic response due to high concentration of D-Trp.

Existing literature is largely incomplete in the case of a lung injury *in vivo*. Following the previous *in vitro* analysis of D-Trp on an epithelial coculture, it was postulated that D-Trp could reduce PMN neutrophil recruitment in the lung after an ALI. This animal experiment confirmed the previous *in vitro* findings, where after LPS (2 µg/mL, 50 µL) and the subsequent D-Trp inhalation by C57BL/6J mice, significantly reduced PMN recruitment in the BAL occurred. This indicates a topical anti-inflammatory phenomenon, confirming in the lungs Kepert et al. results in the gut. Indeed, D-Trp deeply modified the lung immunological landscape, where surface markers associated with PMN (*i.e.* CD11b and Fpr2) were rapidly reduced as well as

Alox12 pro-resolving factor expression was impaired in lung homogenate. This is in accordance with the time course of the inflammation's resolution as described by Kuhn et al. [172].

The strongest cell recruitment reduction was obtained with a D-Trp concentration of 1 mM. The equivalent condition (1 mM) of L-Trp did not present the same reduction of cells recruitment (Figure 28), highlighting the D-Trp stereospecificity effect shown by Kepert et al. [67]. This outcome was confirmed by the CCL17 inflammatory protein simultaneous decrease in the BALF following ALI and 1 mM D-Trp treatment. This data corroborated Thanabalasuriar et al. description of CCL17 as a PMN chemoattractant during lung inflammation [214]. Remarkably, these results challenged previous finding from Chen et al., where CCL17 cytokine release was associated with augmented M2 polarization [215], whereas here, CCL17 secretion was reduced (Figure 30) despite D-Trp induced anti-inflammatory responses and M2 markers increase (Figure 23). Curiously, the overall protein concentration in the BAL after LPS instillation was L-Trp and D-Trp independent (40 µg/mL). This can be explained by the time course of the experiment and the protein level reaching for homeostasis 24h after ALI. Han et al. [216] demonstrated similar results where BAL protein levels do not significantly change during the 24h after ALI.

L- and D-Trp effects on the immune system are mediated via receptors, transporters and enzymes; some of them being isomer specific [217]. More importantly, D-Trp yielded a better uptake and immunomodulatory potency [218]. Moreover, Trp metabolites have been linked to immune modulation through the IDO/kynurenine pathway [102,203,217–221].

5. D-Trp, metabolites and AhR signaling

5.1. D-Trp tolerogenic effect

Several studies agree that D-Trp and D-/L-Trp (racemic) are ligands to the ligand-activated transcription factor AhR. Nguyen et al. described how in macrophages and DCs, AhR promotes an anti-inflammatory phenotype [222]. Furthermore, in AhR deficient mice macrophages produce more pro-inflammatory cytokines [223]. In this study, using BMDM cells issued from AhR deficient mice, Kimura et al. results were corroborated, highlighting an increase of IL-6 production in LPS stimulated $AhR^{-/-}$ macrophages. Besides, the previous findings confirmed that the anti-inflammatory mechanisms triggered by D-Trp were AhR dependent. Indeed, the D-Trp stereoisomer selectively diminished IL-6 gene expression in a dose dependent manner after LPS stimulation of the $AhR^{-/-}$ BMDM. Furthermore, IL-4 treated $AhR^{-/-}$ BMDM showed an increased Arg1 gene expression when being D-Trp treated. This is consistent with the greater anti-inflammatory response observed in M2 macrophages throughout this study. These results support the role of AhR on diminishing acute inflammation proposed by Wu et al. [224].

In extension to other immune cell studies, these results also reinforce Bruhs et al. results, showing that AhR activation leads to immunosuppression by DCs modulation [225], suggesting a common AhR dependent tolerogenic effect.

5.2. AhR signaling and kynurenine pathway

Kynurenine is a Trp metabolite and an AhR ligand, generated after deoxygenation of Trp by the IDO1 enzyme. Julliard et al. demonstrated that the IDO1 expression in DCs leads to kynurenine accumulation which is tolerogenic, inducing a T_{regs} increase [221]. These results refine a previous study by Munn et al. explaining how the degradation of Trp by IDO1 in macrophages leads to suppressed T cells [102].

Zelante et al. discussed how racemic Trp in the gut [66] leads to T_{regs} and IL-10 proliferation, creating an anti-inflammatory phenotype, whereas high concentration of Trp leads to the secretion of the inflammatory cytokine IL-22 [219]. Fallarino [220]

and Li [226] provide evidence that the metabolites resulting from Trp catabolism are responsible for a local tolerogenic environment, essentially by controlling T cells homeostasis.

Results of this PhD thesis reveal that Ido1 is induced in BMDM after high D-Trp doses (100 µM) (Figure 34, Figure 36), whether naïve, LPS, or IL-4 treated. This conflicts with Musso et al. findings describing that IL-4 influences Trp catabolism by inhibiting Ido1 gene expression in PBMC [227]. Considering the similarities between BMDM and PBMC, this suggests that the Trp uptake may be stereospecific and that Ido1 expression is independent to IL-4.

Heath-Pagliuso et al. [228] presented that D-Trp activates through AhR signaling both the kynurenine and the Cyp1a1 pathways. CYP1A1 is one of the targets of AhR signaling (in addition to TLR2 in the gut [229]). As such, it is activated and regulated by a variety of hydrocarbons. In particular, it has already been shown that Trp and its metabolites are selective AhR modulators [230]. Nguyen et al. [231] showed that the D-amino acid oxidase (DAOO) endogenously help the production of AhR ligands through the conversion of D-Trp. Consistently, the results showed that high doses of D-Trp (100 µM) effectively regulate Cyp1a1 through AhR signaling (Figure 34). Moreover, D-Trp displayed a consistent higher potency compared to L-Trp. This could be explained by a higher affinity of the AhR's structure towards D-Trp compared to L-Trp. These results are consistent with the ligand affinity values determined by Heath-Pagliuso et al. [228], which show a higher binding potency of D-Trp to the AhR compared to the L-Trp. However, it is still unclear why the AhR favors competitively the D-Trp isomer.

Additionally, they showed that the Trp metabolites tryptamine (TA) and indole acetic acid (IAA) were not only AhR agonists but were also direct Cyp1a1 ligands [228].

D-Trp reduced Ido1 gene expression (Figure 36). Consequently, it was suggested that Ido1 reduced expression would in turn reduce the kynurenine production as well along the AhR/kynurenine axis, since Ido1 is indirectly responsible for the kynurenine biosynthesis. Several enzymes are responsible for Trp metabolism (IDO2/TDO1/2).

However, their stereospecificity have never been studied. Zhang et al. established that TDO compensates for IDO1 deficiency. With impaired IDO1, Il-17a was also consequently reduced [226], corroborating Li et al.'s findings that Trp catabolism induces local immunosuppressive environments by controlling T cells homeostasis [226].

III- CONCLUSIONS AND COMPARISON OF D-TRP AND 3-OXO-C_{12}-HSL EFFECTS

1. Conclusions

Since AHL-QS had been discovered to be the cornerstone of bacterial virulence for Gram-negative bacteria, various strategies have been set to disrupt QS signaling [232–236], along with the inherent ability of mammalian cells to degrade AHL through paroxonomase enzymes activity, such as the calcium dependent PON2 enzyme [91,237]. QS inhibitors such as furanones [238] and antibiotics, impairing AHL-QS molecules production, or signal detection, have been proven to be an efficient way to selectively inhibit the virulence of *Pseudomonas aeruginosa* [233,234,239].

However, over time bacteria have been shown to develop resistance against the hosts' defense strategies. The QS inhibitor brominated furanone C-30 was once found to reduce virulence as well as posing little selective pressure on the bacteria [240]. Yet, *P. aeruginosa* developed the C-30-resistant, highly pathogenic, mutant *mexR* after treatment with the inhibitor [241]. In plants, AHL can induce subsequent resistance to pathogens through salicylic acid pathway signaling [242]. Conventional antibiotics like macrolides have proven their efficiency in regulating bacteria virulence by inhibiting biofilm formation. [243]. Nonetheless, hypermutable *P. aeruginosa* strains persist to generate higher antibiotic resistance [244].

Following up these results, it was hypothesized that using the QS molecules' role as inter-kingdom mediator would help to positively regulate the host immune system.

Indeed, the idea of employing the same mechanisms as some bacteria use to reduce lung inflammatory response could largely benefit individual with chronic of acute lung inflammatory diseases. Inter-bacterial and cross-kingdom communication represented by AHL-QS could lead to better therapy strategies against opportunistic pathogens. However, despite promising *in vitro* results, demonstrating the AHL ability to reduce innate inflammation by impairing M1 polarization and promoting M2 polarization, could so far not be extended *in vivo*. Indeed, no significant effect of AHL on neutrophil recruitment during ALI was observed, nor any evidence supporting wound repair of the epithelium after an injury. However, the model systems and the application modes used may have to be developed further to finally succeed in positive *in vivo* responses.

The immunomodulation specificity of D-Trp over L-Trp, is a novel finding which needs further research. In this regard, this study demonstrated that the amino acid D-Trp, a metabolite produced by probiotic Gram-positive bacteria like *Lactobacillus casei* strain and others [67], simultaneously impaired the M1 polarization but promoted the M2 polarization of AM *in vitro*. Furthermore, murine intratracheal application of D-Trp after acute lung injury reduced neutrophils recruiting, PMN associated markers in the lung and CCL17 inflammatory cytokine production in the bronchoalveolar lavage (BAL).

With the help of an $AhR^{-/-}$ mouse model, it was found that D-Trp, a direct agonist of the AhR, extinguished IL-6 overexpression in $AhR^{-/-}$ M1 polarized bone marrow derived macrophages (BMDM) cells, highlighting an AhR dependent D-Trp tolerogenic effect.

Considering its anti-inflammatory properties as well as its relative low toxicity *in vivo*, the results obtained suggest that D-Trp would make a good candidate towards a therapeutic approach against acute and chronic lung diseases as a choice target of the aryl hydrocarbon receptor and the downstream regulation of the T_h17/T_{regs} balance. The drug delivery method must however be improved, to allow in the future a more homogenous dispersion of the D-Trp in lung. D-Trp oral supplementation has to be further investigated since initial studies by Kepert et al. [67] showed promising

results. Future basic research should focus on, and strengthen the link between D-Trp pathway, metabolite stereochemistry and receptors affinity as well as other immune cells involvements.

2. Comparison of D-Trp and 3-oxo-C_{12}-HSL effects

In this thesis, the effects of two bacterial molecules on the lung immune system were studied: the 3-oxo-C_{12}-AHL, QS-molecule secreted by the Gram-negative *Pseudomonas aeruginosa's* AHL-QS system, and the D-Trp amino acid, secreted (among others) by the Gram-positive, probiotic bacterium *Lactobacillus casei.*

Both molecules shared *in vitro* a couple of key features. They demonstrated evidence of impaired pro-inflammatory gene expression of M1 in AM cell line culture (Figure 10 and Figure 21). In a coculture model of alveolar epithelial cell type 2 (AECII) and AM (Figure 15), the 3-oxo-C_{12}-AHL, but not D-Trp, caused a reduced expression of pro-inflammatory genes (Figure 15). D-Trp and 3-oxo-C_{12}-AHL treatment increased key anti-inflammatory gene expression in M2 AM, thus further supporting M2 polarization of M2 AM.

Neither D-Trp nor 3-oxo-C_{12}-AHL supported wound repair in an epithelium wound healing assay consisting in a bilayer of AECII and AM. However, the 3-oxo-C_{12}-AHL notably resulted in more cytotoxicity of the epithelium.

An *in vivo* model of acute lung injury was carried out. LPS was applied intratracheally prior to the application of D-Trp or 3-oxo-C_{12}-AHL. The immune response was quantified by the amount of PMN in the inflamed bronchoalveolar lavage (BAL). D-Trp, but not 3-oxo-C_{12}-AHL, displayed a reduction in PMN and protein concentration in the BAL (Figure 28). This result was followed in its downstream signaling and linked to the AhR pathway. These findings suggest D-Trp as a possible candidate for further studies of bacteria-host interactions in the lung.

SUPPLEMENTARY FIGURES

Suppl. Fig. 1. Rosiglitazone (RGZ) pre-treatment on M1 cells reduced Tnf expression after stimulation with 3-oxo-C_{12}-HSL. Joint RGZ/AHL effect on M1 polarized cells was studied in a time response experiment (24h). All cells were LPS (1 µg/mL)/AHL (60 µM) or LPS (1 µg/mL)/RGZ (60 µM) co-stimulated for 6h and then stimulated with RGZ or AHL respectively. ACN: Acetonitrile solvent control (0.2%). (mRNA expression is relative to Hprt, n=3, values represent the mean ± SEM).

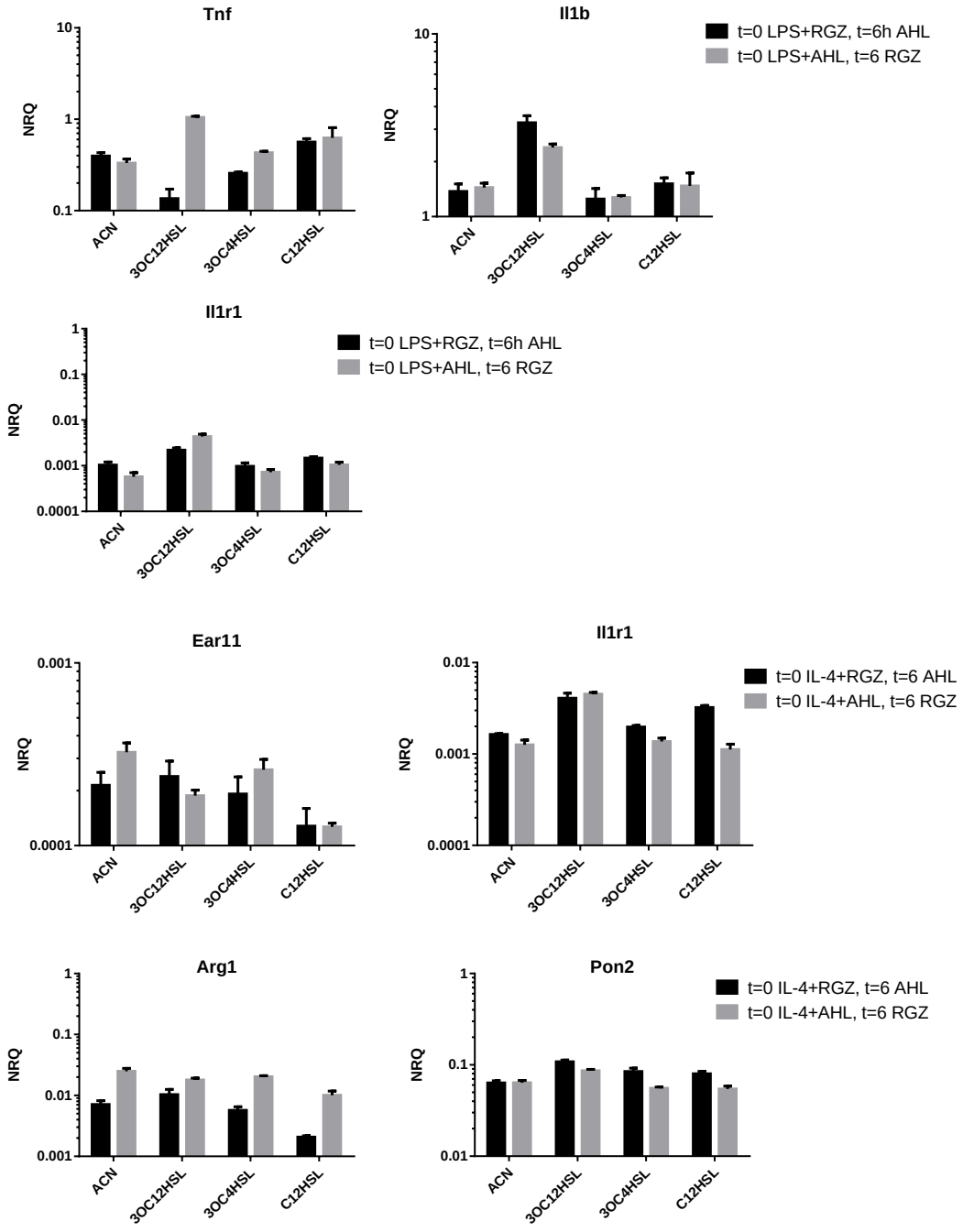

Suppl. Fig. 2. 3-oxo-C_{12}-HSL selectively impairs wound closure of AECII monolayer and AECII/AM coculture independently of LPS. LA-4/MH-S cells were cultivated from 0 to 24h after simultaneous scratch and treatment with ACN (0.6%)/3-oxo-C_{12}-HSL (60µM)/3-oxo-C_4-HSL (60µM)/C_{12}-HSL (60µM)/RGZ (60µM)/LPS (1 µg/mL). Wound widths were determined 0 and 24 hours after wounding. ACN: Acetonitrile solvent control (0.2%). (n=3, values represent the mean ± SEM, *: $p<0.05$)

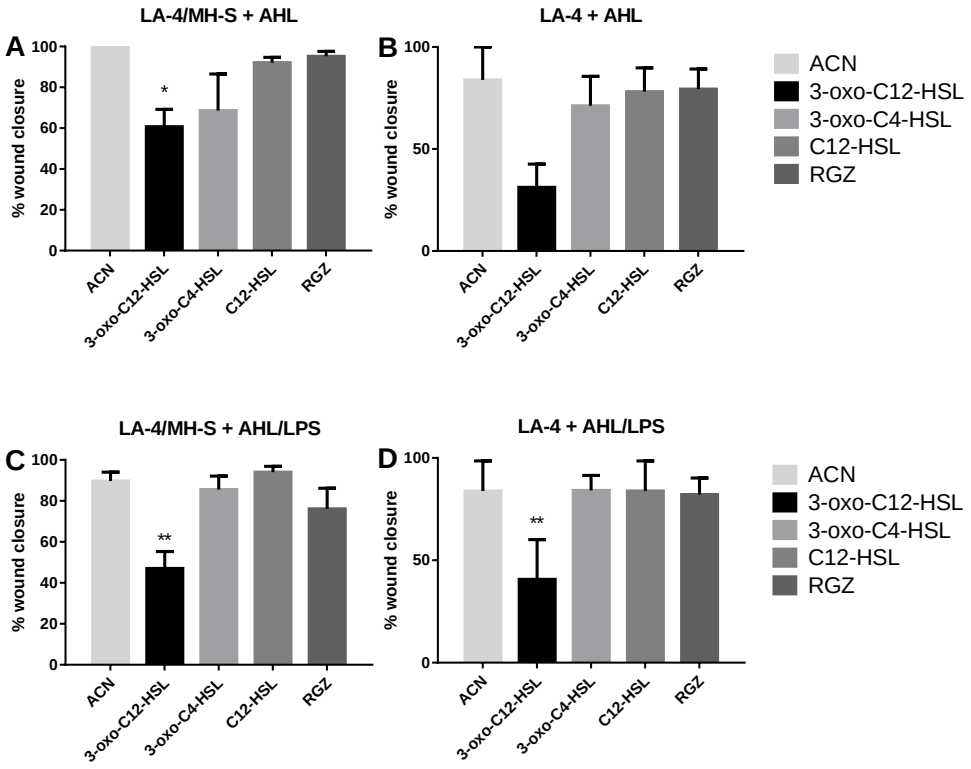

Suppl. Fig. 3. 3-oxo-C_{12}-HSL/LPS treatment reduces Tas2r138 mRNA expression in AM/AECII coculture. MH-S/LA-4 cells were incubated 24h after AHL/LPS treatment. The mRNA expression is relative to Hprt. M0: no polarization; M1: LPS (1 µg/mL). (n=3, values represent the mean ± SEM)

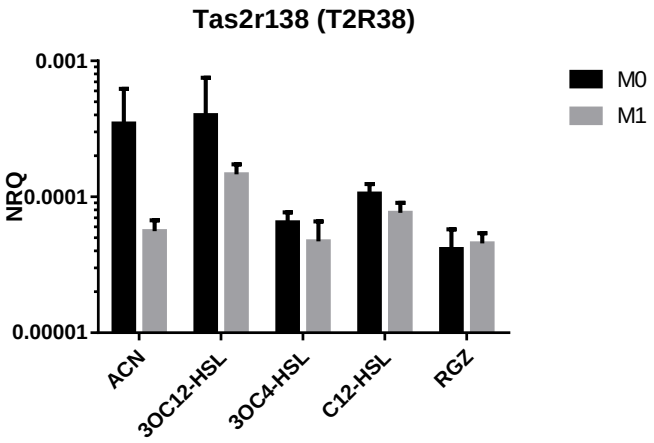

Suppl. Fig. 4. Microarray analysis of gene expression of isolated and polarized wild type alveolar macrophages. Data shows gene expression, a value under 100 is considered low expression - Ingenuity software (Qiagen).

Symbol	WT_M0 Expression	WT_M1 Expression	WT_M2 Expression
Tas1r1	59	58	64
Tas1r2	77	55	69
Tas1r3	65	70	85
Tas2r102	60	61	56
Tas2r104	62	66	59
Tas2r105	93	101	97
Tas2r106	63	67	63
Tas2r107	65	68	70
Tas2r4	44	44	43
Tas2r109	62	72	74
Tas2r110	82	84	80
Tas2r113	61	61	62
Tas2r10	73	69	73
Tas2r115	80	75	77
Tas2r116	48	54	53
Tas2r117	48	47	50
Tas2r117	47	40	45
Tas2r16	70	74	59
Tas2r1	88	84	80
Tas2r46	72	72	69
Tas2r13	64	62	59
Tas2r123	53	58	53
Tas2r124	96	108	90
Tas2r125	93	90	89
Tas2r41	123	118	121
Tas2r129	58	67	66
Tas2r7	81	88	92
Tas2r42	47	51	48
Tas2r134	62	52	65
Tas2r60	60	49	53
Tas2r31	62	64	61
Tas2r3	52	55	45
Tas2r39	52	60	59
Tas2r14	56	52	50
Tas2r143	47	62	52
Tas2r143	69	57	66
Tas2r40	74	79	74

Suppl. Fig. 5. Low dose of D-Trp (<300 μM) inhibited CD36 expression when co-treated with RGZ before being LPS stimulated. Tnf expression is reduced in the same conditions. CD36 is a surface marker induced by RGZ [153]. Joint RGZ/D-Trp effect on M1 polarized cells was studied in a dose-time response experiment (24h). MH-S cells were either RGZ/D-Trp or RGZ/D-Trp/LPS stimulated for 6h and then further stimulated with LPS or PBS respectively. mRNA expression is relative to Hprt (n=3). Control: PBS solvent. (Values represent the mean ± SEM).

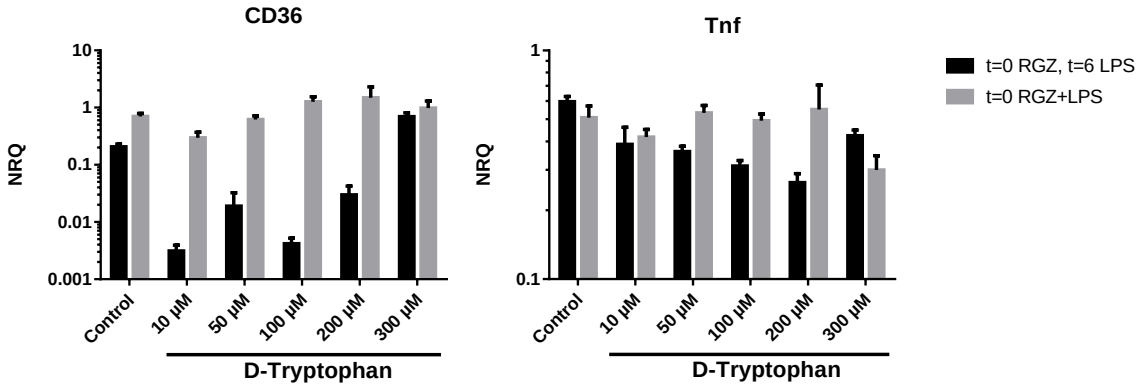

Suppl. Fig. 6. Low doses of D-Trp (10 μM) increased Il1b expression in M1 polarized cells as well as Mrc1 and Arg1 expression in M2 polarized cells. DMSO 1%, All D-amino acids (100μM, DMSO 1%) are used as controls. mRNA expression is relative to Hprt (n=3). M0: no polarization; M1: LPS (1 μg/mL); M2: IL-4 (20 ng/mL). (Values represent the mean ± SEM)

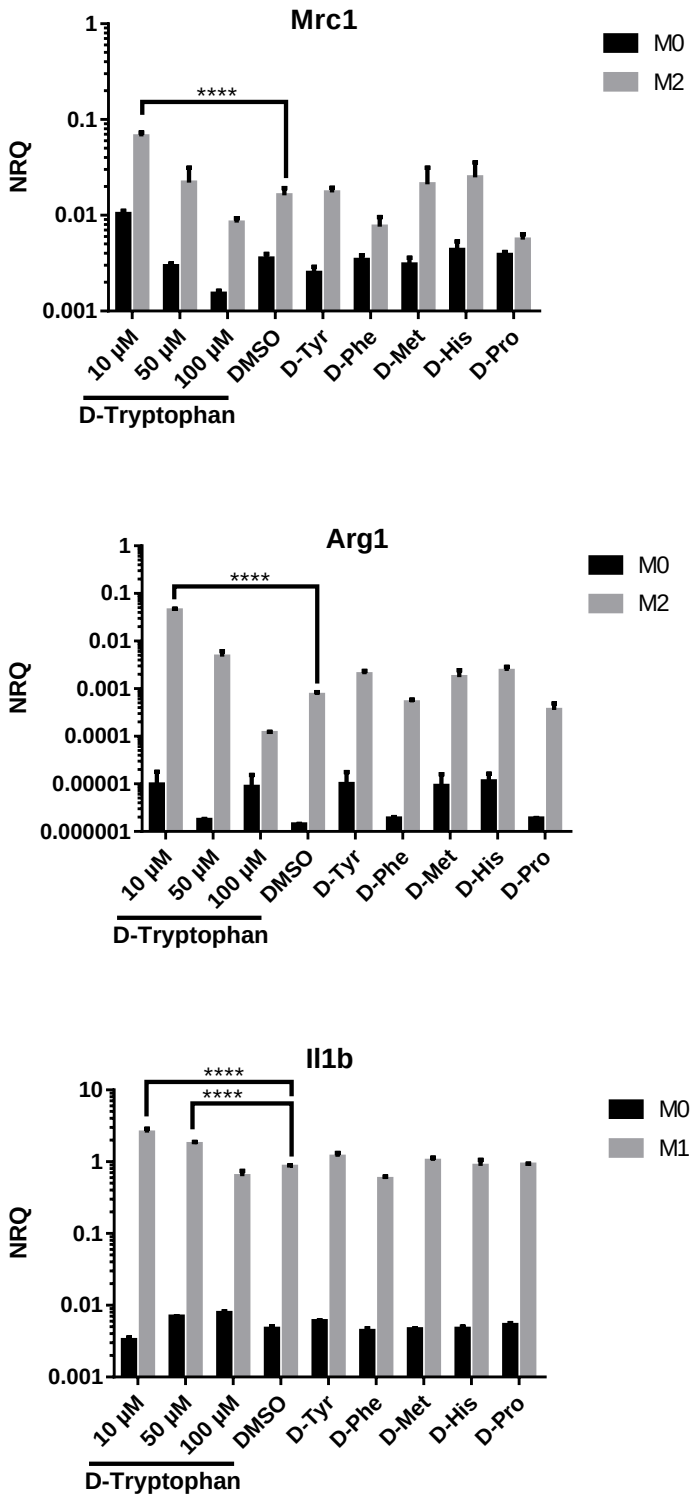

Suppl. Fig. 7. CCL17, CXCL1 and TNFα cytokines concentrations in the BAL are reduced after D-Trp instillation and ALI *in vivo*. ELISA assay of the correlation between protein concentration and cell numbers 24h after D-Trp/L-Trp (1 mM) and ALI. BAL cells consist mostly of AM and PMN. The data points are the cumulation of ELISA BAL experiments (n=5-8).

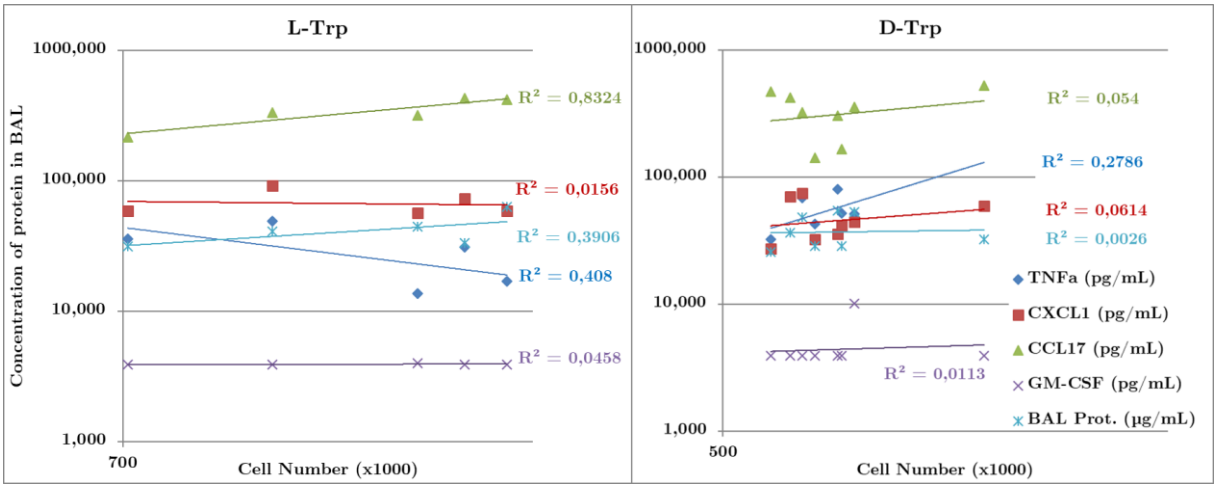

Suppl. Fig. 8. TNF signaling pathway. TNFα is one of the key inflammatory cytokines and its release is a robust indicator of classically activated macrophages. (Generated from www.genome.jp/kegg/).

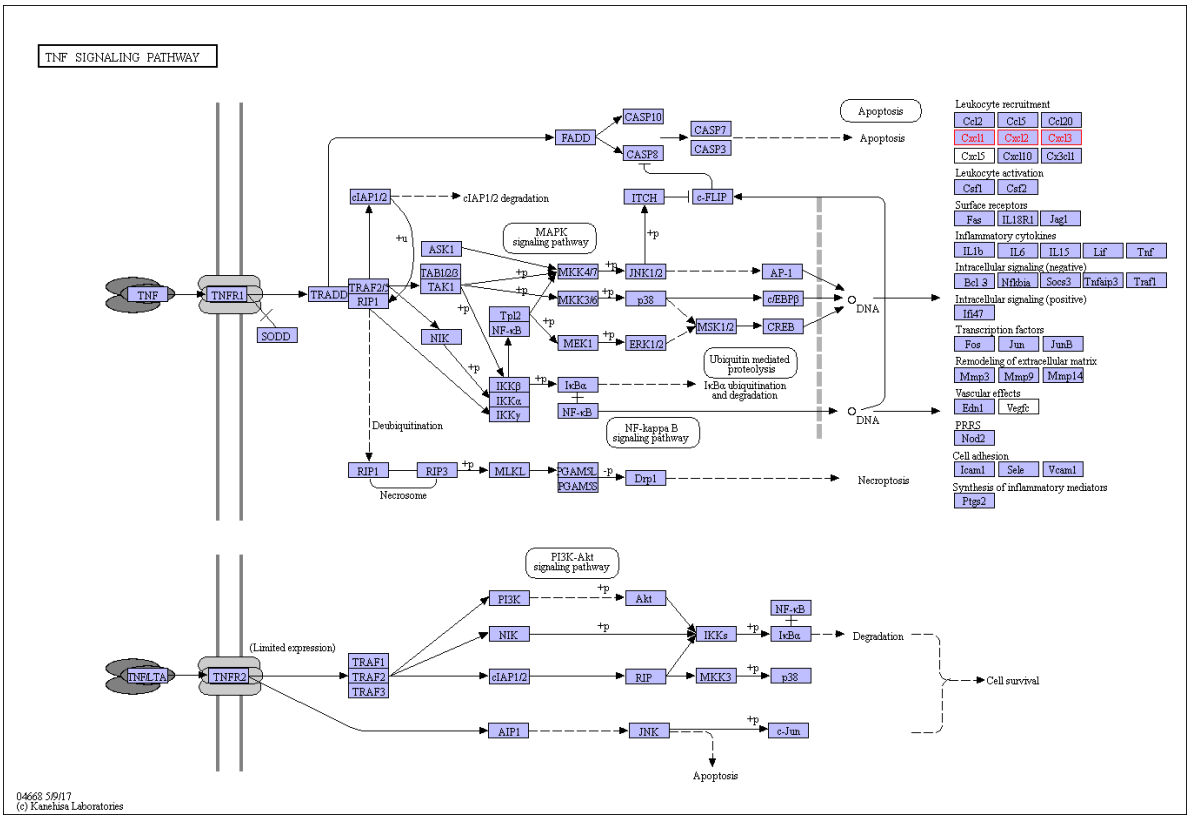

Suppl. Fig. 9. Phenylalanine, Tyrosine and Tryptophan biosynthesis pathway map in fungi, bacteria and plants. These metabolites will then be catabolized in the food chain in eukaryotic mammalian species. (Generated from www.genome.jp/kegg/).

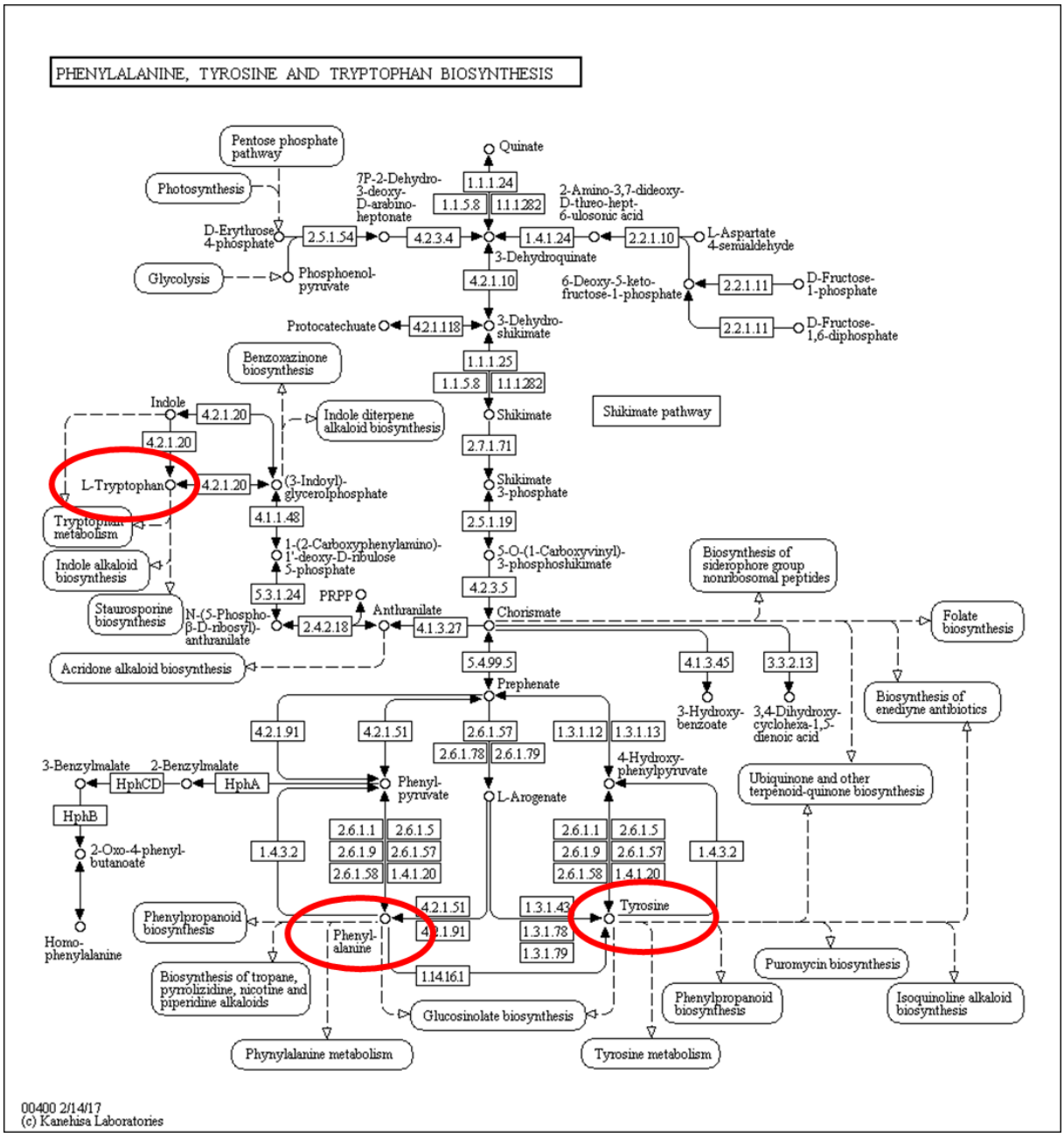

Suppl. Fig. 10. Tryptophan metabolism pathway map. D-Trp and L-Trp are both metabolized by mammalian organisms through the same enzymes of the kynurenine pathway. (Generated from www.genome.jp/kegg/)

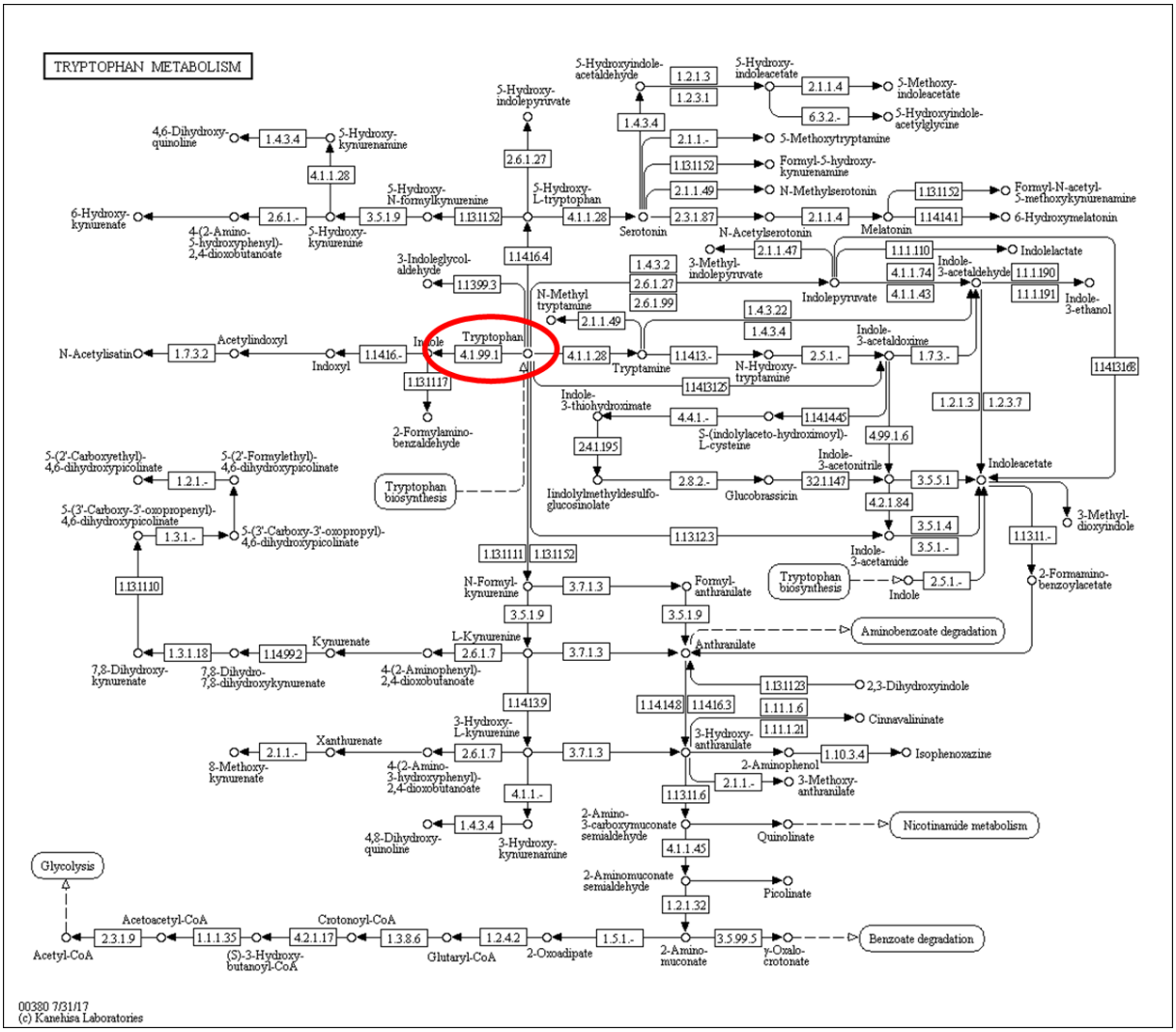

Suppl. Fig. 11. Biosynthesis of the acute inflammation mediators leading to the activation of FPR2/ALXR receptors. Diagram of the acute inflammatory response. In blue: the onset. In red: the propagation. In green: the resolution [245].

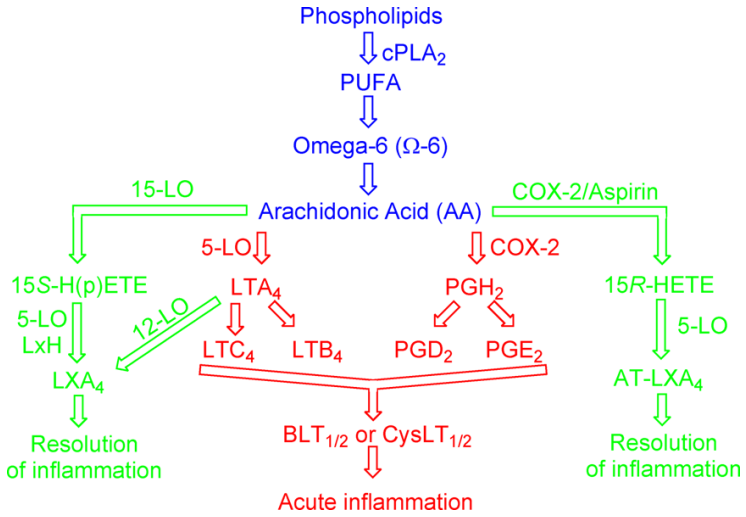

Suppl. Fig. 12. Microbiota: commensal vs pathogenic. Diagram of the underlying mechanism of airway inflammation. Adapted from [246].

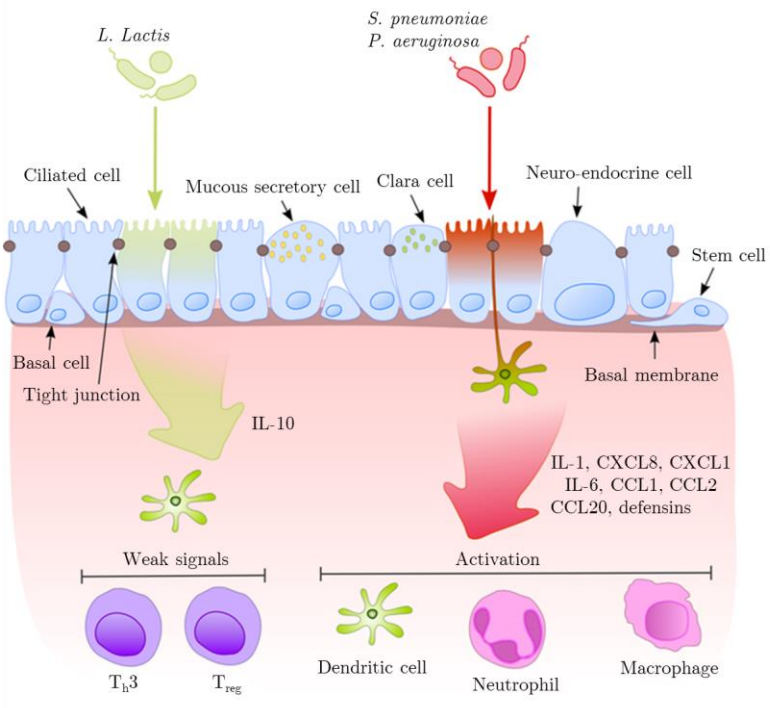

REFERENCES

[1] Ochs M, Nyengaard JR, Jung A, Knudsen L, Voigt M, Wahlers T, et al. The Number of Alveoli in the Human Lung. *Am J Respir Crit Care Med* 2004;169:120–4.

[2] Welch DBM, Huse SM. Microbial Diversity in the Deep Sea and the Underexplored "Rare Biosphere." *Handb Mol Microb Ecol II Metagenomics Differ Habitats* 2011;103:12115–20.

[3] van de Guchte M, Blottière HM, Doré J. Humans as holobionts: implications for prevention and therapy. *Microbiome* 2018;6:81.

[4] Dixit NK. Signaling in innate immunity and inflammation. *Cold Spring Harb Perspect Biol* 2012;4:1–19.

[5] Mogensen TH. Pathogen recognition and inflammatory signaling in innate immune defenses. *Clin Microbiol Rev* 2009;22:240–73.

[6] Scheiermann C, Frenette PS, Hidalgo A. Regulation of leucocyte homeostasis in the circulation. *Cardiovasc Res* 2015;107:340–51.

[7] Vogel DYS, Glim JE, Stavenuiter AWD, Breur M, Heijnen P, Amor S, et al. Human macrophage polarization in vitro: Maturation and activation methods compared. *Immunobiology* 2014;219:695–703.

[8] Miyata R, Bai N, Vincent R, Sin DD, Van Eeden SF. Statins Reduce Ambient Particulate Matter (PM10)-Induced Lung Inflammation by Promoting the Clearance of PM10 from Lung Tissues. *Chest* 2012;143:452–60.

[9] Hogquist KA, Xing Y, Hsu F-C, Smith Shapiro V. T cell adolescence: maturation events beyond positive selection. *J Immunol* 2015;195:1351–7.

[10] Herold S, Mayer K, Lohmeyer J. Acute lung injury: How macrophages orchestrate resolution of inflammation and tissue repair. *Front Immunol* 2011;2:65.

[11] Alberts B, Johnson A, Lewis J, Raff M, Roberts K, Walter P. Chap. 24: Pathogens, Infection, and Innate Immunity. Mol. Biol. Cell. Fifth Edit, *Garland Science*; 2008, p. 1485–538.

[12] Whitsett JA, Alenghat T. Respiratory epithelial cells orchestrate pulmonary innate immunity. *Nat Immunol* 2015;16:27–35.

[13] Jansing NL, McClendon J, Henson PM, Tuder RM, Hyde DM, Zemans RL. Unbiased Quantitation of ATII to ATI Cell Transdifferentiation During Repair After Lung Injury in Mice. *Am J Respir Cell Mol Biol* 2017;57:519–26.

[14] Crestani B, Comillet P, Dehoux M, Rolland C, Guenounou M, Aubier M. Alveolar Type II Epithelial Cells Produce Interleukin-6 In Vitro and In Vivo Regulation by Alveolar Macrophage Secretory Products. *J Clin Invest* 1994;94:731–40.

[15] Barrett EG, Johnston C, Oberdorster G, Finkelstein JN. Silica-induced chemokine expression in alveolar type II cells is mediated by TNF-alpha-induced oxidant stress. *Am J Physiol* 1999;276:L1110–9.

[16] Campus Virtuel Suisse.
http://www.embryology.ch/francais/rrespiratory/phasen07.html.
Vue d'ensemble des voies aériennes pulmonaires n.d.

[17] Ungefroren H, Hyder A, Schulze M, Fawzy El-Sayed KM, Grage-Griebenow E, Nussler AK, et al. Peripheral blood monocytes as adult stem cells: Molecular characterization and improvements in culture conditions to enhance stem cell features and proliferative potential. *Stem Cells Int* 2015;2016:7132751.

[18] Italiani P, Boraschi D. From monocytes to M1/M2 macrophages: Phenotypical vs. functional differentiation. *Front Immunol* 2014;5:514.

[19] Upadhyay S, George L, Ganguly K, Stoeger T. Chap 2: Macrophage Polarization in Lung Biology and Diseases. Lung Inflamm., *Intech*; 2014, p. 29–57.

[20] Marim FM, Silveira TN, Lima DS, Zamboni DS. A Method for Generation of Bone Marrow-Derived Macrophages from Cryopreserved Mouse Bone Marrow Cells. *PLoS One* 2010;5:e15263.

[21] Benoit M, Desnues B, Mege J-L. Macrophage Polarization in Bacterial Infections. *J Immunol* 2008;181:3733–9.

[22] Mills CD, Ley K. M1 and M2 macrophages: The chicken and the egg of immunity. *J Innate Immun* 2014;6:716–26.

[23] Martinez FO, Gordon S. The M1 and M2 paradigm of macrophage activation: time for reassessment. *F1000Prime Rep* 2014;6:13.

[24] Kisspng. www.kisspng.com/png-phagocyte-macrophage-phagocytosis-diagram-lymphocy-6315397/download-png.html. Phagocytosis diagram n.d.

[25] Enfield GP, Leibovich SJ. Macrophage Heterogeneity and Wound Healing. *Adv Wound Care* 2011;2:89–95.

[26] Mosser DM, Edwards JP. Exploring the full spectrum of macrophage activation. *Nat Rev Immunol* 2010;8:958–69.

[27] Gordon S, Martinez FO. Alternative activation of macrophages: Mechanism and functions. *Immunity* 2010;32:593–604.

[28] Martinez FO. Macrophage activation and polarization. *Front Biosci* 2008;13:453–61.

[29] Asada K, Sasaki S, Suda T, Chida K, Nakamura H. Antiinflammatory Roles of Peroxisome Proliferator-activated Receptor γ in Human Alveolar Macrophages. *Am J Respir Crit Care Med* 2004;169:195–200.

[30] Epelman S, Lavine KJ, Randolph GJ. Origin and Functions of Tissue Macrophages. *Immunity* 2014;41:21–35.

[31] Guilliams M, De Kleer I, Henri S, Post S, Vanhoutte L, De Prijck S, et al. Alveolar macrophages develop from fetal monocytes that differentiate into long-lived cells in the first week of life via GM-CSF. *J Exp Med* 2013;210:1977–92.

[32] Shi C, Pamer EG. Monocyte recruitment during infection and inflammation. *Nat Rev Immunol* 2011;11:762–74.

[33] Davies LC, Rosas M, Jenkins SJ, Liao C, Scurr MJ, Brombacher F, et al. Distinct bone marrow-derived and tissue resident macrophage- lineages proliferate at key stages during inflammation. *Nat Commun* 2013;4:1886.

[34] Hussell T, Bell TJ. Alveolar macrophages: plasticity in a tissue-specific context. *Nat Rev Immunol* 2014;14:81–93.

[35] Gosselin D, Link VM, Romanoski CE, Fonseca GJ, Eichenfield DZ, Spann NJ, et al. Environment drives selection and function of enhancers controlling tissue-specific macrophage identities. *Cell* 2014;159:1327–40.

[36] Lambrecht BN. Alveolar Macrophage in the Driver's Seat. *Immunity* 2006;24:366–8.

[37] Lavin Y, Winter D, Blecher-Gonen R, David E, Keren-Shaul H, Merad M, et al. Tissue-resident macrophage enhancer landscapes are shaped by the local microenvironment. *Cell* 2014;159:1312–26.

[38] Dethloff LA, Lehnert BE. Pulmonary interstitial macrophages: isolation and flow cytometric comparisons with alveolar macrophages and blood monocytes. *J Leukoc Biol* 1988;43:80–90.

[39] Johnston LK, Rims CR, Gill SE, McGuire JK, Manicone AM. Pulmonary macrophage subpopulations in the induction and resolution of acute lung injury. *Am J Respir Cell Mol Biol* 2012;47:417–26.

[40] Romagnani S. T-cell subsets (Th1 versus Th2). *Ann Allergy, Asthma Immunol* 2000;85:9–21.

[41] Zheng SG. Regulatory T cells vs Th17: differentiation of Th17 versus Treg, are the mutually exclusive? *Am J Clin Exp Immunol* 2013;2:94–106.

[42] Baumann C, Bonilla W V., Fröhlich A, Helmstetter C, Peine M, Hegazy AN, et al. T-bet– and STAT4–dependent IL-33 receptor expression directly promotes antiviral Th1 cell responses. *Proc Natl Acad Sci* 2015;112:4056–61.

[43] Murray PJ, Allen JE, Biswas SK, Fisher EA, Gilroy DW, Goerdt S, et al. Macrophage Activation and Polarization: Nomenclature and Experimental Guidelines. *Immunity* 2014;41:14–20.

[44] Maier E, Duschl A, Horejs-Hoeck J. STAT6-dependent and -independent mechanisms in Th2 polarization. *Eur J Immunol* 2012;42:2827–33.

[45] Mosmann TR, Coffman RL. Th1 and Th2 Cells: Different Patterns of Lymphokine Secretion Lead to Different Functional Properties. *Annu Rev Immunol* 1989;7:145–73.

[46] Ouyang W, Kolls J, Zheng Y. The biological functions of Th17 cell effector cytokines in inflammation. *Immunity* 2012;28:454–67.

[47] Sakaguchi S, Yamaguchi T, Nomura T, Ono M. Regulatory T Cells and Immune Tolerance. *Cell* 2008;133:775–87.

[48] Josefowicz SZ, Lu L-F, Rudensky AY. Regulatory T Cells: Mechanisms of Differentiation and Function. *Annu Rev Immunol* 2012;30:531–64.

[49] von Boehmer H. Mechanisms of suppression by suppressor T cells. *Nat Immunol* 2005;6:338–44.

[50] Shevach EM, DiPaolo RA, Andersson J, Zhao D-M, Stephens GL, Thornton AM. The lifestyle of naturally occurring CD4+ CD25+ Foxp3+ regulatory T cells. *Immunol Rev* 2006;212:60–73.

[51] van der Poll T, Calvano SE, Kumar A, Braxton CC, Coyle SM, Barbosa K, et al. Endotoxin Induces Downregulation of Tumor Necrosis Factor Receptors on Circulating Monocytes and Granulocytes in Humans. *Blood* 1995;86:2754–9.

[52] Martich GD, Boujoukos AJ, Suffredini AF. Response of man to endotoxin. *Immunobiology* 1993;187:403–16.

[53] Liu Y-C, Zou X-B, Chai Y-F, Yao Y-M. Macrophage Polarization in Inflammatory Diseases. *Int J Biol Sci* 2014;10:520–9.

[54] Hao N, Whitelaw ML. The emerging roles of AhR in physiology and immunity. *Biochem Pharmacol* 2013;86:561–70.

[55] Duarte JH, Di Meglio P, Hirota K, Ahlfors H, Stockinger B. Differential influences of the aryl hydrocarbon receptor on Th17 mediated responses in vitro and in vivo. *PLoS One* 2013;8:e79819.

[56] Negishi T, Kato Y, Ooneda O, Mimura J, Takada T, Mochizuki H, et al. Effects of Aryl Hydrocarbon Receptor Signaling on the Modulation of Th1/Th2 Balance. *J Immunol* 2005;175:7348–56.

[57] Suzuki TA. Links between natural variation in the microbiome and host fitness in wild mammals. *Integr Comp Biol* 2017;57:756–69.

[58] Carvajal-Gonzalez JM, Roman AC, Cerezo-Guisado MI, Rico-Leo EM, Martin-Partido G, Fernandez-Salguero PM. Loss of dioxin-receptor expression accelerates wound healing in vivo by a mechanism involving TGFβ. *J Cell Sci* 2009;122:1823–33.

[59] Couzin-Frankel J. Bacteria and Asthma: Untangling the Links. *Science (80-)* 2010;330:1168–9.

[60] Nakajima T, Palchevsky V, Perkins DL, Belperio JA, Finn PW. Lung transplantation: Infection, inflammation, and the microbiome. *Semin Immunopathol* 2011;33:135–56.

[61] Zemanick ET, Sagel SD, Harris JK. The airway microbiome in cystic fibrosis and implications for treatment. *Curr Opin Pediatr* 2011;23:319–24.

[62] Beck JM. ABCs of the lung microbiome. *Ann Am Thorac Soc* 2014;11:S3–6.

[63] Beck JM, Young VB, Huffnagle GB. The Microbiome of the Lung. *Transl Res* 2012;160:258–66.

[64] Morris A, Beck JM, Schloss PD, Campbell TB, Crothers K, Curtis JL, et al. Comparison of the respiratory microbiome in healthy nonsmokers and smokers. *Am J Respir Crit Care Med* 2013;187:1067–75.

[65] Konkel L. The Environment Within. *Environ Health Perspect* 2013;121:276–81.

[66] Marsland BJ. Regulating inflammation with microbial metabolites. *Nat Med* 2016;22:581–3.

[67] Kepert I, Fonseca J, Müller C, Milger K, Hochwind K, Kostric M, et al. D-tryptophan from probiotic bacteria influences the gut microbiome and allergic airway disease. *J Allergy Clin Immunol* 2017;139:1525–35.

[68] Wang Z, Bafadhel M, Haldar K, Spivak A, Mayhew D, Miller BE, et al. Lung microbiome dynamics in chronic obstructive pulmonary disease exacerbations. *Eur Respir J* 2016;47:1082–92.

[69] Hartl D, Griese M, Kappler M, Zissel G, Reinhardt D, Rebhan C, et al. Pulmonary Th2 response in *Pseudomonas aeruginosa*-infected patients with cystic fibrosis. *J Allergy Clin Immunol* 2006;117:204–11.

[70] Williams P. Quorum sensing, communication and cross-kingdom signalling in the bacterial world. *Microbiology* 2007;153:3923–38.

[71] Doğaner BA, Yan LKQ, Youk H. Autocrine Signaling and Quorum Sensing: Extreme Ends of a Common Spectrum. *Trends Cell Biol* 2015;26:262–71.

[72] Bleves S, Soscia C, Nogueira-orlandi P, Filloux A. Quorum Sensing Negatively Controls Type III Secretion Regulon Expression in *Pseudomonas aeruginosa* PAO1. *J Bacteriol* 2005;187:3898–902.

[73] Ruimy R, Andremont A. Quorum sensing in *Pseudomonas aeruginosa*: molecular mechanism, clinical impact, and inhibition. *Reanimation* 2004;13:176–84.

[74] Hooi DSW, Bycroft BW, Chhabra SR, Williams P, Pritchard DI. Differential Immune Modulatory Activity of *Pseudomonas aeruginosa* Quorum-Sensing Signal Molecules. *Infect Immun* 2004;72:6463–70.

[75] Wagner C, Zimmermann S, Brenner-Weiss G, Hug F, Prior B, Obst U, et al. The quorum-sensing molecule N-3-oxododecanoyl homoserine lactone (3OC12-HSL) enhances the host defence by activating human polymorphonuclear neutrophils (PMN). *Anal Bioanal Chem* 2007;387:481–7.

[76] Jahoor A, Patel R, Bryan A, Do C, Krier J, Watters C, et al. Peroxisome proliferator-activated receptors mediate host cell proinflammatory responses to *Pseudomonas aeruginosa* autoinducer. *J Bacteriol* 2008;190:4408–15.

[77] Telford G, Wheeler D, Williams P, Tomkins PT, Sewell H, Stewart GSAB, et al. The *Pseudomonas aeruginosa* Quorum-Sensing Signal Molecule N-(3-Oxododecanoyl)-L-Homoserine Lactone Has Immunomodulatory Activity. *Infect Immun* 1998;66:36–42.

[78] Glucksam-Galnoy Y, Sananes R, Silberstein N, Krief P, Kravchenko V V., Meijler MM, et al. The bacterial quorum-sensing signal molecule N-3-oxo-dodecanoyl-L-homoserine lactone reciprocally modulates pro- and anti-inflammatory cytokines in activated macrophages. *J Immunol* 2013;191:337–44.

[79] Shiner EK, Terentyev D, Bryan A, Sennoune S, Martinez-Zaguilan R, Li G, et al. *Pseudomonas aeruginosa* autoinducer modulates host cell responses through calcium signalling. *Cell Microbiol* 2006;8:1601–10.

[80] Holban A-M, Bleotu C, Chifiriuc MC, Bezirtzoglou E, Lazar V. Role of *Pseudomonas aeruginosa* quorum sensing (QS) molecules on the viability and cytokine profile of human mesenchymal stem cells. *Virulence* 2014;5:303–10.

[81] Tateda K, Ishii Y, Horikawa M, Matsumoto T, Miyairi S, Pechere JC, et al. The *Pseudomonas aeruginosa* Autoinducer N -3-Oxododecanoyl Homoserine Lactone Accelerates Apoptosis in Macrophages and Neutrophils. *Infect Immun* 2003;71:5785–93.

[82] Vikström E, Bui L, Konradsson P, Magnusson KE. Role of calcium signalling and phosphorylations in disruption of the epithelial junctions by *Pseudomonas aeruginosa* quorum sensing molecule. *Eur J Cell Biol* 2010;89:584–97.

[83] Vikström E, Bui L, Konradsson P, Magnusson KE. The junctional integrity of epithelial cells is modulated by *Pseudomonas aeruginosa* quorum sensing molecule through phosphorylation-dependent mechanisms. *Exp Cell Res* 2009;315:313–26.

[84] Smith RS, Fedyk ER, Springer TA, Mukaida N, Iglewski BH, Phipps RP. IL-8 Production in Human Lung Fibroblasts and Epithelial Cells Activated by the *Pseudomonas* Autoinducer N -3-Oxododecanoyl Homoserine Lactone Is Transcriptionally Regulated by NF- ϰB and Activator Protein-2. *J Immunol* 2001;167:366–74.

[85] Khajanchi BK, Kirtley ML, Brackman SM, Chopra AK. Immunomodulatory and protective Roles of quorum-sensing signaling molecules N-Acyl homoserine lactones during infection of mice with *Aeromonas hydrophila*. *Infect Immun* 2011;79:2646–57.

[86] Holm A, Vikström E. Quorum sensing communication between bacteria and human cells: signals, targets, and functions. *Front Plant Sci* 2014;5:309.

[87] Ritchie AJ, Jansson A, Stallberg J, Nilsson P, Cooley MA, Lysaght P. The *Pseudomonas aeruginosa* Quorum-Sensing Molecule N -3-(Oxododecanoyl)-l-Homoserine Lactone Inhibits T-Cell Differentiation and Cytokine Production by a Mechanism Involving an Early Step in T-Cell Activation. *Infect Immun* 2005;73:1648–55.

[88] Zimmermann S, Wagner C, Müller W, Brenner-Weiss G, Hug F, Prior B, et al. Induction of neutrophil chemotaxis by the quorum-sensing molecule N-(3-oxododecanoyl)-L-homoserine lactone. *Infect Immun* 2006;74:5687–92.

[89] Kravchenko V V, Kaufmann GF, Mathison JC, Scott DA, Katz AZ, Grauer DC, et al. Modulation of Gene Expression via Disruption of NF-κB Signaling by a Bacterial Small Molecule. *Science (80-)* 2008;321:259–63.

[90] Kravchenko V V., Kaufmann GF, Mathison JC, Scott D a., Katz AZ, Wood MR, et al. N-(3-oxo-acyl)homoserine lactones signal cell activation through a mechanism distinct from the canonical pathogen-associated molecular pattern recognition receptor pathways. *J Biol Chem* 2006;281:28822–30.

[91] Griffin PE, Roddam LF, Belessis YC, Strachan R, Beggs S, Jaffe A, et al. Expression of PPARγ and paraoxonase 2 correlated with *Pseudomonas aeruginosa* infection in cystic fibrosis. *PLoS One* 2012;7:e42241.

[92] Maurer S, Wabnitz GH, Kahle NA, Stegmaier S, Prior B, Giese T, et al. Tasting *Pseudomonas aeruginosa* Biofilms: Human Neutrophils Express the Bitter Receptor T2R38 as Sensor for the Quorum Sensing Molecule N-(3-Oxododecanoyl)-l-Homoserine Lactone. *Front Immunol* 2015;6:369.

[93] Schikora A, Schenk ST, Hartmann A. Beneficial effects of bacteria-plant communication based on quorum sensing molecules of the N-acyl homoserine lactone group. *Plant Mol Biol* 2016;90:605–12.

[94] Schenk ST, Hernandez-Reyes C, Schikora M, Neumann C, Stein E, Kogel K-H, et al. N-Acyl-Homoserine Lactone Primes Plants for Cell Wall Reinforcement and Induces Resistance to Bacterial Pathogens via the Salicylic Acid/Oxylipin Pathway. *Plant Cell* 2014;26:2708–23.

[95] Trent MS, Stead CM, Tran AX, Hankins J V. Diversity of endotoxin and its impact on pathogenesis. *J Endotoxin Res* 2006;12:205–23.

[96] Liu YC, Chan KG, Chang CY. Modulation of host biology by *Pseudomonas aeruginosa* quorum sensing signal molecules: Messengers or traitors. *Front Microbiol* 2015;6:1226.

[97] Moffett JR, Namboodiri MA. Tryptophan and the immune response. *Immunol Cell Biol* 2003;81:247–65.

[98] Widner B, Ledochowski M, Fuchs D. Interferon gama induced Tryptophan Degradation: Neuropsychiatric and Immunological Consequences. *Curr Drug Metab* 2000;1:193–204.

[99] Choy DF, Hart KM, Borthwick LA, Shikotra A, Nagarkar DR, Siddiqui S, et al. Th2 and Th17 inflammatory pathways are reciprocally regulated in asthma. *Sci Transl Med* 2015;7:301ra129.

[100] Divangahi M, King IL, Pernet E. Alveolar macrophages and type I IFN in airway homeostasis and immunity. *Trends Immunol* 2015;36:307–14.

[101] Mathie SA, Dixon KL, Walker SA, Tyrrell V, Mondhe M, O'Donnell VB, et al. Alveolar macrophages are sentinels of murine pulmonary homeostasis following inhaled antigen challenge. *Allergy Eur J Allergy Clin Immunol* 2015;70:80–9.

[102] Munn DH, Shafizadeh E, Attwood JT, Bondarev I, Pashine A, Mellor AL. Inhibition of T cell proliferation by macrophage tryptophan catabolism. *J Exp Med* 1999;189:1363–72.

[103] Chiarugi A, Rovida E, Sbarba P Dello, Moroni F. Tryptophan availability selectively limits NO-synthase induction in macrophages. *J Leukoc Biol* 2003;73:172–7.

[104] Biswas SK, Mantovani A. Orchestration of metabolism by macrophages. *Cell Metab* 2012;15:432–7.

[105] Makita N, Hizukuri Y, Yamashiro K, Murakawa M, Hayashi Y. IL-10 enhances the phenotype of M2 macrophages induced by IL-4 and confers the ability to increase eosinophil migration. *Int Immunol* 2015;27:131–41.

[106] Crabbé A, Sarker SF, Van Houdt R, Ott CM, Leys N, Cornelis P, et al. Alveolar epithelium protects macrophages from quorum sensing-induced cytotoxicity in a three-dimensional co-culture model. *Cell Microbiol* 2011;13:469–81.

[107] Mosmann T. Rapid colorimetric assay for cellular growth and survival: Application to proliferation and cytotoxicity assays. *J Immunol Methods* 1983;65:55–63.

[108] Bedoya SK, Wilson TD, Collins EL, Lau K, Larkin J. Isolation and Th17 Differentiation of Naive CD4 T Lymphocytes. *J Vis Exp* 2013;79:e50765.

[109] Yang L, Anderson DE, Baecher-Allan C, Hastings WD, Bettelli E, Oukka M, et al. IL-21 and TGF-β are required for differentiation of human TH17 cells. *Nature* 2008;454:350–2.

[110] Mangan PR, Harrington LE, O'Quinn DB, Helms WS, Bullard DC, Elson CO, et al. Transforming growth factor-β induces development of the Th17 lineage. *Nature* 2006;441:231–4.

[111] Veldhoen M, Hocking RJ, Atkins CJ, Locksley RM, Stockinger B. TGFβ in the context of an inflammatory cytokine milieu supports de novo differentiation of IL-17-producing T cells. *Immunity* 2006;24:179–89.

[112] Gaisford W, Pritchard DI, Cooke A. OdDHL inhibits T cell subset differentiation and delays diabetes onset in NOD mice. *Clin Vaccine Immunol* 2011;18:1213–20.

[113] Laskin DL, Sunil VR, Gardner CR, Laskin JD. Macrophages and Tissue Injury: Agents of Defense or Destruction? *Annu Rev Pharmacol Toxicol* 2011;51:267–88.

[114] Galván-Peña S, O'Neill LAJ. Metabolic reprograming in macrophage polarization. *Front Immunol* 2014;5:420.

[115] Jiang Z, Zhu L. Update on the role of alternatively activated macrophages in asthma. *J Asthma Allergy* 2016;9:101–7.

[116] Weber A, Wasiliew P, Kracht M. Interleukin-1 (IL-1) Pathway. *Sci Signal* 2010;3:cm1.

[117] Takeda K, Ichiki T, Narabayashi E, Inanaga K, Miyazaki R, Hashimoto T, et al. Inhibition of prolyl hydroxylase domain-containing protein suppressed lipopolysaccharide-induced TNF-α expression. *Arterioscler Thromb Vasc Biol* 2009;29:2132–7.

[118] Loke P, Nair MG, Parkinson J, Guiliano D, Blaxter M, Allen JE. IL-4 dependent alternatively-activated macrophages have a distinctive in vivo gene expression phenotype. *BMC Immunol* 2002;3:7.

[119] Tarrand JJ, LaSala PR, Han XY, Rolston K V., Kontoyiannis DP. Dimethyl sulfoxide enhances effectiveness of skin antiseptics and reduces contamination rates of blood cultures. *J Clin Microbiol* 2012;50:1552–7.

[120] Elisia I, Nakamura H, Lam V, Hofs E, Cederberg R, Cait J, et al. DMSO represses inflammatory cytokine production from human blood cells and reduces autoimmune arthritis. *PLoS One* 2016;11:e0152538.

[121] Liang J, Zhang Y, Xie T, Liu N, Chen H, Geng Y, et al. Hyaluronan and TLR4 promote surfactant-protein-C-positive alveolar progenitor cell renewal and prevent severe pulmonary fibrosis in mice. *Nat Med* 2016;22:1285–93.

[122] Ishii H, Hayashi S, Hogg JC, Fujii T, Goto Y, Sakamoto N, et al. Alveolar macrophage-epithelial cell interaction following exposure to atmospheric particles induces the release of mediators involved in monocyte mobilization and recruitment. *Respir Res* 2005;6:87.

[123] Cakarova L. Macrophage-Epithelial Crosstalk during Alveolar Epithelial Repair following Pathogen-induced Pulmonary Inflammation. Justus Liebig University Giessen, 2009.

[124] Lin CF, Young KC, Bai CH, Yu BC, Ma CT, Chien YC, et al. Rosiglitazone regulates anti-inflammation and growth inhibition via PTEN. *Biomed Res Int* 2014;2014:ID787924.

[125] Liu D, Zeng BX, Zhang SH, Yao SL. Rosiglitazone, an agonist of peroxisome proliferator-activated receptor gamma, reduces pulmonary inflammatory response in a rat model of endotoxemia. *Inflamm Res* 2005;54:464–70.

[126] Xu Y, Romero R, Miller D, Kadam L, Mial TN, Plazyo O, et al. An M1-like Macrophage Polarization in Decidual Tissue during Spontaneous Preterm Labor That Is Attenuated by Rosiglitazone Treatment. *J Immunol* 2016;196:2476–91.

[127] Thorley AJ, Grandolfo D, Lim E, Goldstraw P, Young A, Tetley TD. Innate immune responses to bacterial ligands in the peripheral human Lung - Role of alveolar epithelial TLR expression and signalling. *PLoS One* 2011;6:e21827.

[128] Pechkovsky DV, Zissel G, Stamme C, Goldmann T, Ari Jaffe H, Einhaus M, et al. Human alveolar epithelial cells induce nitric oxide synthase-2 expression in alveolar macrophages. *Eur Respir J* 2002;19:672–83.

[129] Ferkol T, Schraufnagel D. The global burden of respiratory disease. *Ann Am Thorac Soc* 2014;11:404–6.

[130] Crapo JD, Barry BE, Gehr P, Bachofen M, Weibel ER. Cell number and cell characteristics of the normal human lung. *Am Rev Respir Dis* 1982;126:332–7.

[131] Hogan BLM, Barkauskas CE, Chapman HA, Epstein JA, Jain R, Hsia CCW, et al. Repair and regeneration of the respiratory system: Complexity, plasticity, and mechanisms of lung stem cell function. *Cell Stem Cell* 2014;15:123–38.

[132] Ware LB, Matthay MA. Alveolar fluid clearance is impaired in the majority of patients with acute lung injury and the acute respiratory distress syndrome. *Am J Respir Crit Care Med* 2001;163:1376–83.

[133] Ahdieh M, Vandenbos T, Youakim A. Lung epithelial barrier function and wound healing are decreased by IL-4 and IL-13 and enhanced by IFN-gamma. *Am J Physiol Cell Physiol* 2001;281:C2029–38.

[134] Mir-Kasimov M, Sturrock A, McManus M, Paine R. Effect of alveolar epithelial cell plasticity on the regulation of GM-CSF expression. *Am J Physiol Lung Cell Mol Physiol* 2012;302:L504-11.

[135] Stoner GD, Kikkawa Y, Kniazeff AJ, Stoner D, Kniazeff J, Wagner M. Clonal Isolation of Epithelial Cells from Mouse Lung Adenoma Clonal Isolation of Epithelial Cells from Mouse Lung Adenoma. *Cancer Res* 1975;35:2177–85.

[136] Wikenheiser KA, Clark JC, Linnoila RI, Stahlman MT, Whitsett JA. Simian Virus 40 Large T Antigen Directed by Transcriptional Elements of the Human Surfactant Protein C Gene Produces Pulmonary Adenocarcinomas in Transgenic Mice1. *Cancer Res* 1992;52:5342–52.

[137] Liu Y-C, Hussain F, Negm O, Paiva AC, Halliday N, Dubern J-F, et al. Contribution of the Alkylquinolone Quorum-Sensing System to the Interaction of Pseudomonas aeruginosa With Bronchial Epithelial Cells. *Front Microbiol* 2018;9:3018.

[138] Glessner A, Smith RS, Iglewski BH, Robinson JB. Roles of *Pseudomonas aeruginosa las* and *rhl* Quorum-Sensing Systems in Control of Elastase and Rhamnolipid Biosynthesis Genes. *J Bacteriol* 1999;181:1623–9.

[139] Wilder CN, Diggle SP, Schuster M. Cooperation and cheating in *Pseudomonas aeruginosa*: The roles of the *las*, *rhl* and *pqs* quorum-sensing systems. *ISME J* 2011;5:1332–43.

[140] Wu M, Huang H, Zhang W, Kannan S, Weaver A, McKibben M, et al. Host DNA repair proteins in response to *Pseudomonas aeruginosa* in lung epithelial cells and in mice. *Infect Immun* 2011;79:75–87.

[141] Li Y, Petrova OE, Su S, Lau GW, Panmanee W, Na R, et al. BdlA, DipA and Induced Dispersion Contribute to Acute Virulence and Chronic Persistence of *Pseudomonas aeruginosa*. *PLoS Pathog* 2014;10:e1004168.

[142] Webb JS, Thompson LS, James S, Charlton T, Tolker-Nielsen T, Koch B, et al. Cell Death in *Pseudomonas aeruginosa* Biofilm Development. *J Bacteriol* 2003;185:4585–92.

[143] Matute-bello G, Frevert CW, Martin TR. Animal models of acute lung injury. *Am J Physiol Lung Cell Mol Physiol* 2008;295:L379–99.

[144] Huebener P, Schwabe RF. Regulation of Wound Healing and Organ Fibrosis by Toll-like Receptors. *Biochim Biophys Acta* 2013;1832:1005–17.

[145] Vernooy JHJ, Dentener MA, van Suylen RJ, Buurman WA, Wouters EFM. Intratracheal instillation of lipopolysaccharide in mice induces apoptosis in bronchial epithelial cells. No role for tumor necrosis factor-α and infiltrating neutrophils. *Am J Respir Cell Mol Biol* 2001;24:569–76.

[146] Li L, Ma P, Liu Y, Huang C, O W-S, Tang F, et al. Intermedin Attenuates LPS-induced Inflammation in the Rat Testis. *PLoS One* 2013;8:e65278.

[147] Morokata T, Ishikawa J, Ida K, Yamada T. C57BL/6 mice are more susceptible to antigen-induced pulmonary eosinophilia than BALB/c mice , irrespective of systemic T helper 1/T helper 2 responses. *Immunology* 1999;98:345–51.

[148] Harrison CM, Andersen CC. Exhaled breath measures of inflammation: are they useful in neonatal chronic lung disease? *Arch Dis Child Fetal Neonatal Ed* 2005;90:F6-10.

[149] Kolaczkowska E, Kubes P. Neutrophil recruitment and function in health and inflammation. *Nat Rev Immunol* 2013;13:159–75.

[150] Brinkmann V. Neutrophil Extracellular Traps Kill Bacteria. *Science (80-)* 2004;303:1532–5.

[151] Phillipson M, Kubes P. The neutrophil in vascular inflammation. *Nat Med* 2011;17:1381–90.

[152] Santa Cruz Biotechnology. D-Tryptophan 2009:1–5.

[153] Kannan S, Huang H, Seeger D, Audet A, Chen Y, Huang C, et al. Alveolar epithelial type II cells activate alveolar macrophages and mitigate *P. aeruginosa* infection. *PLoS One* 2009;4:e4891.

[154] Grabiner MA, Fu Z, Wu T, Barry KC, Schwarzer C, Machen TE. *Pseudomonas aeruginosa* Quorum-Sensing Molecule Homoserine Lactone Modulates Inflammatory Signaling through PERK and eI-F2. *J Immunol* 2014;193:1459–67.

[155] Salazar F, Hall L, Negm OH, Awuah D, Tighe PJ, Shakib F, et al. The mannose receptor negatively modulates the Toll-like receptor 4-aryl hydrocarbon receptor-indoleamine 2,3-dioxygenase axis in dendritic cells affecting T helper cell polarization. *J Allergy Clin Immunol* 2016;137:1841–51.

[156] Fernando MR, Reyes JL, Iannuzzi J, Leung G, McKay DM. The pro-inflammatory cytokine, interleukin-6, enhances the polarization of alternatively activated macrophages. *PLoS One* 2014;9:e94188.

[157] Brandenburg KS, Calderon DF, Kierski PR, Brown AL, Shah NM, Abbott NL, et al. Inhibition of *Pseudomonas aeruginosa* biofilm formation on wound dressings. *Wound Repair Regen* 2015;23:842–54.

[158] Bandeira LG, Bortolot BS, Cecatto MJ, Monte-Alto-Costa A, Romana-Souza B. Exogenous tryptophan promotes cutaneous wound healing of chronically stressed mice through inhibition of TNF-α and IDO activation. *PLoS One* 2015;10:e0128439.

[159] Borthwick LA, McIlroy EI, Gorowiec MR, Brodlie M, Johnson GE, Ward C, et al. Inflammation and epithelial to mesenchymal transition in lung transplant recipients: Role in dysregulated epithelial wound repair. *Am J Transplant* 2010;10:498–509.

[160] Sarasija S, Patil J. Pulmonary drug delivery strategies: A concise, systematic review. *Lung India* 2012;29:44–9.

[161] Xue B, Wu Y, Yin Z, Zhang H, Sun S, Yi T, et al. Regulation of lipopolysaccharide-induced inflammatory response by glutathione S-transferase P1 in RAW264.7 cells. *FEBS Lett* 2005;579:4081–7.

[162] Lotter K, Höcherl K, Bucher M, Kees F. In vivo efficacy of telithromycin on cytokine and nitric oxide formation in lipopolysaccharide-induced acute systemic inflammation in mice. *J Antimicrob Chemother* 2006;58:615–21.

[163] Cai S, Batra S, Lira SA, Kolls JK, Jeyaseelan S. CXCL1 Regulates Pulmonary Host Defense to Klebsiella Infection via CXCL2, CXCL5, NF-ϰB, and MAPKs. *J Immunol* 2010;185:6214–25.

[164] Heiseke AF, Faul AC, Lehr H, Förster I, Schmid RM, Krug AB, et al. CCL17 promotes intestinal inflammation in mice and counteracts regulatory T cell mediated protection from colitis. *Gastroenterology* 2012;142:335–45.

[165] Weber C, Meiler S, Döring Y, Koch M, Drechsler M, Megens RTA, et al. CCL17-expressing dendritic cells drive atherosclerosis by restraining regulatory T cell homeostasis in mice. *J Clin Invest* 2011;121:2898–910.

[166] Staples KJ, Hinks TSC, Ward JA, Gunn V, Smith C, Djukanović R. Phenotypic characterization of lung macrophages in asthmatic patients: Overexpression of CCL17. *J Allergy Clin Immunol* 2012;130:1404–12.

[167] Duan M, Steinfort DP, Smallwood D, Hew M, Chen W, Ernst M, et al. CD11b immunophenotyping identifies inflammatory profiles in the mouse and human lungs. *Mucosal Immunol* 2016;9:550–63.

[168] Siegmund S V., Schlosser M, Schildberg FA, Seki E, De Minicis S, Uchinami H, et al. Serum amyloid a induces inflammation, proliferation and cell death in activated hepatic stellate cells. *PLoS One* 2016;11:e0150893.

[169] Uderhardt S, Krönke G. 12/15-Lipoxygenase during the regulation of inflammation, immunity, and self-tolerance. *J Mol Med* 2012;90:1247–56.

[170] Byers DE, Holtzman MJ. Alternatively activated macrophages and airway disease. *Chest* 2011;140:768–74.

[171] Uderhardt S, Herrmann M, Oskolkova O V., Aschermann S, Bicker W, Ipseiz N, et al. 12/15-Lipoxygenase Orchestrates the Clearance of Apoptotic Cells and Maintains Immunologic Tolerance. *Immunity* 2012;36:834–46.

[172] Kuhn H, Banthiya S, Van Leyen K V. Mammalian lipoxygenases and their biological relevance. *Biochim Biophys Acta* 2015;1851:308–30.

[173] Adhyatmika A, Putri KSS, Beljaars L, Melgert BN. The Elusive Antifibrotic Macrophage. *Front Med* 2015;2:81.

[174] Liu Y, Chen K, Wang JM. Chap 91: FPR Ligands. Handb. Biol. Act. Pept. Second Edi, *Elsevier Inc.*; 2013, p. 671–80.

[175] Schmidt J V, Su GH, Reddy JK, Simon MC, Bradfield CA. Characterization of a murine Ahr null allele: involvement of the Ah receptor in hepatic growth and development. *Proc Natl Acad Sci U S A* 1996;93:6731–6.

[176] Vogel CFA, Khan EM, Leung PSC, Gershwin ME, Chang WLW, Wu D, et al. Cross-talk between aryl hydrocarbon receptor and the inflammatory response: A role for nuclear factor-κB. *J Biol Chem* 2014;289:1866–75.

[177] Bessede A, Gargaro M, Pallotta MT, Matino D, Servillo G, Brunacci C, et al. Aryl hydrocarbon receptor control of a disease tolerance defence pathway. *Nature* 2014;511:184–90.

[178] Denison MS, Nagy SR. Activation Of The Aryl Hydrocarbon Receptor By Structurally Diverse Exogenous And Endogenous Chemicals. *Annu Rev Pharmacol Toxicol* 2003;43:309–34.

[179] Bardaweel SK. D-amino Acids : Prospects for New Therapeutic Agents. *J Med Bioeng* 2014;3:195–8.

[180] Quintana FJ, Sherr DH. Aryl hydrocarbon receptor control of adaptive immunity. *Pharmacol Rev* 2013;65:1148–61.

[181] Nguyen NT, Nakahama T, Le DH, Van Son L, Chu HH, Kishimoto T. Aryl hydrocarbon receptor and kynurenine: Recent advances in autoimmune disease research. *Front Immunol* 2014;5:551.

[182] Vogel CFA, Goth SR, Dong B, Pessah IN, Matsumura F. Aryl hydrocarbon receptor signaling mediates expression of indoleamine 2,3-dioxygenase. *Biochem Biophys Res Commun* 2008;375:331–5.

[183] Bivar Xavier K. Bacterial interspecies quorum sensing in the mammalian gut microbiota. *Comptes Rendus - Biol* 2018;341:297–9.

[184] Marques JC, Lamosa P, Russell C, Ventura R, Maycock C, Semmelhack MF, et al. Processing the interspecies quorum-sensing signal autoinducer-2 (AI-2): Characterization of phospho-(S)-4,5-dihydroxy-2,3-pentanedione isomerization by LsrG protein. *J Biol Chem* 2011;286:18331–43.

[185] Holm A, Magnusson K-E, Vikström E. *Pseudomonas aeruginosa* N-3-oxo-dodecanoyl-homoserine Lactone Elicits Changes in Cell Volume, Morphology, and AQP9 Characteristics in Macrophages. *Front Cell Infect Microbiol* 2016;6:32.

[186] Lee J, Zhang L. The hierarchy quorum sensing network in *Pseudomonas aeruginosa*. *Protein Cell* 2014;6:26–41.

[187] Heurlier K, Dénervaud V, Haas D. Impact of quorum sensing on fitness of *Pseudomonas aeruginosa*. *Int J Med Microbiol* 2006;296:93–102.

[188] Liu J, Feng Y, Yang K, Li Q, Ye L, Han L, et al. Early production of IL-17 protects against acute pulmonary *Pseudomonas aeruginosa* infection in mice. *FEMS Immunol Med Microbiol* 2011;61:179–88.

[189] Jørgensen TN, Haase C, Michelsen BK. Treatment of an immortalized APC cell line with both cytokines and LPS ensures effective T-cell activation In vitro. *Scand J Immunol* 2002;56:492–503.

[190] Ma J, Chen T, Mandelin J, Ceponis A, Miller NE, Hukkanen M, et al. Regulation of macrophage activation. *Cell Mol Life Sci* 2003;60:2334–46.

[191] Stone KC, Mercer RR, Gehr P, Stockstill B, Crapo JD. Allometric Relationships of Cell Numbers and Size in the Mammalian Lung. *Am J Respir Cell Mol Biol* 1992;6:235–43.

[192] Dobbs L, Johnson M, Vanderbilt J, Allen L, Gonzalez R. The great big alveolar TI cell: Evolving concepts and paradigms. *Cell Physiol Biochem* 2010;25:55–62.

[193] Herzog EL, Brody AR, Colby T V, Mason R, Williams MC. Knowns and unknowns of the alveolus. *Proc Am Thorac Soc* 2008;5:778–82.

[194] Aggarwal NR, King LS, D'Alessio FR. Diverse macrophage populations mediate acute lung inflammation and resolution. *Am J Physiol Lung Cell Mol Physiol* 2014;306:L709–25.

[195] Zhang J, Gong F, Li L, Zhao M, Song J. *Pseudomonas aeruginosa* quorum-sensing molecule N-(3-oxododecanoyl) homoserine lactone attenuates lipopolysaccharide-induced inflammation by activating the unfolded protein response. *Biomed Reports* 2014;2:233–8.

[196] Michalik L, Wahli W. Involvement of PPAR nuclear receptors in tissue injury and wound repair. *Clin Invest* 2006;116:598–606.

[197] Vikström E, Magnusson K-E, Pivoriūnas A. The *Pseudomonas aeruginosa* quorum-sensing molecule N-(3-oxododecanoyl)-L-homoserine lactone stimulates phagocytic activity in human macrophages through the p38 MAPK pathway. *Microbes Infect* 2005;7:1512–8.

[198] Karlsson T, Turkina M V, Yakymenko O, Magnusson K-E, Vikström E. The *Pseudomonas aeruginosa* N-acylhomoserine lactone quorum sensing molecules target IQGAP1 and modulate epithelial cell migration. *PLoS Pathog* 2012;8:e1002953.

[199] Lee RJ, Chen B, Redding KM, Margolskee RF, Cohen NA. Mouse nasal epithelial innate immune responses to *Pseudomonas aeruginosa* quorum-sensing molecules require taste signaling components. *Innate Immun* 2013;20:606–17.

[200] Cooley MA, Whittall C, Rolph MS. *Pseudomonas* signal molecule 3-oxo-C12-homoserine lactone interferes with binding of rosiglitazone to human PPARg. *Microbes Infect* 2010;12:231–7.

[201] Gaida MM, Dapunt U, Hänsch GM. Sensing developing biofilms: the bitter receptor T2R38 on myeloid cells. *Pathog Dis* 2016;74:ftw004.

[202] Genchi G. An overview on d-amino acids. *Amino Acids* 2017;49:1521–33.

[203] Li P, Yin Y-L, Li D, Woo Kim S, Wu G. Amino acids and immune function. *Br J Nutr* 2007;98:237–52.

[204] Macpherson AJ, Harris NL. Interactions between commensal intestinal bacteria and the immune system. *Nat Rev Immunol* 2004;4:478–85.

[205] Hayes CL, Dong J, Galipeau HJ, Jury J, McCarville J, Huang X, et al. Commensal microbiota induces colonic barrier structure and functions that contribute to homeostasis. *Sci Rep* 2018;8:14184.

[206] Muñoz A, López-García B, Pérez-Payá E, Marcos JF. Antimicrobial properties of derivatives of the cationic tryptophan-rich hexapeptide PAF26. *Biochem Biophys Res Commun* 2007;354:172–7.

[207] Velmourougane K, Prasanna R. Influence of L-amino acids on aggregation and biofilm formation in *Azotobacter chroococcum* and *Trichoderma viride*. *J Appl Microbiol* 2017;123:977–91.

[208] Kao WTK, Frye M, Gagnon P, Vogel JP, Chole R. D-amino acids do not inhibit *Pseudomonas aeruginosa* biofilm formation. *Laryngoscope Investig Otolaryngol* 2017;2:4–9.

[209] Kolodkin-gal I, Romero D, Cao S, Clardy J, Kolter R, Losick R. D-Amino Acids Trigger Biofilm Disassembly. *Science (80-)* 2010;328:627–9.

[210] Leiman SA, May JM, Lebar MD, Kahne D, Kolter R, Losick R. D-Amino Acids Indirectly Inhibit Biofilm Formation in *Bacillus subtilis* by Interfering with Protein Synthesis. *J Bacteriol* 2013;195:5391–5.

[211] Mikkelsen H, McMullan R, Filloux A. The *Pseudomonas aeruginosa* reference strain PA14 displays increased virulence due to a mutation in *ladS*. *PLoS One* 2011;6:e29113.

[212] Koseki S, Nakamura N, Shiina T. Growth Inhibition of *Listeria* monocytogenes, *Salmonella enterica*, and *Escherichia coli* O157:H7 by D-Tryptophan as an Incompatible Solute. *J Food Prot* 2015;78:819–24.

[213] Chan DI, Prenner EJ, Vogel HJ. Tryptophan- and arginine-rich antimicrobial peptides: Structures and mechanisms of action. *Biochim Biophys Acta* 2006;1758:1184–202.

[214] Thanabalasuriar A, Neupane AS, Wang J, M.F. K, Kubes P. iNKT Cell Emigration out of the Lung Vasculature Requires Neutrophils and Monocyte-Derived Dendritic Cells in Inflammation. *Cell Rep* 2016;16:3260–3272.

[215] Chen S, Kammerl IE, Vosyka O, Baumann T, Yu Y, Wu Y, et al. Immunoproteasome dysfunction augments alternative polarization of alveolar macrophages. *Cell Death Differ* 2016;23:1026–37.

[216] Han W, Li H, Cai J, Gleaves LA, Polosukhin V V., Segal BH, et al. NADPH Oxidase Limits Lipopolysaccharide-Induced Lung Inflammation and Injury in Mice through Reduction-Oxidation Regulation of NF-ϰB Activity. *J Immunol* 2013;190:4786–94.

[217] Belladonna ML, Grohmann U, Guidetti P, Volpi C, Bianchi R, Fioretti MC, et al. Kynurenine Pathway Enzymes in Dendritic Cells Initiate Tolerogenesis in the Absence of Functional IDO. *J Immunol* 2006;177:130–7.

[218] Silk JD, Lakhal S, Laynes R, Vallius L, Karydis I, Marcea C, et al. IDO induces expression of a novel tryptophan transporter in mouse and human tumor cells. *J Immunol* 2011;187:1617–25.

[219] Zelante T, Iannitti RG, Cunha C, DeLuca A, Giovannini G, Pieraccini G, et al. Tryptophan catabolites from microbiota engage aryl hydrocarbon receptor and balance mucosal reactivity via interleukin-22. *Immunity* 2013;39:372–85.

[220] Fallarino F, Grohmann U, You S, McGrath BC, Cavener DR, Vacca C, et al. The Combined Effects of Tryptophan Starvation and Tryptophan Catabolites Down-Regulate T Cell Receptor ζ-Chain and Induce a Regulatory Phenotype in Naive T Cells. *J Immunol* 2006;176:6752–61.

[221] Julliard W, Fechner JH, Mezrich JD. The aryl hydrocarbon receptor meets immunology: Friend or foe? A little of both. *Front Immunol* 2014;5:458.

[222] Nguyen NT, Hanieh H, Nakahama T, Kishimoto T. The roles of aryl hydrocarbon receptor in immune responses. *Int Immunol* 2013;25:335–43.

[223] Kimura A, Abe H, Tsuruta S, Chiba S, Fujii-Kuriyama Y, Sekiya T, et al. Aryl hydrocarbon receptor protects against bacterial infection by promoting macrophage survival and reactive oxygen species production. *Int Immunol* 2014;26:209–20.

[224] Wu D, Li W, Lok P, Matsumura F, Adam Vogel CF. AhR deficiency impairs expression of LPS-induced inflammatory genes in mice. *Biochem Biophys Res Commun* 2011;410:358–63.

[225] Bruhs A, Haarmann-Stemmann T, Frauenstein K, Krutmann J, Schwarz T, Schwarz A. Activation of the arylhydrocarbon receptor causes immunosuppression primarily by modulating dendritic cells. *J Invest Dermatol* 2015;135:435–44.

[226] Liu Y, Liang X, Yin X, Lv J, Tang K, Ma J, et al. Blockade of IDO-kynurenine-AhR metabolic circuitry abrogates IFN-γ-induced immunologic dormancy of tumor-repopulating cells. *Nat Commun* 2017;8:15207.

[227] Musso T, Gusella GL, Brooks A, Longo DL, Varesio L. Interleukin-4 inhibits indoleamine 2,3-dioxygenase expression in human monocytes. *Blood* 1994;83:1408–11.

[228] Heath-Pagliuso S, Rogers WJ, Tullis K, Seidel SD, Cenijn PH, Brouwer A, et al. Activation of the Ah receptor by tryptophan and tryptophan metabolites. *Biochemistry* 1998;37:11508–15.

[229] Nguyen Do K, Nielsen Fink L, Elbenhardt Jensen T, Gautier L, Parlesak A. TLR2 controls intestinal carcinogen detoxication by CYP1A1. *PLoS One* 2012;7:e32309.

[230] Cheng Y, Jin U-H, Allred CD, Jayraman A, Chapkin RS, Safe S. Aryl Hydrocarbon Receptor Activity of Tryptophan Metabolites in Young Adult Mouse Colonocytes. *Drug Metab Dispos* 2015;43:1526–43.

[231] Nguyen LP, Hsu EL, Chowdhury G, Dostalek M, Stec DF, Guengerich FP, et al. Structural identification of diindole agonists of the aryl hydrocarbon receptor derived from degradation of indole-3-pyruvic acid. *Chem Res Toxicol* 2009;22:1905–12.

[232] Kalia VC, Wood TK, Kumar P. Evolution of Resistance to Quorum-Sensing Inhibitors. *Microb Ecol* 2014;68:13–23.

[233] Kalia VC. Quorum sensing inhibitors: An overview. *Biotechnol Adv* 2013;31:224–45.

[234] Kalia VC, Purohit HJ. Quenching the quorum sensing system: Potential antibacterial drug targets. *Crit Rev Microbiol* 2011;37:121–40.

[235] Fischbach MA, Losick R, Kolter R, Chu F, Lopez D. Structurally diverse natural products that cause potassium leakage trigger multicellularity in Bacillus subtilis. *Proc Natl Acad Sci* 2008;106:280–5.

[236] García-Contreras R, Maeda T, Wood TK. Resistance to Quorum-Quenching Compounds. *Appl Environ Microbiol* 2013;79:6840–6.

[237] Teiber JF, Horke S, Haines DC, Chowdhary PK, Xiao J, Kramer GL, et al. Dominant role of paraoxonases in inactivation of the *Pseudomonas aeruginosa* quorum-sensing signal N-(3-oxododecanoyl)-L-homoserine lactone. *Infect Immun* 2008;76:2512–9.

[238] LaSarre B, Federle MJ. Exploiting quorum sensing to confuse bacterial pathogens. *Microbiol Mol Biol Rev* 2013;77:73–111.

[239] Hentzer M, Wu H, Andersen JB, Riedel K, Rasmussen TB, Bagge N, et al. Attenuation of *Pseudomonas aeruginosa* virulence by quorum sensing inhibitors. *EMBO J* 2003;22:3803–15.

[240] Defoirdt T, Sorgeloos P, Bossier P. Alternatives to antibiotics for the control of bacterial disease in aquaculture. *Curr Opin Microbiol* 2011;14:251–8.

[241] Maeda T, García-Contreras R, Pu M, Sheng L, Garcia LR, Tomás M, et al. Quorum quenching quandary: Resistance to antivirulence compounds. *ISME J* 2012;6:493–501.

[242] Teplitski M, Mathesius U, Rumbaugh KP. Perception and degradation of N-Acyl homoserine lactone quorum sensing signals by mammalian and plant cells. *Chem Rev* 2011;111:100–16.

[243] Tateda K, Standiford TJ, Pechere JC, Yamaguchi K. Regulatory Effects of Macrolides on Bacterial Virulence : Potential Role as Quorum-Sensing Inhibitors. *Curr Pharm Des* 2004;10:3055–65.

[244] Oliver A, Cantón R, Campo P, Baquero F, Blázquez J. High frequency of hypermutable *Pseudomonas aeruginosa* in cystic fibrosis lung infection. *Science (80-)* 2000;288:1251–3.

[245] Corminboeuf O, Leroy X. FPR2 / ALXR Agonists and the Resolution of Inflammation. *J Med Chem* 2015;58:537–59.

[246] Wikimedia Commons Contributors. Commensals vs pathogens mechanism. https://commons.wikimedia.org/w/index.php?title=File:Commensals_vs_pathogens_mechanism.png&oldid=292398243. *Wikimedia Commons, Free Media Repos* n.d.

ABBREVIATIONS

Ab	Antibody
ABP	Activity-based probe
ACN	Acetonitrile
Actb	Actin, beta
AECII	Alveolar Epithelial Cells type 2
AHL	N-Acyl Homoserine Lactones
AP-1	Activator protein 1
ALI	Acute lung injury
AM	Alveolar Macrophage
APC	Antigen presenting cell
AQ	2-alkyl-4(1H)-quinolone
Arg1	Arginase 1
BAL	Bronchoalveolar lavage
BMDM	Bone Marrow Derived Macrophage
BSA	Bovine serum albumin
CCL17	Chemokine (C-C motif) ligand 17
CCL2	Chemokine (C-C motif) ligand 2
CD	Cluster of differentiation
cDNA	Complementary DNA
COPD	Chronic obstructive pulmonary disease
CpG	CpG motifs
CSF-2	Colony stimulating factor 2
Ct	Cycle threshold
CXCL5	C-X-C motif chemokine 5
DAAO	D-amino acid oxidase
DCs	Dendritic cells
DMEM	Dulbecco's Modified Eagle Medium

DMSO	Dimethyl sulfoxide
DNA	Deoxyribonucleic acid
DTT	Dithiothreitol
D-Phe/His/Met/ Pro/Tyr/Trp	D-Phenylalanine/Histidine/Methionine/Proline/Tyrosine/ Tryptophan
EDTA	Ethyldiaminetetraacetate
ELISA	Enzyme-linked immunosorbent assay
FACS	Fluorescence-activated cell sorting (flow cytometry)
FBS	Fetal Bovine Serum
HDL	High-density lipoprotein
HRP	Horseradish peroxidase
HSL	Homoserine Lactone
IAA	Indole acetic acid
IDO1/2	Indoleamine 2,3-dioxygenase 1/2
IL-12β	Interleukin 12 beta
IL-1β	Interleukin-1 beta
IL-4Rα	Interleukin-4 receptor alpha chain
IL-6	Interleukin 6
iNOS	Inducible nitric oxide synthase
IPF	Idiopathic pulmonary fibrosis
IRF	Interferon-regulatory factor
JAK	Janus Kinase
KO, -/-	Knock out
LasI	Acyl-homoserine-lactone synthase
Lcn2	Lipocalin-2
LPS	Lipopolysaccharides
M1 macrophage	Classically activated macrophage
M2 macrophage	Alternatively activated macrophage
M-CSF	Macrophage colony-stimulating factor

MHC	Major histocompatibility complex
MRC1	Mannose Receptor C-Type 1
NF-ϰB	Nuclear factor kappa-light-chain-enhancer of activated B cells
NRQ	Normalized relative quantity
OD	Optical density
PAO1	*Pseudomonas aeruginosa* strain PAO1
P/S	Penicillin/Streptomycin
PBS	Phosphate buffer saline
PBMC	Peripheral blood mononuclear cell
PBST	Phosphate buffered saline with Tween 20
PCR	Polymerase chain reaction
PMA	Phorbol 12-myristate 13-acetate
PMN	Polymorphonuclear neutrophil
PRR	Pattern recognition receptor
qPCR	Quantitative real-time polymerase chain reaction
QS	Quorum sensing
Retnlα	Resistin-like molecule alpha
Rhl	Acyl-homoserine-lactone synthase
RIPA	Radioimmunoprecipitation assay buffer
RGZ	Rosiglitazone
RNA	Ribose nucleic acid
RT	Room temperature
RT-PCR	Reverse transcription PCR
SAA	Serum amyloid A
SEM	Standard error of the mean
STAT	Signal transducer and activator of transcription
T2R38	Taste receptor, Type 2, Member 38
TA	Tryptamine
TCR	T cell receptor

TDO	Tryptophan 2,3-dioxygenase
TEMED	Tetramethylethylenediamine
TGFβ	Transforming growth factor beta
T_h	T helper cells
TLR	Toll-like receptor
TNFα	Tumor necrosis factor α
T_{reg}	Regulatory T cell
WT	Wild type

ACKNOWLEDGEMENTS

I would like to express all my gratitude to the people that have supported me from close and far since the beginning of my work at the CPC: Susanne for believing in me since my master's degree, Tobias Stöger and Toni Hartmann for supporting and advising me in the good and the bad days of this adventure. I could not have gathered all this knowledge and make it until here without working in groups of a rare quality. To the Dr. Caspar Ohnmacht for the KO mice thanks to which I could close this thesis. I am grateful to Stefan, Katrin and Marc who taught me most of the techniques I used the last years: as well as my fellow "Doktoranden" from Großhadern and Neuherberg, Petra, Sabine, Jeremias, and after Nunja, Shanze, Roberta, Youjia, Mehwish and Ernesto. It has been a delight to count on Rabea, David and Anna to assist me during a lot of experiments, and to share more than science with Ryan and Garreth. My work life would not have been the same without the extended lunch break with the all the Yildirim's lab: Önder, Gerrit, Tom, Rim, Jie, Gizem and Zeynep.

The Comprehensive Pneumology Center, Großhadern (CPC) was a second family for several years and I want to thank everybody for the many happy moments. Natalia, Aina, Vlady, Nina, Flavia, Carolina, Rita, Deniz, Nadine, and Kyra our friendship means the world to me. I am highly indebted and thoroughly grateful to Hoeke, Claudia, and Melanie for helping me becoming a better scientist during the many Research School classes; and of course, Camille, Doreen, and Kathleen for your enthusiasm and your help in the day to day administrative life.

I want to thank the HELENA initiative for the opportunities that were created, and for all the great people I met during the course, like Eva, Susie, the two Martin and the rest of the soft skill gang that I met periodically these last 3 years.

The completion of this manuscript did not only depend on my professional life but also on my personal life and the people I had the pleasure to live with: Jakob, Hamza Franzi and Alexandra supporting me like no one else did. My fellow Herzogis: Pauline, Caro, Kadda, Marcel, Aldo, Eva, Basti, Alex Double B and all the others,

and the one I spent most of my free time with Victor and Mickaëla. I want to thank my Wing Chun mates: Simon, Rene, David, Julia, Peter, Annette, Anna, Martina, Lukas, Armin, Julian, Augusto, Sven, Boris, and Meister Björn. I am grateful to the highest point to Sevi and Julia who have been there for me for a long time and I hope that they will still stay long after. I am so thankful to Nico, who showed me never ending kindness when I was in doubt.

I want to thank everyone who put me back in the right tracks when I was lost, especially Irene, who gave me peace in the chaos. I cannot thank enough Stephan and David for being the amazing friends they are, available and listening, every time and everywhere, I can never repay the debt I owe you. To my lifelong *Brigade* friends who showed me how much I mattered to them.

I do not forget my family, far but supportive; for whom I was not often present, but they should know they were always in my heart.

Finally, I am thankful to Kristin, my better half, who gives me strength and endless love every day.